WADD TECHNICAL REPORT 60-699
VOLUME VI

ENERGY CONVERSION SYSTEMS REFERENCE HANDBOOK

VOLUME VI — CHEMICAL SYSTEMS

W. R. Menetrey
J. Chrisney

Electro-Optical Systems, Inc.

SEPTEMBER 1960

Flight Accessories Laboratory
Contract Nr. AF 33(616)-6791
Project Nr. 4769
Task Nr. 61048

WRIGHT AIR DEVELOPMENT DIVISION
AIR RESEARCH AND DEVELOPMENT COMMAND
UNITED STATES AIR FORCE
WRIGHT-PATTERSON AIR FORCE BASE, OHIO

700 — May 1961 — 30-1130

A B S T R A C T

Power systems which use chemical fuel as the energy source appear useful in a variety of space applications, and offer weight advantages for durations below about 100 hours. This volume discusses primary and secondary batteries, primary and regenerative fuel cells, reciprocating engines using hydrogen and oxygen bipropellant, monopropellant and bipropellant turbines and cryogenic storage of hydrogen and oxygen. The theoretical and practical performance of the converters is reviewed, and the weight of various systems is predicted. Other factors besides power system weight may lead to the selection of a chemical system in preference to others. For example, liquid hydrogen provides an excellent heat sink for environmental control. While batteries may be approaching the limits of their capability, major advances still will be accomplished in the fuel cell and dynamic engine area. For durations of more than several hours primary system weights of 1 to 1.5 lb/hp hr and secondary specific weights of up to 100 whr/lb appear possible by 1970.

ENERGY CONVERSION SYSTEMS REFERENCE HANDBOOK

LIST OF VOLUME AND SECTION TITLES WITH AUTHORS

LIST OF VOLUME AND SECTION TITLES WITH AUTHORS (CONT'D)

A complete detailed Table of Contents for all volumes of Energy Conversion Systems Reference Handbook is included in Volume I.

PREFACE

It is the purpose of this volume to discuss subsystems containing chemical reactions which play an important role in energy transformation -- both open cycle (primary) and closed cycle (secondary) systems.

Primary systems involve the storage of chemical reactants until useful energy is desired. Of most interest to this text is the conversion of chemical to electric energy (electrochemical) and thermal energy (exothermic reaction).

The primary systems discussed here include the following:

a. Batteries -- electrochemical systems composed essentially of two dissimilar electrodes, an electrolyte, and electrode spacers in a suitable container. Prior to discharges, one electrode is in a reduced state, and the other is in an oxidized state. On use, the reduced electrode is oxidized (electron source), and the other electrode is reduced (electron sink).

b. Primary fuel cell -- an electrochemical system where the chemical reactants are not stored within the battery but are fed into the system.

c. Open cycle engines -- rotating or reciprocating engines which use the hot pressurized combustion products from a monopropellant or bipropellant fuel as a source of mechanical energy and exhaust these products to the atmosphere.

d. Combustion devices -- devices which use (hot) combustion products to heat a structure which conducts thermal energy to a static heat engine or working fluid.

In secondary systems, additional equipment is provided whereby the chemical reactants are regenerated using solar and/or nuclear energy sources. Regeneration systems of many types are being actively investigated, including those which use chemical, photochemical, radiochemical, thermochemical, and electrolytic reactions.

Secondary systems under discussion in this text include the following:

a. Secondary batteries - - systems in which the anode and cathode reactants of the battery are regenerated by electrolysis with electric current from solar or nuclear power systems.

b. Regenerative fuel cells - - systems in which anode and cathode reactants are regenerated by a variety of processes mentioned above using energy from solar or nuclear sources.

Included in the discussion are electrochemical storage mechanisms which could be used, for example, in solar systems during the dark portion of the satellite orbit and for peak load application. The other major storage system of interest, thermal storage, is discussed in Volume II.

A fundamental limitation in conversion efficiency occurs when heat is used as an intermediate form of energy, as differentiated from the heat generated incidentally as a result of irreversibility. In any cycle where heat energy occurs as an intermediate form, the theoretical efficiency is that of a Carnot cycle, as given below.

$$\eta_{Carnot} = \frac{T_2 - T_1}{T_2}$$

where

T_2 = the temperature of the heat source and

T_1 = the temperature of the heat sink.

In practice, the efficiency of converting fuel chemical energy to electric energy, using an intermediate heat process, will not be greater than 40 percent. Because electrochemical devices are not subject to Carnot efficiency, the theoretical limit is 100 percent of the free energy change. This theoretical advance in conversion efficiency has stimulated particular interest in fuel cells, since in many cases the chemical reactants used in combustion and/or electrochemical processes are the same.

The emphasis in this text is on power levels greater than 10 watts and durations greater than one day -- the latter restriction eliminates chemical power systems useful in short-term, high-rate applications such as launch boosters. Eliminated devices include monopropellant gas turbines, special types of high-rate batteries such as the thermal battery, and others which are generally advantageous for durations less than a few minutes.

As compared with solar and nuclear, the primary advantage of chemical systems is the ability to store energy for long periods of time without fuel consumption. Thus, high peak loads of short durations required in the latter stages of a space vehicle mission may be satisfied by small amounts of chemical reactants and a suitable converter, rather than requiring the additional heavy fixed weight of a solar or nuclear system. Thermal storage, the only major competitor to chemical storage, suffers from gradual energy leakage through radiation and from the inability to deviate from rather fixed temperatures depending on the heat storage material.

In addition, chemical systems generally offer the lightest weight, lowest cost, and highest reliability for durations of one day to several weeks depending on the specific application (See Vol. I).

ENERGY CONVERSION SYSTEMS REFERENCE HANDBOOK

Volume VI - Chemical Systems

Section A

BATTERIES PRIMARY AND SECONDARY

W. R. Menetrey
Energy Research Division
ELECTRO-OPTICAL SYSTEMS, INC.

Manuscript released by the author
September 1960 for publication in this
Energy Conversion Systems Reference Handbook

WADD Technical Report 60-699

VI-A BATTERIES -- PRIMARY AND SECONDARY

C O N T E N T S

ILLUSTRATIONS

VI-A BATTERIES -- PRIMARY AND SECONDARY

TABLES

A. BATTERIES -- PRIMARY AND SECONDARY

The wide variety of batteries available for military application are of three general types:

1. Primary batteries, which may be stored and subjected to intermittent or continuous discharges on demand.
2. Reserve batteries, which are activated immediately prior to use and then used in "one shot" applications.
3. Secondary or storage batteries, which are recharged and submitted to many cycles of charging and discharging.

For use in space vehicles, batteries suffer several different disadvantages. For long duration application, primary batteries are heavy and bulky as compared with other power supplies. In addition, secondary batteries at present have limited cycle life and relatively low efficiency in a storage application.

Balanced against these limitations, chemical batteries can be easily built to meet severe mechanical launch requirements. Space vehicle engineering can provide sufficient temperature control to make them operate satisfactorily and reliably. Batteries have no serious handicap in the outer space environment, because vacuum effects are overcome by proper sealing; and zero-g effects, by proper design. Battery supplies have an exceptionally high degree of reliability, and battery cost is relatively cheap.

The discussion here is limited to several battery systems which perform well at relatively long discharge periods and which appear to offer advantages in weight, cycle life, good voltage regulation, or other categories at present or possibly in the near future. These are listed in Table VI-A-1 below, along with:

1. Their theoretical capacity.
2. The actual capacity reported thus far at low discharge rate, room temperature conditions (20 percent voltage drop).
3. The estimated ultimate energy level possible in a practical battery.
4. The cost range of presently available batteries, with minimum cost generally corresponding to the larger batteries.

TABLE VI-A-1

ENERGY DENSITY OF BATTERIES -- PRIMARY APPLICATION

System	Energy Density whr/lb Theory	Actual	Ultimate	Energy Density whr/in^3 Actual	Ultimate	COST Actual (1) ($/kw hr)
Commercially Available						
Zinc-Silver Oxide Zn/KOH/AgO	137	80	95(1)	5.3	6.85(1)	$1000 - 6000
Mercury Alkaline Zn/KOH/HgO	104	55	60(2)	7.75	8.5(2)	$500 - 200
LeClanche Cell $Zn/NH_4Cl/MnO_2$	140	45	67(2)	3.5	4.75(2)	$20 - 10
Silver-Cadmium $Cd/KOH/Ag_2O_2$	111	33	40(1)	2.7	3.3(1)	$1000 - 8000
Lead Acid $Pb/H_2SO_4/PbO_2$	74	20	32(2)	1.5	2.4(2)	$ 300 - 1000
Nickel-Cadmium Cd/KOH/NiO OH	96	17	20(2)	1.2	1.6(2)	$ 300 - 1000
Future Systems						
Organic Depolarized $Mg/MgBr_2$/m - Dinitrobenzene	770	90(3)	130(1)	4.5(3)	6.5	--
Magnesium Cell $Mg/MgBr_2/MnO_2$	193	65(3)	90(1)	4.2(3)	5.8	--
$Mg/Mg(ClO_4)_2/MnO_2$	193	55-85(3)	90(1)	4.2	5.8	--

(1) Manufacturer's estimate.
(2) Signal Corp estimates (Ref. VI-A-6).
(3) Experimental Data.

Many battery systems of possible use in special applications (e.g., low-temperature types) are not mentioned due to time limits.

The mercury alkaline and LeClanche cell are primary dry cells now commercially available, whereas the magnesium and organic depolarized dry cells will become available within a few years. The nickel-cadmium, silver-cadmium, and lead-acid batteries are suitable for storage applications with many cycles of life. The zinc-silver oxide battery may be used as a reserve or primary battery, depending on the application, and also has a limited cycle life in storage applications. Estimates of energy density are derived from several sources, including the Signal Corps, and from conversations with battery manufacturers. A partial list of manufacturers is included in Table VI-A-2 below.

Characteristics important for evaluating batteries include weight, volume, storage life, and discharge characteristics including percentage change in voltage, effect of temperature, effect of discharge rate, and other factors. For secondary application, cycle life and storage efficiency must be high.

Approximate weight figures for several battery systems are shown in Figure VI-A-1 as a function of the discharge rate of the battery. The weights for commercial batteries are based on selected models and do not apply to all models or sizes of any particular type. Variations in individual battery performance can be appreciable, with one sigma values of 5 percent being common for several systems (e.g., silver zinc). Battery weight is severely affected by the ambient temperatures of battery operation, as demonstrated in Figure VI-A-2. Shown here are typical variations in the available energy density of batteries as affected by discharge temperature.

TABLE VI-A-2

BATTERY MANUFACTURERS (Partial)

TYPE	MANUFACTURERS
Zinc-Silver Oxide	Yardney Electric Corporation Electric Storage Battery Company Eagle-Picher Company Frank R. Cook Company American Machine and Foundry Company
Mercury Alkaline	P. R. Mallory and Co., Inc.
LeClanche Cell	P. R. Mallory and Co., Inc. National Carbon Company ("Eveready") Burgess Battery Company R. C. A. Ray-O-Vac
Silver-Cadmium	Yardney Electric Corporation
Lead-Acid	Gould National Batteries, Inc. Electric Storage Battery Company and many others
Nickel-Cadmium	Sonotone Corporation Gould National Batteries, Inc., Nicad Div. Gulton Industries, Inc., Nicad Div. Eagle-Picher Company
Organic Depolarized	R. C. A.
Magnesium Dry Cell	R. C. A. National Carbon Company

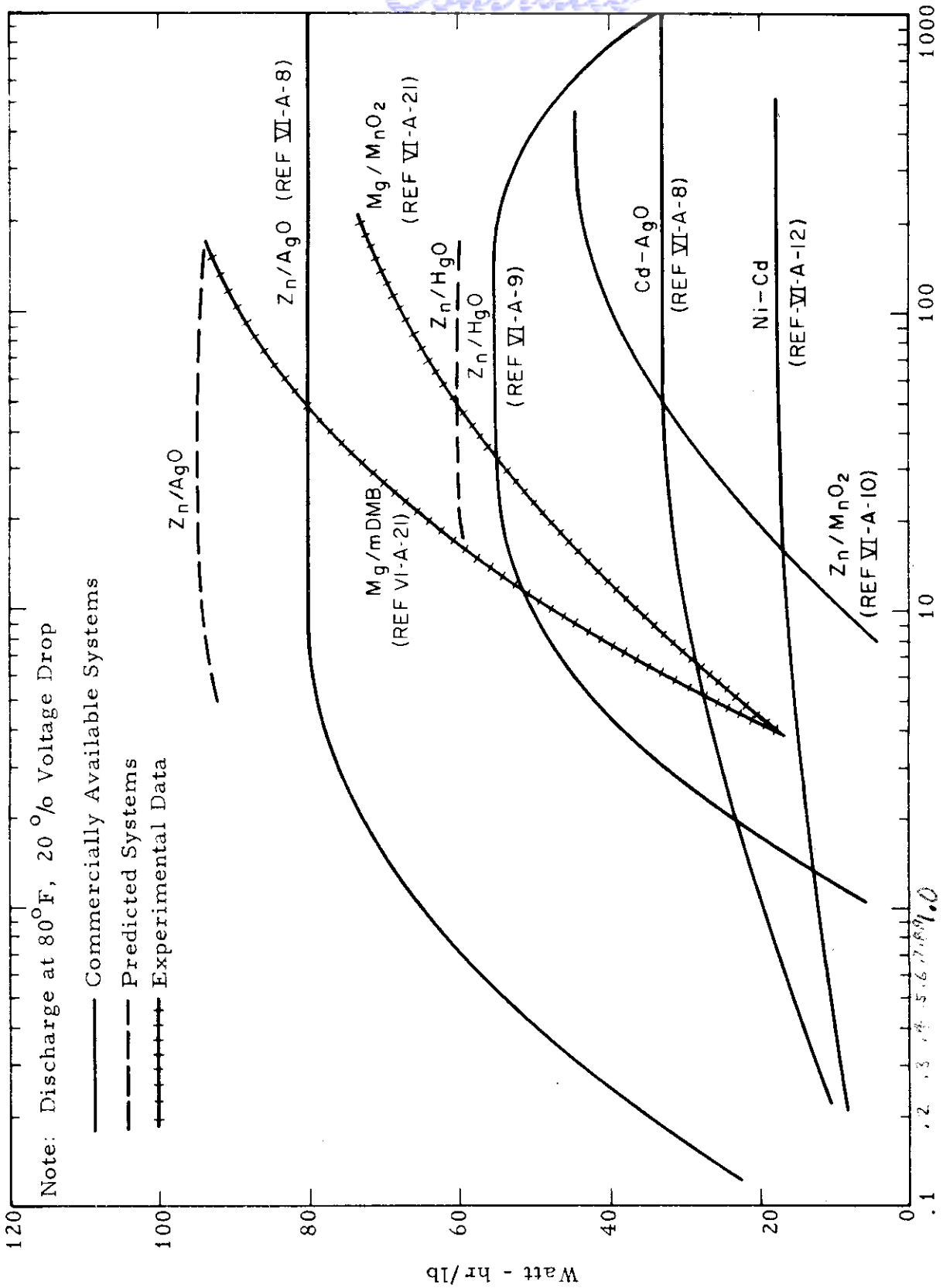

FIG. VI-A-1 WATT-HOURS/POUND VS. DISCHARGE RATE (primary cells)

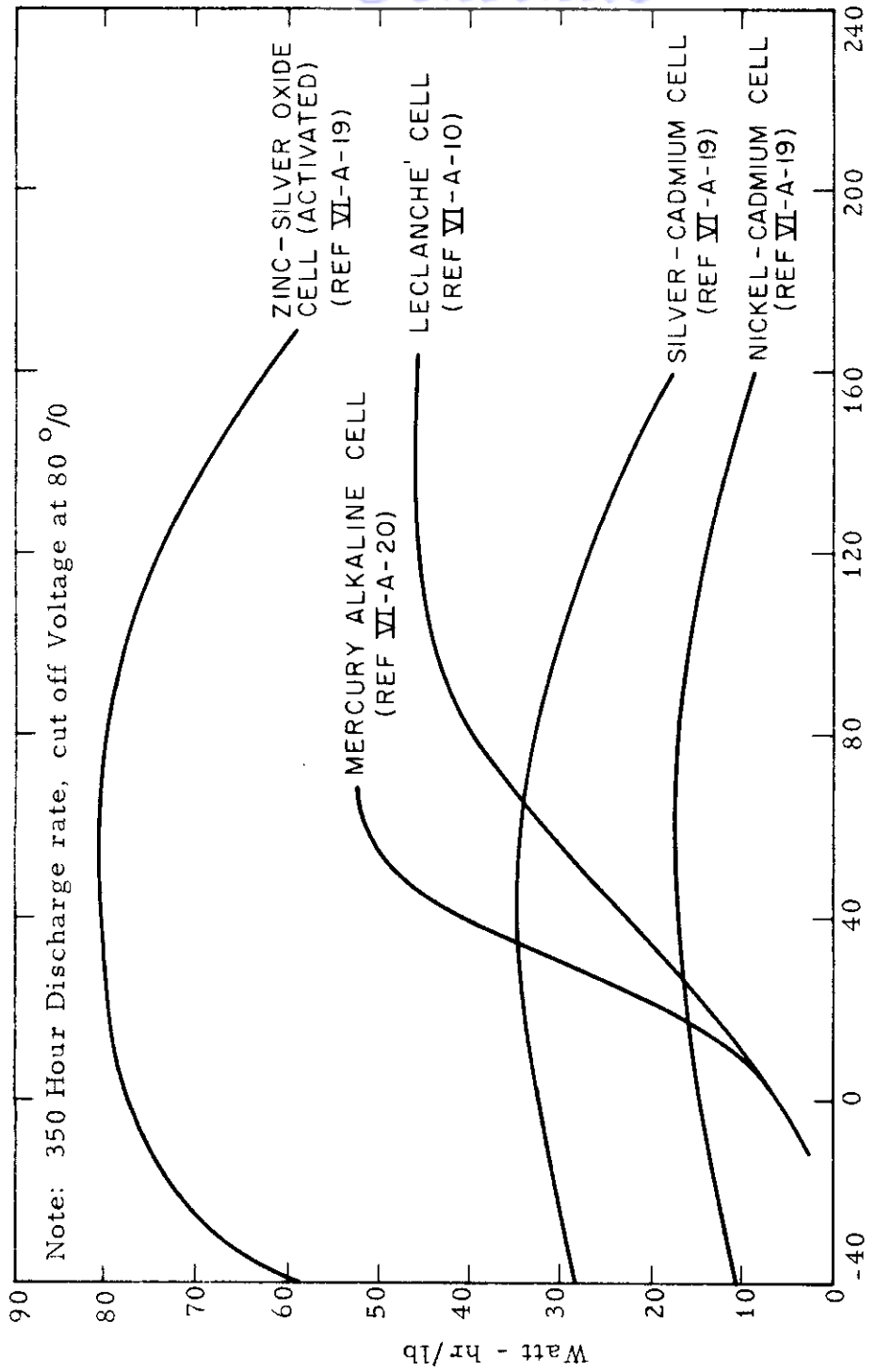

FIG VI-A-2 MAXIMUM BATTERY CAPACITY VS. TEMPERATURE

The batteries may be stored for long durations prior to use on the ground or during a space mission. High-temperature storage will, in general, severely decrease the percent of energy density retained during storage. Figure VI-A-3 shows data from several sources regarding storage life, with straight lines on a semilog scale extrapolated between several data points. The curves are only approximate, because storage life can vary considerably, depending on the construction of any particular cell.

Batteries discussed here share several general problem areas. One is the relatively poor utilization of energy available in the active materials used. Another is additional material required to produce desired performance, thereby creating much extra volume and weight. In a dry cell, for example, zinc and manganese dioxide are the two active materials; yet, carbon black, carbon rods, separators, sealing compounds, and other materials are all required for satisfactory performance. These two factors account for most of the discrepancy in Table VI-A-1 between the theoretical energies of the active materials used and the actual energies realized.

Increased capacities and utilization can be obtained by reducing the current densities in any given system. Since the discharge rate for any given application is generally fixed, a decrease in current density must be obtained through an increase in the electrode surface area in each cell system. Thus, by increasing the electrode surfaces and maintaining fixed drains on equipment, current densities are reduced; and, in turn, greater utilization of active materials can be realized. This principle is being adopted by most battery manufacturers.

Mechanical and thermal design of the battery will be important in space application. Decreased volume, for example, results from using flat rectangular shapes, rather than round cells, in a battery pack. During discharge,

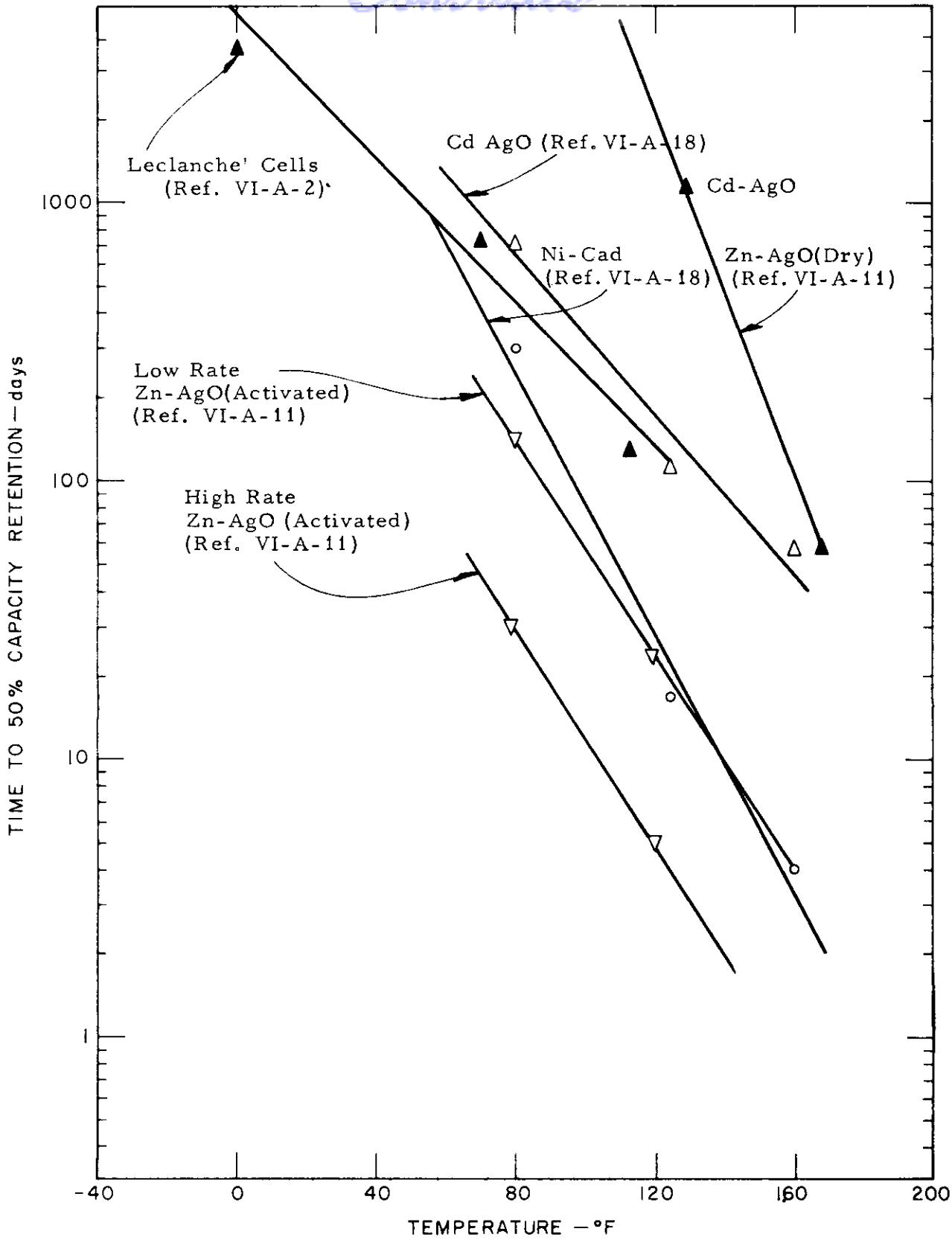

FIGURE VI-A-3 BATTERY SHELF LIFE (approximate)

battery inefficiency will result in heat which must be conducted to the outside surface and then removed by radiation or a cooling mechanism. For large battery packs, the interior of the battery may reach temperatures such that the over-all battery performance is severely degraded unless careful thermal analysis is performed on each individual battery pack. The mechanical design of each battery must account for the space environment (e.g., several electrochemical systems will gas during discharge and charge, and the battery case must be sealed in order to avoid loss of capacity).

These and other problems will be mentioned during the following discussion of individual batteries. Increased battery energies resulting from the utilization of newer electrochemical systems will be discussed here, including the use of organic depolarizer compounds, new anode materials such as magnesium, and new electrolytes.

A number of cells in series will be required to provide higher voltages than are available from each individual cell. The reliability and life of the series-connected circuit is strongly dependent upon the shortest life battery. Short circuiting of a battery through separator deterioration and other effects will increase the current density and hasten the deterioration of the other batteries in a series circuit. The primary dry cell has been developed to a reliability of over .99. Improved manufacturing techniques are rapidly increasing the wet primary cells (e.g., Zn-AgO) to this reliability figure. In a secondary application, the necessary data on long-term cycle life under a variety of conditions are inadequate, and high reliability can only be incorporated into a system by using low discharge rates and by using only a small percent of battery capacity. This conclusion is based on empirical test data. The basic mechanism of storage battery failure is as yet not understood.

1.0 NICKEL-CADMIUM BATTERIES

Sealed nickel-cadmium batteries are at present the only electrochemical storage mechanism combining high cycle life in a satellite application with a reasonable weight. In addition, the nickel-cadmium battery is highly reliable, has good low-temperature characteristics, and is mechanically rugged. The cost is high, relative to other batteries, but low in comparison with over-all costs of space power systems. Sonatone Corporation has thus far been the leader among commercial battery manufacturers in the development of nickel-cadmium batteries for space application. Test and development programs are also taking place in various private and government organizations generally associated with satellite and space probe construction, such as USAERDL, Lockheed (LMSVD), R.C.A., G.E. (MSVD), Bell Laboratories and others.

Nickel-cadmium cells have been used in several satellites as the storage mechanism for a system using photovoltaic cells as the primary energy source, and the majority of satellite power systems planned in the near future will use this same type of system. There is nothing fundamentally peculiar about the battery which prevents it from being used with power systems other than photovoltaic, such as thermoelectric. More data have been accumulated on nickel-cadmium for satellite storage than any other battery. The basic mechanisms of failure, however, are not yet understood, and performance estimates are based on limited empirical data.

1.1 Physical Construction

Nickel-cadmium batteries are made in two basic types: those with pocket-tubular electrodes and those with plate construction. The sintered plate cell may be sealed, will sustain higher current densities, and at low

designated as $T_c(t)$ and $T_h(t)$ respectively. The rate at which heat is absorbed at the cold junctions is $P_c(t)$ and the rate at which heat is liberated at the hot junctions is $P_h(t)$. The electric current and electric terminal voltage are defined as I(t) and v(t) respectively in such a way that the electrical power input is VI.

The homogeneous isotropic thermoelements are described by Seebeck coefficients α_n and α_p, electrical resistivities ρ_n and ρ_p, thermal conductivities k_n and k_p, and per-unit-volume specific heats C_n and C_p. The Thomson coefficients are τ_n and τ_p, where a positive coefficient designates the liberation of heat if the temperature gradient and the electric current are positive in the same direction. The cross-sectional areas of the elements are A_n and A_p, and the lengths are ℓ.

2.1.3 Basic Equations of the System

The basic heat pump shown in Figure IV-A-6 can be described completely by five equations. The first two of these, which are obtained by applying the principle of conservation of energy to a differential segment of thermoelement, are the partial differential equations for the temperature distributions in the two thermoelements (Ref. IV-A-4).

$$\frac{\partial}{\partial x}\left[k_p A_p \frac{\partial T_p}{\partial x}\right] + \tau_p I \frac{\partial T_p}{\partial x} - C_p A_p \frac{\partial T_p}{\partial t} + \frac{\rho_p}{A_p} I^2 = 0 \qquad (2.1)$$

$$\frac{\partial}{\partial x}\left[k_n A_n \frac{\partial T_n}{\partial x}\right] - \tau_n I \frac{\partial T_n}{\partial x} - C_n A_n \frac{\partial T_n}{\partial t} + \frac{\rho_n}{A_n} I^2 = 0 \qquad (2.2)$$

The next two equations are the power balances at the two junctions, at the cold end:

$$P_c = \alpha_c T_c I - k_p A_p \frac{\partial T_p}{\partial x}\bigg|_{x=0} - k_n A_n \frac{\partial T_n}{\partial x}\bigg|_{x=0} \qquad (2.3)$$

It has, therefore, been the practice to package rectangular cells as groups within magnesium cases having sufficient strength to prevent deformation of the individual cell cases. This practice allows the use of lighter cell walls and a greater energy-to-weight ratio in the entire system. Satellite batteries generally have cell walls made of low carbon steel. Because of the high pressures encountered, plastic cases are subject to deformation. In addition, plastic is not as impermeable to water vapor and gas as is low carbon steel. Package design is primarily determined by internal thermal requirements and the necessity of electrical insulation. To maintain internal temperatures of less than about 105°F, surface temperatures are generally limited to 90 to 105°F for long cycle life.

In the cylindrical cell used in several satellite applications, the plates are rolled like two newspapers and then placed in a cylindrical can which is the negative terminal. In the latest hermetically sealed cell, the top is welded on. The lead from the positive terminal is brought out through a glass-metal seal. Previous sealing techniques used a nylon-plastic gasket seal which tended to leak when under vacuum or at high temperatures. Sealed cell batteries have been made ranging in size from milliampere-hour to about 160 ampere-hours. For rectangular cells, it is necessary to use a plastic, rather than a glass-to-metal, seal because of the lack of rigidity. In practical system application, a pressure release valve has lack of rigidity. In practical system application, a pressure release valve has been provided to take care of any system situation resulting in temperature malfunction and battery abuse. Tests have indicated high reliability and satisfactory operation of this valve.

A nickel-cadmium dry cell (Hermetac) is available commercially but offers inferior characteristics for satellite application. Performance figures are as follows: 10.5 watt hr/lb and 1 watt hr/in^3 at 80°F, rising to 11.5 watt hr/lb at 113°F and falling to 0 watt hr/lb at about -10°F. These cells

give about 300 cycles at moderate discharge rates; then the capacity is about 50 per cent of the original. Although these cells are "hermetically" sealed, they evolve gas on normal charge and discharge up to 0.7 mm/day. A 10 per cent loss of capacity is suffered after about three months of storage. The dry cell construction does offer inherent advantages in ruggedness and resistance to shock.

1.2 Battery Selection and Performance

The choice of cell size is determined by the required ampere-hour capacity as effected by the following: charge and discharge rate, permissible voltage range, method of charging and expected overcharge, desired cycle life, cell temperatures during operation, and related factors.

1.2.1 Voltage Characteristics

Greater voltage range will allow greater ampere-hour capacity per cell. Discharge can be carried on as low as .6 volts; however, the additional capacity gained by dropping from one volt to .6 volts for an end point is not large and should not be used in a storage application, as illustrated in the typical discharge curves of Figure VI-A-4. Using a 1.0 voltage end point, decreasing temperature will lower the available room temperature (80°F) capacity to 80-85 per cent at 0°F and to 40-50 per cent at 40°F. Nominal open circuit voltage is about 1.33 volts, whereas an average operating voltage is between 1.25 and 1.10 volts. As shown, plateau voltages will also decrease with increased discharge rate and decreased temperature. A typical charge-discharge curve for a battery used in a satellite application is shown in Figure VI-A-5.

1.2.2 Cycle Life

In the sealed battery an overcharge will result in an excess amount of heat, resulting in cell deterioration, particularly in the separator. The useful cycle life of a cell can, therefore, decrease if high charging rates are used and if the excess energy is converted to heat.

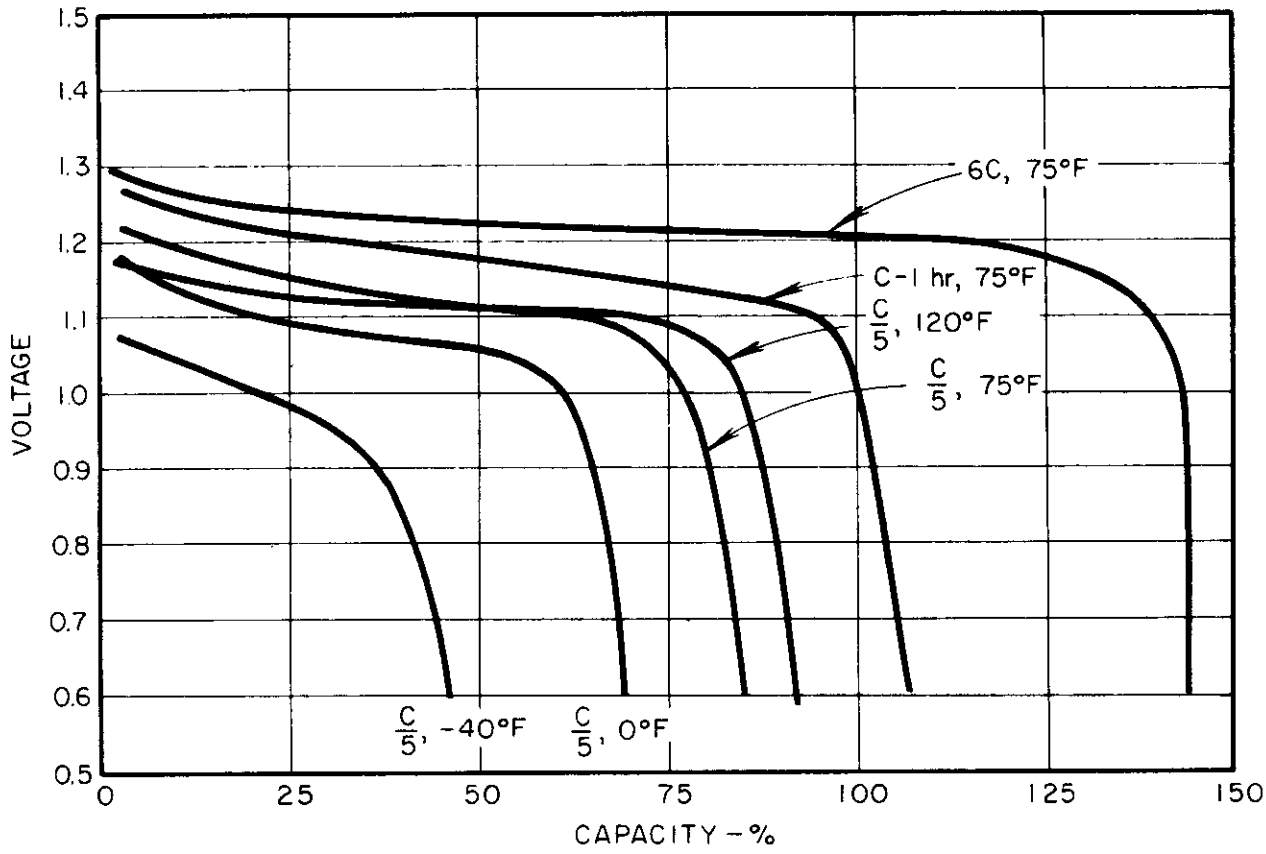

FIGURE VI-A-4 TYPICAL DISCHARGE VOLTAGE CHARACTERISTICS NICKEL-CADMIUM BATTERIES (Ref. VI-A-12, VI-A-22)

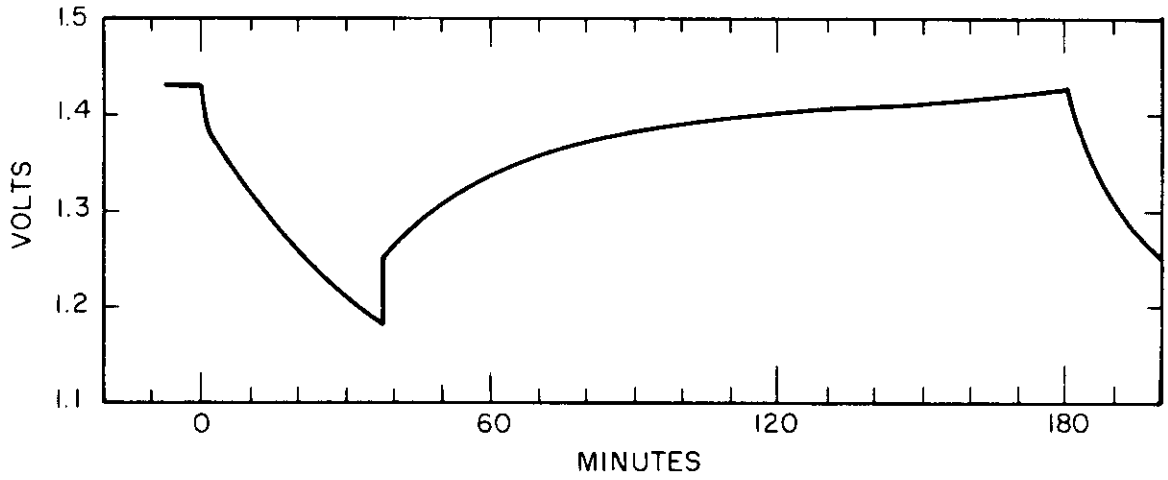

FIGURE VI-A-5 CHARGE-DISCHARGE CHARACTERISTICS--NICKEL CADMIUM BATTERY

During overcharge, oxygen is evolved at the positive plates at a rate proportional to the current being passed. The rate of consumption of oxygen at the negative is determined by the partial pressure of oxygen within the cell. Consequently, as the cell becomes fully charged and oxygen begins to be formed, the internal pressure builds up until the rate of consumption equals the rate of production. Hence there is a steady-state pressure corresponding to each overcharge current. If the overcharge rate is too high, the steady-state pressure may exceed safe limits. For very high overcharging currents some hydrogen may be evolved at the negative. This will cause very sharp rises in voltage and internal pressure which will lead to cell failure. Thus, one of the most important limitations on the use of sealed nickel-cadmium cells is the maximum steady-state overcharge current which can be safely tolerated.

The cellulosic (paper) separators presently used will dissolve in the potassium hydroxide electrolyte at high temperatures. The separator must also have a wetting property such that the KOH is absorbed -- a necessary step in many applications, for example, where spin stabilization is used and where the electrolyte must be held in the proper place in the battery. The separator must also be porous enough to allow recombination of the oxygen. Sonatone Corporation recommends that cell temperatures be held below a level of 100°F for long life. The use of new separator materials such as Teflon (which has shown favorable results at 130°F), nylon, and others might raise this temperature barrier.

Data are somewhat limited regarding cycle life as a function of charging rate, overcharge, temperature, discharge depth, and other parameters and causes of ultimate failure are unknown. Failure has resulted from drying out of the cell through faulty seals, separator failure, and deterioration of the sintered nickel plaque and some shedding of the positive

active material with prolonged cycling.

It is generally believed that this deterioration is more rapid the more frequent the cycles of charge and discharge and that deep discharges, i.e., those which involve large fractions of the total battery capacity, cause more deterioration per cycle.

Using the criterion that the voltage difference from the end of charge to discharge will not exceed 20 per cent, Table VI-A-3 shows the range of cycle life that was obtained at S. C. E. L. using a 60-40 minute cycle.

TABLE VI-A-3

RANGE OF CYCLE LIFE

Temperature	No. of Cycles	Per Cent Capacity Removed	Per Cent Overcharge
80°F	1,400-11,000+	6.6-11.0	30-100
20°F	360- 6,400+	14.0-22.0	0-31
120°F	1,025- 1,930+	15.0-26.6	15-110

The cells tested at 80°F were charged by silicon solar converters exposed to artificial light, whereas constant potentials of 1.5 and 1.45 volts/cell were used at 20°F and 120°F, respectively. Cell failure in many cases could be attributed to water leakage which should not occur in the new hermetically sealed batteries. Furthermore, the cells could be rejuvenated by adding water.

A test program at Bell Laboratories was reported in detail by U. Thomas, and used an available "hermetically-sealed" nickel-

cadmium cell with a nominal capacity of 4 ampere hours. The cell used, a Sonotone "F" cell, is a steel cylinder 9.3 cm high and 3.4 cm in diameter weighing 270 grams. For test purposes a 3-hour cycle was chosen with a discharge time of 37.5 minutes (0.625 hr) and a charge time of 142.5 minutes (2.375 hr), corresponding to the maximum dark time for a circular polar orbit of approximately 2260 miles altitude. For cycle-life testing, charge and discharge were at constant current.

In initial trials the charge current was set at 500 ma and the discharge at 1.6 amperes. Operation on this cycle for several days showed that the charge and discharge curves changed very little from cycle to cycle and hence it was decided to raise the overcharge rate and decrease the amount of overcharge per cycle. As a result of these exploratory tests, overcharge currents of 580 ma and a discharge of 2.4 amperes were chosen for the majority of the test cycles described below.

The cell was first given a prolonged charge, about 5 hours, and then discharged and recharged repeatedly as indicated. The end-of-discharge voltage decreased from 1.25 volts on the first cycle to about 1.18 volts after 30 cycles, at which value it remained approximately constant with further cycling. A typical voltage-time curve is given in Figure VI-A-5. The cell was operated for nearly 600 3-hour cycles, interrupted from time to time for capacity determination and other special tests, the longest uninterrupted series lasting about 200 cycles.

It was noted that repeated cycling, after a prolonged charge, changes the shape of the discharge curve. In particular, the final discharge voltage decreased. This effect is illustrated in Figure VI-A-6. The final voltage however tends toward a limiting value after many cycles. The low final voltage apparently is not caused by any permanent change in the cell, since the higher discharge curve can be restored by deep cycling or by prolonged overcharge.

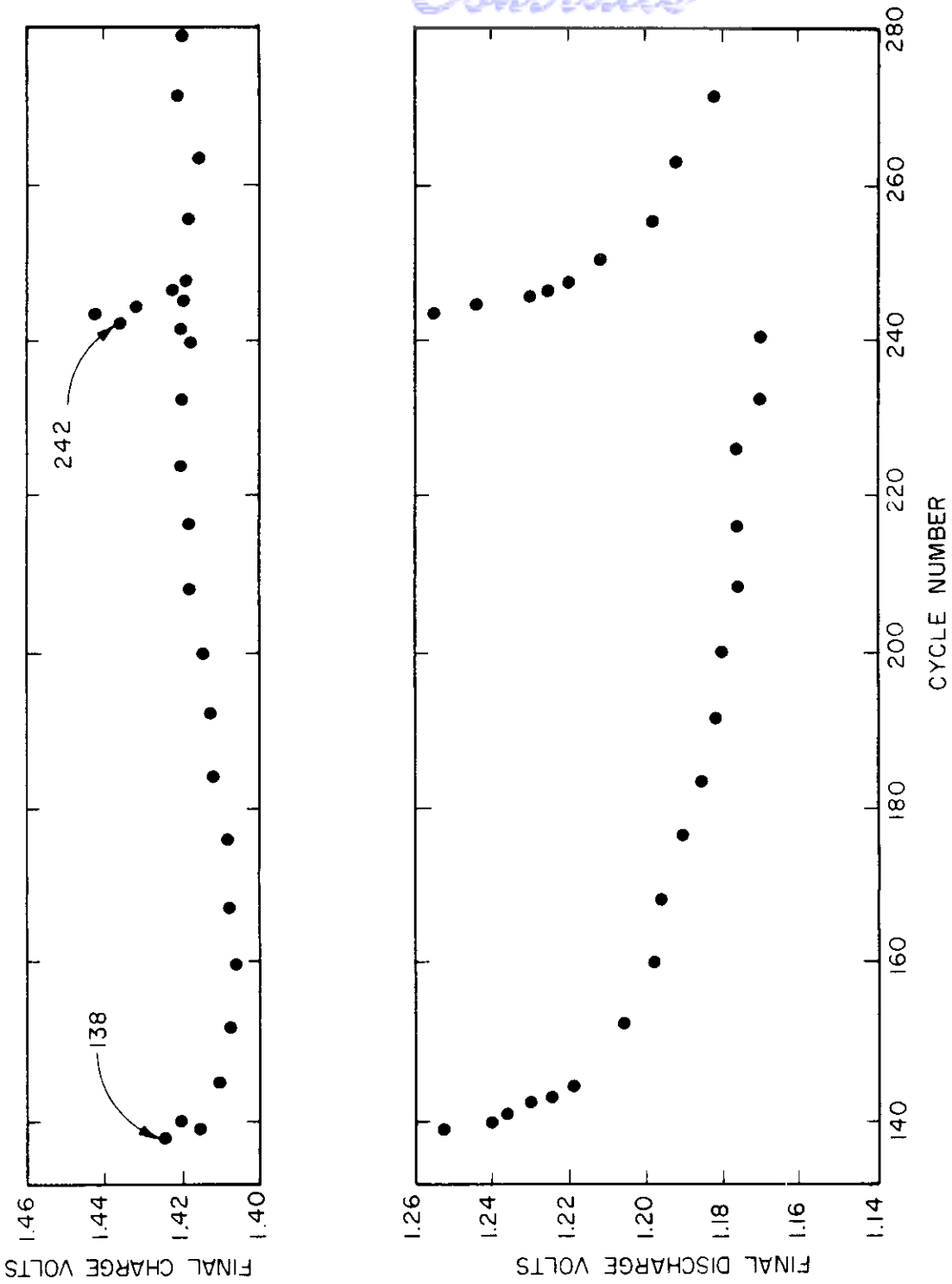

FIGURE VI-A-6 FINAL VOLTS -- NICKEL CADMIUM BATTERY

After 200 repeated standard cycles the final voltage seems to have stabilized at about 1.18 volts. A particular discharge was continued at 2 amperes until the cell voltage had dropped to 1.0 volt. The discharge curve is shown in Figure VI-A-7, where it is compared with a "normal" curve obtained after a deep cycle and an overcharge of 6.7 ampere hours. There are several interesting features to the curve for discharge No. 530. The voltage from 5-18 minutes is higher than for the normal discharge, and the discharge curve is much steeper, almost entirely lacking the usual plateau between 1.25 and 1.20 volts. The total capacity to a 1.0 volt cutoff was 2.38 ampere hours as compared to nearly 4.0 ampere hours for the normal discharge. It will also be noted that there is a particularly rapid voltage drop near the usual end of the cycle, i.e., from 30-37.5 minutes. It is as though the cell "anticipated" the usual cycle.

These tests differ from satellite operation in a number of respects which must be considered before predicting cycle life. In a circular polar orbit, the period of darkness will vary with the season. Thus, the changes in the discharge curve brought on by repeated cycling may be modified by prolonged overcharge.

Also, in a space environment the heat generated in the cell must be dissipated into space by radiation and hence the present tests do not give an accurate picture of cell temperature. The problem of heat balance must be separately studied.

In general, the exceptionally long cycle lives reported have been singular cases which are not predictable by source of manufacture, size, or other criteria. Nothing definite can be reported at this time except that preliminary tests indicate that thousands of cycles are attainable under suitable discharge-charge conditions.

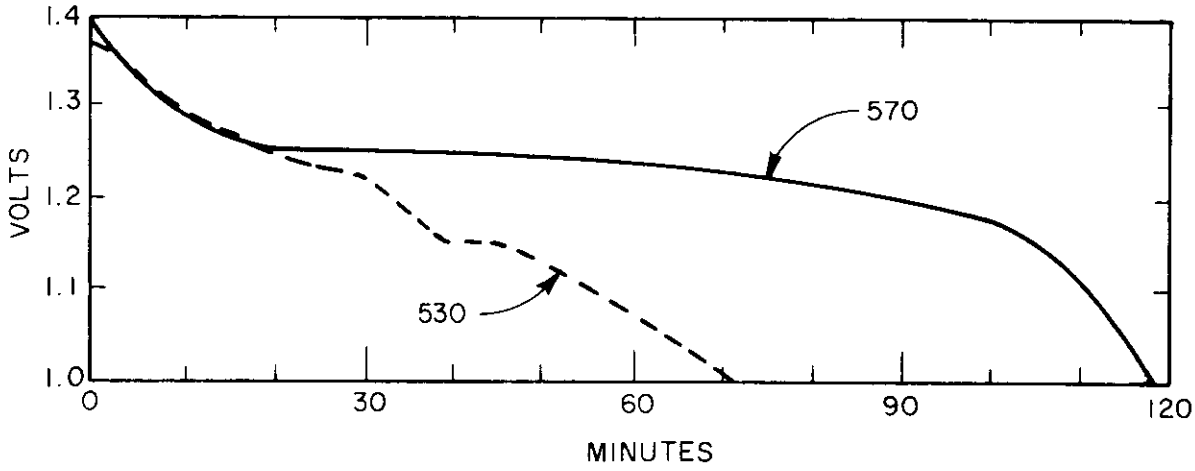

FIGURE VI-A-7 END DISCHARGE VOLTAGE --NICKEL CADMIUM BATTERY

1.2.3 Charging Characteristics

The charge-discharge efficiency of a sealed nickel-cadmium battery is dependent on the overcharge necessary to maintain battery capacity, battery temperature, discharge rate, and related factors. For a 10 per cent overcharge, the ampere-hour efficiency is approximately 90 per cent. The watt hour efficiency--approximately the amp-hour efficiency times the voltage efficiency--corresponds to the voltage difference on charge and discharge. To prevent gassing, charge voltage is limited to 1.45 volts. If the battery is discharged to 1.1 volts, the voltage efficiency is .76, and the watt-hour efficiency would be about 0.9 x 0.76 = 68 per cent. Tests have shown that efficiency is even higher if a portion of the midrange of the charge-discharge curve is used. This use also results in a reduction of the voltage range.

The maximum charge rate is limited by the rate at which gas can recombine on the negative electrode. In satellite operations to date, the battery charging system has been an effective constant current charge. Under constant current, Sonatone estimates that the maximum charging rate allowable for long cycle life should not exceed that required to charge the battery in some 16 hr. It has been found that glass-to-metal seals permit somewhat higher rates of charge. Sonatone also states that the cells can be charged at a much higher rate, such as the two-hour rate, provided that the charging system is limited to about 1.5 volts/cell at any one time and that charging ceases or is reduced to this 16 hour rate when this voltage is reached. Pulse charging, wherein the battery is fully charged to a specified voltage and then allowed to stand, in practice has resulted in voltage fading and loss of capacity. A higher temperature separator will allow a higher charge rate and, therefore, a battery with less ampere-hour capacity for any satellite application.

Thomas of Bell Labs reports successful operation at a 10-hour charge rate. Maximum charge rates vary from 20 to 5 hours, depending

on manufacturer and individual cell variations. By plotting voltage vs. current when charging at a constant temperature, it is possible to determine this maximum charge rate for any given battery. In general, the overcharge will vary during the life of a satellite. For example, in a 24-hour orbit, the maximum period of darkness will be 72 minutes, and in only 40 out of 180 days will there be a period of darkness. During most of its lifetime, therefore, the nickel-cadmium cell must be compatible with a 100 percent continuous overcharge. To avoid excessive deterioration, therefore, low charging rates must be maintained. The nickel-cadmium cell has demonstrated the ability to maintain continuous overcharge. Sonatone Corporation, for example, has achieved three years of continual overcharge at the 16-hour rate at room temperature.

With a 25 percent discharge depth, the Signal Corps reports that voltage can be maintained with only 12 to 20 percent overcharge. Thomas at Bell Labs reports that 10 percent overcharge is adequate for maintaining voltage level. For a greater depth of discharge, a greater amount of overcharge has been indicated in experiments, although no definite data are available. For system design calculations, a figure of 10 percent for overcharge is probably minimum (i.e., 70 percent whr storage efficiency).

The voltage variation from the battery supply will be rather high during the lifetime of the system. For example, a 28-volt power supply might vary from 29.5 to 24 volts during its lifetime. The need for voltage regulation will be determined by the design of electronic load.

1.2.4 Capacity Required

The capacity of a battery required in terms of ampere hours can be estimated from the following approximate equation (accredited to U. Thomas, Bell Labs) for any specific application:

$$C = I_1 H_c \left[f(1 + \beta) \right]$$

where

C = Capacity of the battery in ampere-hours

I_l = Load current supplied by battery

H_c = Maximum permissible charging rate in hours, which is the time required to charge the battery from 0 to 100 percent

f = Battery discharge time/battery charge time

β = Minimum overcharge necessary for a continuous cycling program, which is a fraction of the capacity removed on discharge.

As an example, assume a two-hour orbit where the battery must supply 500 watts for a maximum of 40 minutes, approximately 12 ampere-hours assuming a 28-volt supply is used. During the 80 minutes of light, the battery will be recharged with a 10-percent overcharge, or approximately 14.4 ampere-hours is needed. Assume also a maximum charging rate of 10 hours to insure cycle life. The capacity then is given by:

$$C = (18)(10)\left[\frac{40}{80}(1 + .1)\right]$$

or $C = 99$ ampere-hours.

The percent depth of discharge during orbit would be 12 percent (12/99). The battery of this example not only would be able to supply orbital requirements but also would have a large excess capacity for ascent requirements plus supplying energy for the first orbit.

To supply the necessary 28 volts, approximately 24 batteries must be connected in series, perhaps in sealed rectangular nickel cadmium cells. Each package case would be made of magnesium, and the arrangement of the cells would be based on heat transfer as well as electrical considerations. The individual cell cases would be electrically insulated from each other as well as from the magnesium case. For the example specified above,

a total capacity of about 3,060 whr is required. Including packaging leads, dimensions, and other hardware, the total weight of the battery supply would be approximately 300 pounds, or an equivalent of 1.6 lb/watt.

1.2.5 Environmental Effects

The space environment should have negligible effect upon battery operation, Nickel-cadmium batteries have worked successfully under zero-g conditions. Under normal operating conditions, no excess gas should be generated. The likelihood of permanent damage to the cells due to an improper connection and reverse charging may be alleviated by providing a pressure vent on the sealed cells. Such vents have been constructed and proved satisfactory in operation.

The nickel-cadmium battery has been subjected to the vibration and shock requirements of a missile launch system and found highly reliable. The cell can be checked out on the ground with individual cell voltage checks and individual battery group checks for current distribution and balance.

1.2.6 Life and Reliability

Sonatone indicates that the operational life of the batteries is described statistically by random failure--an exponential decay curve rather than a Gaussian or normal type of failure. Primary problems appear to be mechanical in nature, including the manufacture of uniform plates, separator construction, uniform electrode separation, and other factors. The most sensitive battery component, the separator, will perform satisfactorily if temperature limits are maintained.

In many applications, the battery might be required to stand for long periods of time before use. Shelf life is long, with the time to 50-percent capacity retention being on the order of 300 days at 80°F, 17 days at 125°F, and 4 days at 160°F. Storage temperatures, therefore, should be low.

1.2.7 Weight

The energy density of the nickel-cadmium battery will vary with temperature and discharge rate, as was shown in Figures VI-A-1 and VI-A-2. Maximum performance provides about 17 whr/lb at 80°F and low discharge rates based on a 30-percent voltage drop. This performance corresponds to about 1.1 whr/in^3.

Using Equation A-1 and knowing the energy density of the battery, it is possible to estimate the weight of the storage system required for any mission, as below:

$$W = P \frac{.H_c}{\rho} \left[f(1+\beta)\right] \qquad (A-2)$$

where W = total weight.

P = power level required during battery discharge.

ρ = whr/lb of battery.

Equation A-2 is depicted in Table VI-A-4 below, where it is assumed that a satellite mission requires a given power, P, during the entire dark period and that the entire light period is used for recharging. The specific weight (lb/kw) is shown as a function of satellite altitude. In practice, the entire light period may not be available, or other peak loads may increase f. At present, specific weight of about 10 whr/lb could be safely applied to the nickel-cadmium battery including extra weight due to packaging, leads, and other extra equipment. As an extrapolation into the future (1965), calculations are made assuming H_c = 5 hours and ρ = .02 kwhr/lb.

TABLE VI-A-4

SPECIFIC WEIGHT OF BATTERY STORAGE SYSTEM

Satellite Altitude (miles)	f	Specific Weight (lb/kw)	
		1962	1965
300	.6	660	165
1000	.37	408	102
5000	.156	171.5	43
22,400	.045	49.5	12.5

1962

H_c = 10 hours

β = .1

ρ = .01 kwhr/lb

1965

H_c = 5 hours

β = .1

ρ = .02 kwhr/lb

2.0 SILVER-ZINC BATTERIES

The silver zinc battery offers the highest energy density for any primary system commercially available and can be used as a storage battery over a limited number of cycles. The cell consists essentially of porous silver oxide positive plates, zinc negative plates, and a potassium hydroxide electrolyte. Porous celluloid separators physically separate the plates and are saturated with electrolyte. Cell cases are plastic (e.g., nylon, bakelite), and for lightweight applications, a pressurized rectangular magnesium case is used. For applications where long storage is required, automatic activation mechanisms have been constructed consisting essentially of a storage container and a pressurization mechanism for transfer of electrolyte to the battery when desired.

For low-temperature application, an electric heater blanket raises the temperature to about -20°F. Heater requirements might be on the order of 1/2 watt/hr/in^2 surface area at -65°F.

The silver-zinc cell is commercially available in a variety of sizes (from .1 to 300 amp-hours) and in several models, each model designed for a different cycle life and maximum discharge rate. The primary difference

in models lies in the thickness and type of separator material used. A thick separator will provide long cycle life and/or long active life but will provide generally less energy density and require longer initial activation times.

Yardney Electric Corporation, for example, has four basic models: an automatic activated primary model; a manual primary (PM); a high rate secondary battery (HR series); and a low-rate secondary series (LR series). The differences in performance are illustrated in Table VI-A-5 below:

TABLE VI-A-5

YARDNEY SILVER-ZINC BATTERY MODEL COMPARISON

Performance	Automatic Activated Primary	Manual Primary (PM)	High-Rate Secondary (HR)	Low-Rate Secondary (LR)
Maximum whr/lb	40	80	56	60
Maximum Cycle Life*	5-10	5-10	20-25	80-100
Soak Time (for full discharge)	30 min	30 min	72 hr	150 hr
Minimum Active Life (70°F)	2 mo	2 mo	6-9 mo	12-18 mo

* 1 hour discharge, deep discharge, end of life occurs when output drops to 80 percent of nominal capacity.

Other manufacturers offer similar variation in battery types. Eagle-Picher, for example, offers high, medium, and low-rate cells. Manufacturers also include Yardney Corporation, A.M.F., Frank R. Cook, and Exide.

Typical voltage characteristics are illustrated in Figure VI-A-8 (Eagle-Picher, Ref. VI-A-11). Over most of its useful life, the silver zinc cell has a characteristic flat plateau region which will decrease with increased

Curve A 80°F
Curve B 32°F
Curve C 0°F
Curve D -20°F
Curve E -40°F

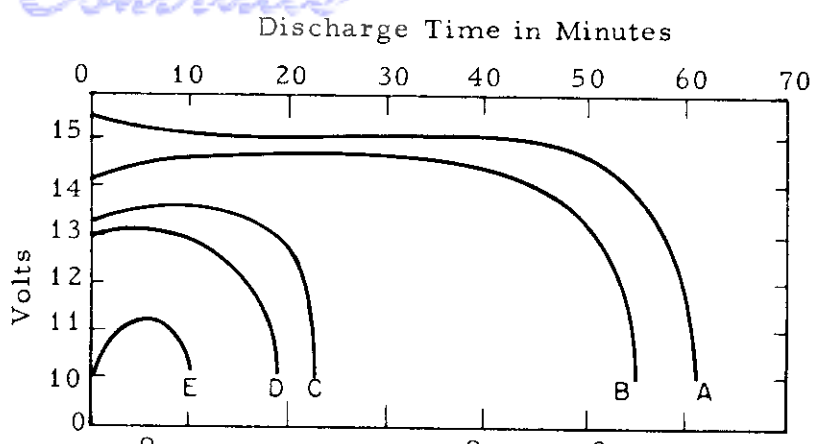

80°F. 1 Hour Rate -40° to 80°F.
Applicable to High and Medium Rate Series.

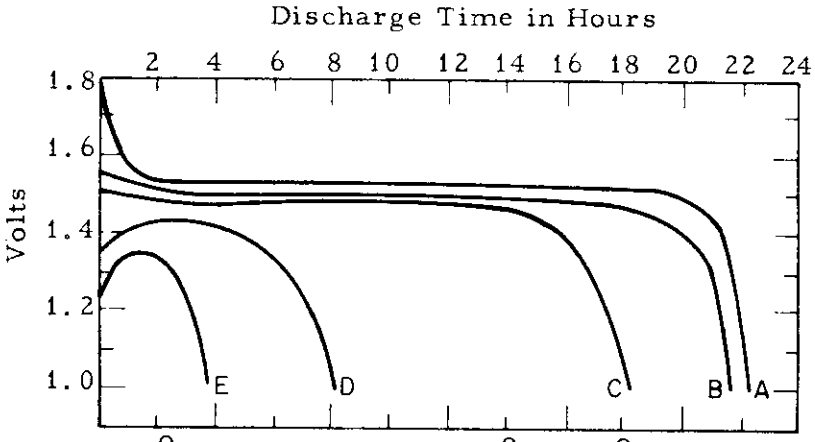

80°F. 24 Hour Rate -40° to 80°F
Applicable to Medium and Low Rate Series.

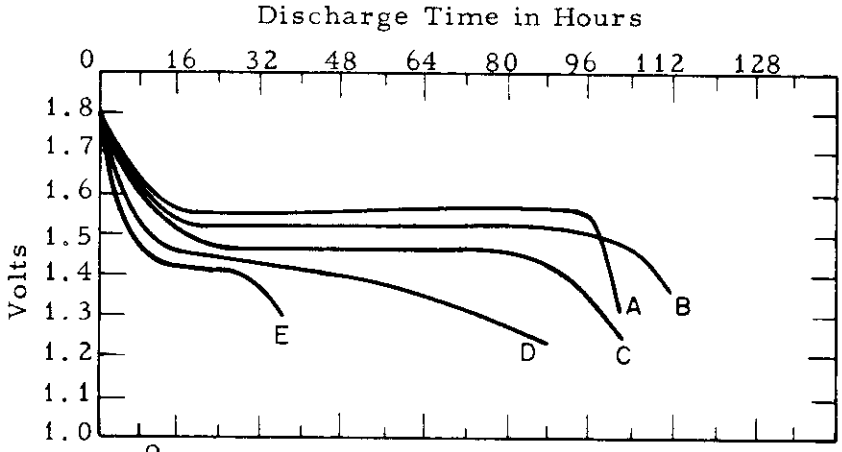

80°F. 100 Hour Rate
Applicable to Low Rate Series

FIGURE VI-A-8 DISCHARGE CHARACTERISTICS - SILVER-ZINC CELLS
Eagle-Picher "A" Series (Ref. VI-A-11)

discharge rate and lower temperature. Nominal open circuit voltage is 1.86 volts; the nominal voltage underload is 1.5 volts; and plateau regulation is ± 2 percent at a fixed load and temperature limits with ± 2 percent. If energy is immediately demanded, a PM type of battery would be used where soak times of approximately 30 minutes are adequate to allow full-scale discharge. Otherwise, soak times of many hours must be allowed.

As shown in Table VI-A-5, cycle life is limited to about 100 cycles at a one-hour discharge. At longer discharge rates and shallow discharges (e.g., 10 percent), a few hundred cycles may be achieved by Yardney's estimate.

The energy output (per unit weight of volume) of the base system is usually much higher than that of the final packaged unit. The extent of energy output reduction is dependent upon the ruggedness required, and low-rate types generally offer the highest energy density. In lab experiments, Eagle-Picher individual cells have achieved 105 watt hr/lb (Ref. VI-A-23), with a mean value for that model of 86 watt hr/lb and a lower third sigma rating of 64.5 watt hr/lb. Capacity is about 80 whr/lb and 5-6 whr/in^3 at discharge rates greater than two hours with present selected commercial primary batteries. This capacity may be increased to 95 whr/lb but is not expected to go higher. The high energy density is achieved only with the larger batteries (e.g., Yardney, PM-200), with density generally decreasing in small sizes. Secondary batteries offer about 60 whr/lb and 4.4 whr/in^3 in certain models but generally fall in the 40-50 whr/lb and 2.5-3.2 whr/in^3 category. The effect of temperature on capacity is shown in Figure VI-A-9.

The active wet life of the Yardney cell ranges from 2 to 18 months, depending on the model and temperatures of operation. Storage characteristics of the Eagle-Picher cell are shown in Figure VI-A-3. Dry shelf life estimates

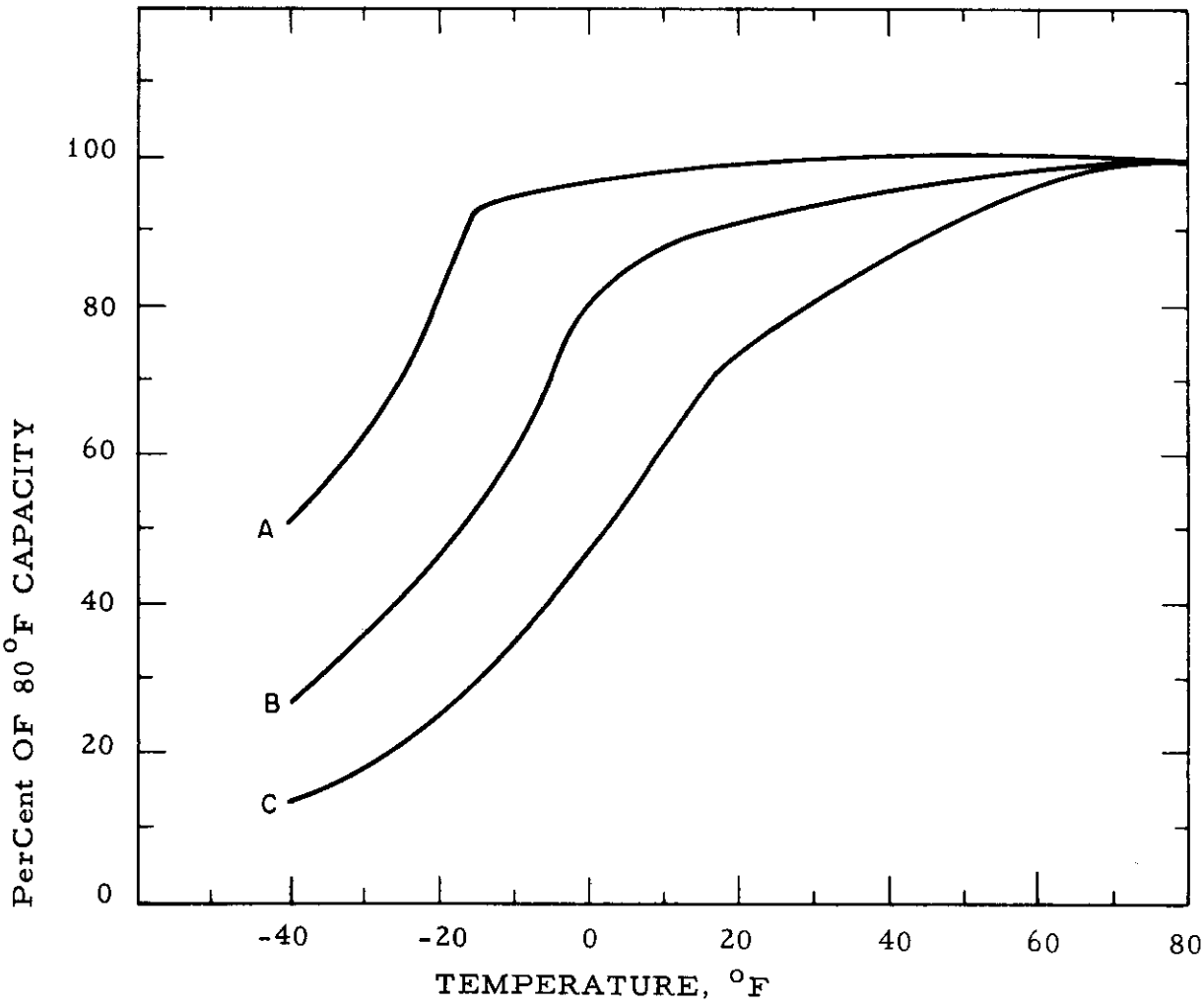

FIGURE VI-A-9 EFFECT OF TEMPERATURE ON CAPACITY AT CONSTANT DISCHARGE RATE
Eagle-Picher "A" and "B" Batteries

Curve A 100 Hr. Rate at 80°F
Curve B 24 Hr. Rate at 80°F
Curve C 1 Hr. Rate at 80°F

are over 5 years at 80°F, 2-1/2 years at 125°F, and 2 months at 165°F for 50-percent capacity retention.

For secondary use, it is not certain whether the battery can be sealed, because appreciable gassing does occur during charge. For a constant charge, it is recommended that voltages be carefully regulated between 1.6 and 1.97 volts. Typical charging characteristics are shown in Figure VI-A-10. The recommended charging rate is 10 to 20 hours, depending on battery type.

The battery is extremely rugged, can be built in a leak proof configuration, and has successfully demonstrated resistance to launch shock and acceleration conditions. Lack of sealing will cause problems under vacuum conditions, but little data are available. The effect of zero gravity is unknown; however, it is expected that the lack of free convection at the plates will create a heavy density of gas particles and loss of performance. Some type of forced convection mechanism may have to be employed. (Ref. VI-A-17)

Complete quantitative data are not available concerning reliability in a space application. The battery used in the Discoverer program successfully completed all functional, environmental, and life tests in a qualification program which utilized 30 cells and 5 complete batteries. Conversations with manufacturers have indicated that reliability is extremely high, and USAERDL tests confirm this opinion (Ref VI-A-6).

The battery performance is affected by the dimensions of the plates. Long, narrow, rectangular plates offer a higher maximum discharge rate than does a square configuration. For many applications, the silver-zinc cell will be required to stand inactive for many months, and an automatic activated primary configuration may be desired. This consists basically of a storage tank, a mechanism for creating internal pressure to force the electrolyte into the cell, a seal which is broken when required, a manifolding system to distribute evenly

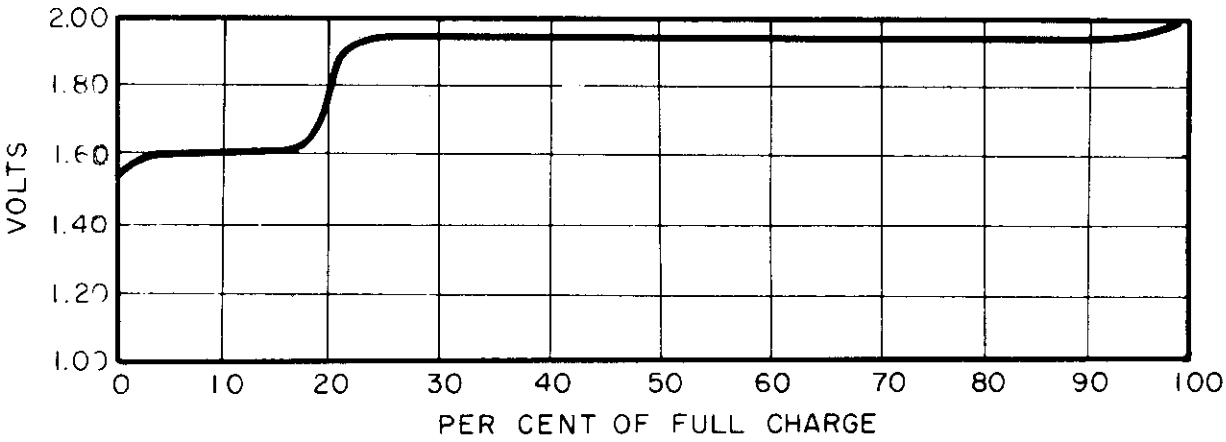

FIGURE VI-A-10 TYPICAL CHARGE CURVE OF THE SILVER-ZINC SYSTEM (VI-A-8)-Yardney

the electrolyte throughout the cell, and a heating system for the electrolyte. (See Ref. VI-A-24) The heavy weight of the activating mechanism increases by roughly 40 percent the primary weight, resulting in an energy density on the order of 40 - 50 whr/lb for long discharge application.

3.0 SILVER-CADMIUM BATTERIES

The silver-cadmium battery shows several advantages in a storage application and offers a compromise between the long cycle life, low capacity of the nickel-cadmium cell and the high capacity, low cycle life of the silver-zinc battery. Lives of 3,000 cycles at shallow discharge and weights of 33 watt hr/lb have been reported (Ref. VI-A-8).

The "Silcad" battery is manufactured exclusively by Yardney Electric Corporation in sizes ranging from 1/10 to 300 ampere-hours. The cell cases are rectangular and employ bakelite, nylon, or other durable plastics. When several cells are used, battery cases made of stainless steel or magnesium are generally provided.

The positive plate is a porous structure which contains graded sintered silver, whereas the negative electrode contains compacted cadmium compounds. A semipermeable membrane separator is used between the two electrodes. In the zinc-silver oxide battery, dendritic electroplating of zinc on the separators may cause damage during the overcharge period. Because of its relative insolubility, cadmium negatives cause no similar separator damage under overcharge or other severe operating conditions. They are not subject to negative corrosion that is evident on zinc electrodes. Consequently, the silver cadmium cell system is more durable than the silver-zinc system due principally to the difference in negative solubility. The electrolyte is a potassium hydroxide solution held within the absorbing separator.

The Silcad battery exhibits a long flat plateau voltage range, as illustrated in Figure VI-A-11. Under given discharge rates and temperatures, the plateau voltage regulation will be about ±5 percent at a fixed load. As shown in Figure VI-A-12, the plateau voltage will drop with a decrease in operating temperature. At a one-hour discharge, open circuit voltage is about 1.25 volts, and load voltage is about 1.15 volts.

Under most conditions of service, the maximum watt hr/lb figure obtainable varies from 24 to 33 and from 1.9 to 2.7 watt hr/ cu in., as shown in Figure VI-A-1. The operating temperature range may be extended up to 165°F and to below -65°F if heaters are provided.

Limited data are available on the cycle life of Silcad batteries. With a discharge depth of less than 10 percent, cycle lives on the order of 2,000 to 3,000 might be expected on the basis of Signal Corps test results. For deep discharges, on the order of 50 percent, a cycle life of 300 to 500 might be anticipated (Ref. VI-A-8). No data on charging efficiency are available.

The battery has an excellent dry storage life. After activation, the discharge retention is also high, with as much as 85 percent of the original capacity remaining after one year's charged wet stand at approximately 70°F (Ref. VI-A-8). The time for 50-percent capacity retention dry storage is about two years at 80°F, 115 days at 125°F, and 58 days at 160°F (Ref. VI-A-18). Dry shelf life is over three years with negligible capacity loss.

On a constant current charge, initial voltage will be 1.2 volts, corresponding to the reduction of cadmium oxide and the oxidation of silver to a lower oxide. After approximately 25 percent of the charge at this voltage, the level rises to 1.45 volts, corresponding to the continued reduction of cadmium oxide to cadmium and the oxidation of the positive anode to the higher silver oxide. When the cell is fully charged, the voltage rises to the gassing

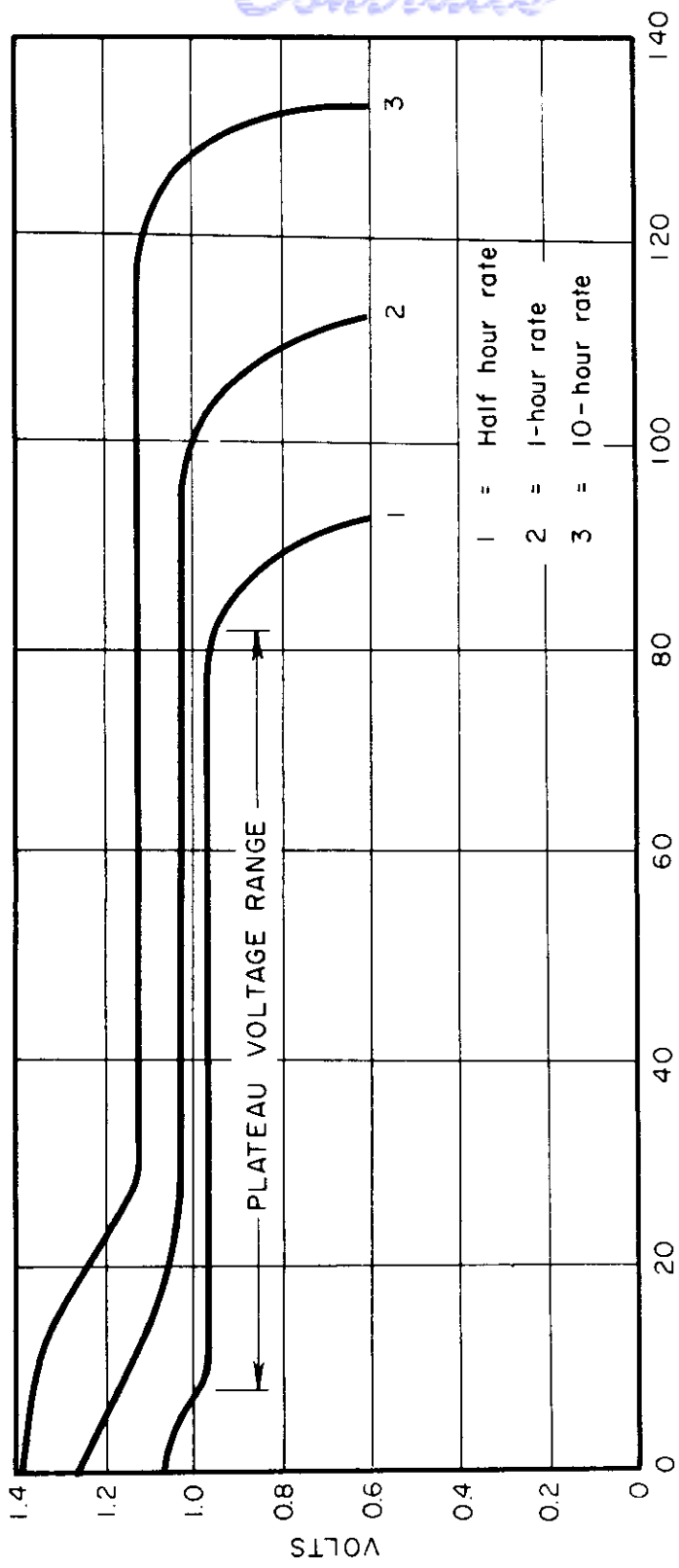

FIGURE VI-A-11 TYPICAL VOLTAGE DISCHARGE CHARACTERISTICS - SILVER-CADMIUM BATTERY (Ref. VI-A-8)

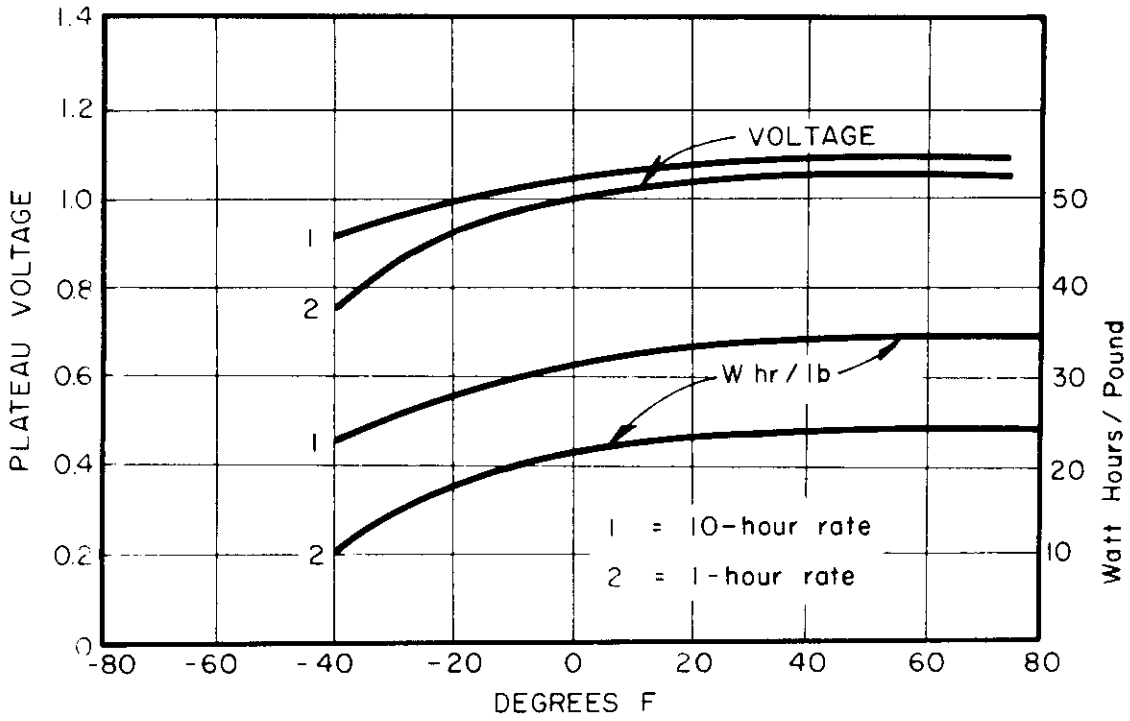

FIG. VI-A-12 TYPICAL EFFECT OF TEMPERATURE ON DISCHARGE VOLTAGE AND ENERGY/UNIT WEIGHT FOR SILCAD CELLS DISCHARGED WITHOUT HEATERS (Ref. VI-A-8)

potential (which is in the neighborhood of 2 volts), and the electrodes gas freely. This voltage rise is demonstrated in Figure VI-A-13. The large abrupt voltage rise at the end of charge is a useful characteristic allowing simplification of charge design. Gassing becomes heavy at about 2 volts but is negligible below this point. Sealing would probably increase the cycle life appreciably, because a loss of water was indicated as a primary limitation.

A constant current charge, therefore, should be held to about 1.55 volts for long cycle life. Recommended charging rate varies from 10 to 14 hours; however, no correlation has been derived between cycle life, charging rates, and charging temperatures.

This extremely rugged Silcad battery has successfully passed missile launch shock and acceleration requirements. The batteries have been made thus far in a leak-proof configuration, and although they have not been sealed, there appears to be no inherent reason why sealing could not be applied. The operating attitude and zero-g environment should make no difference to operation.

Yardney data indicate that during continued cycling the capacity of the battery will drop, as illustrated in Figure VI-A-14 which shows a decrease in capacity as the number of complete discharges and recharges increases.

4.0 MERCURY CELLS

The modern mercury battery consists essentially of a mercuric oxide cathode with a small percentage of graphite, a wound corrugated ribbon anode of amalgamated zinc with approximately 10 percent mercury, and a concentrated aqueous electrolyte of potassium hydroxide saturated with zincate. The electrolyte is immobilized in various forms of cellulosic materials. Accessory parts include a permeable barrier to prevent migration of solid particles from the cathode, electrolyte pads, an inner steel cell case, an outer nickel-plated steel

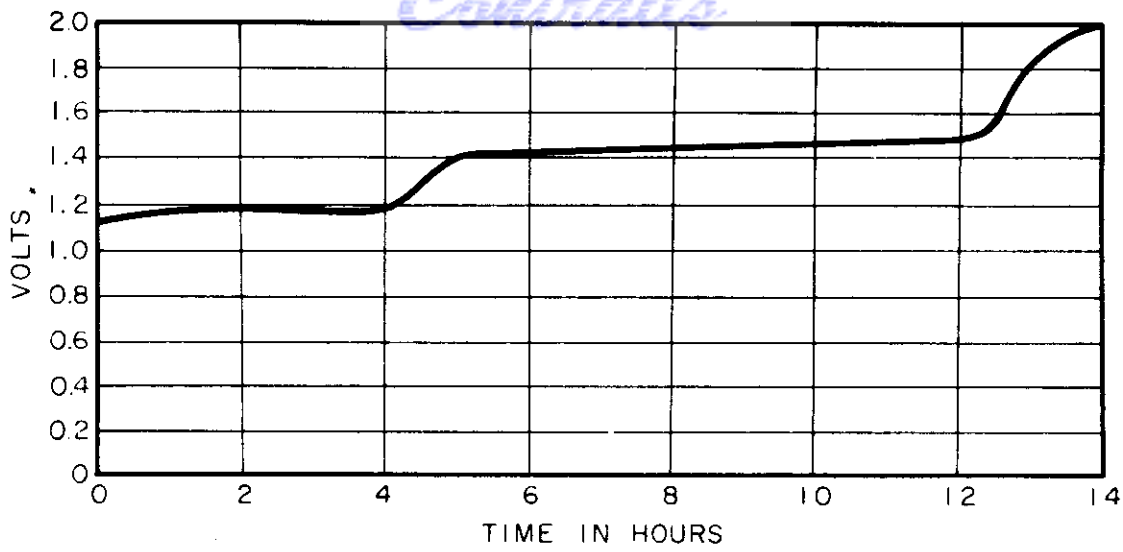

FIGURE VI-A-13 TYPICAL CHARGE CURVE OF A SILCAD CELL

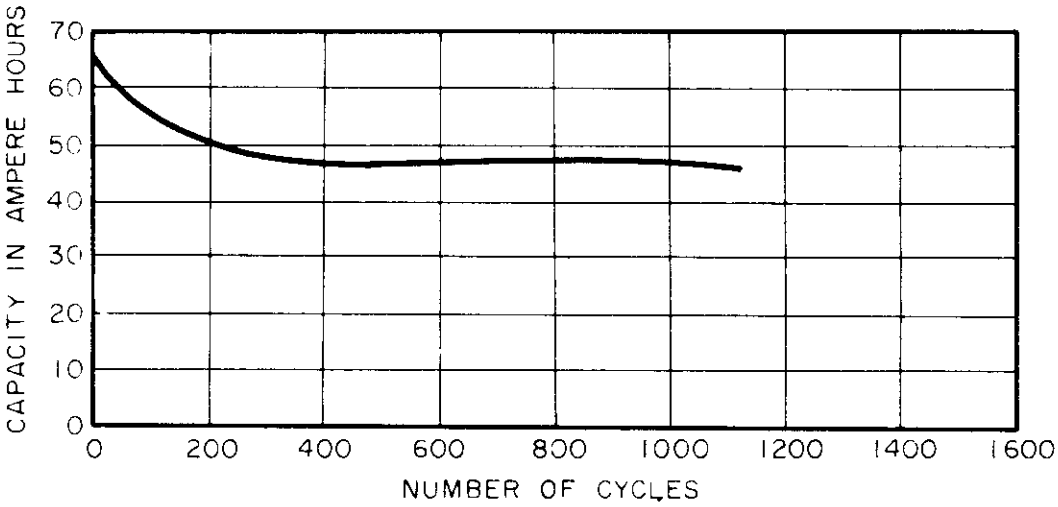

FIGURE VI-A-14 EFFECT OF CYCLING ON CAPACITY OF A SILCAD CELL

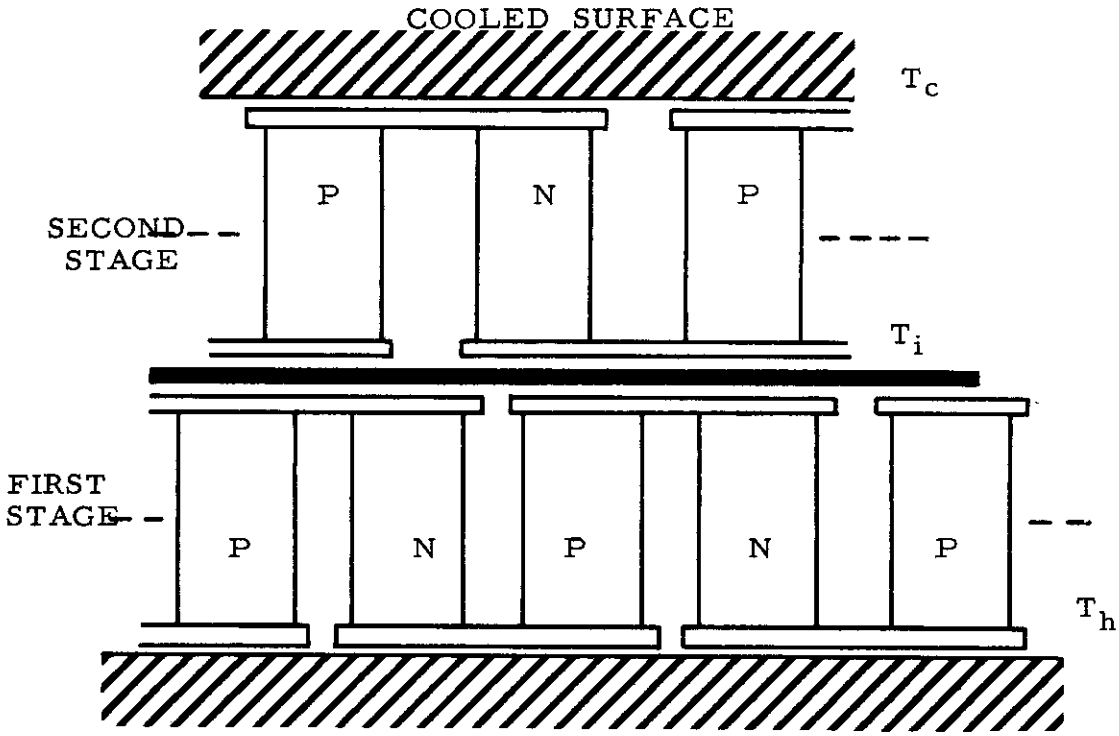

FIGURE IV-A-13 TWO STAGE CASCADED HEAT PUMP

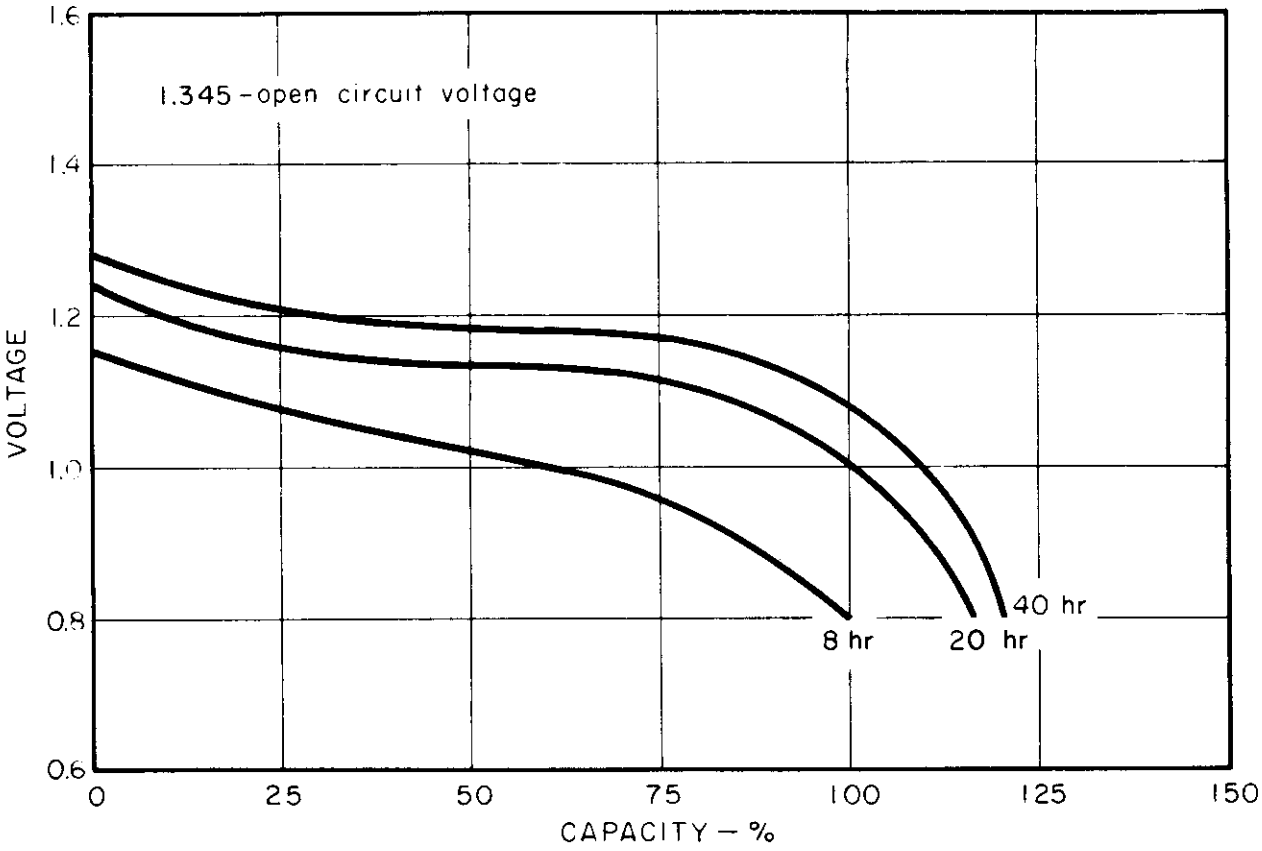

FIGURE VI-A-15 TYPICAL DISCHARGE VOLTAGE CURVES
MERCURY DRY CELL (P.R. Mallory)

Mercury battery storage life is excellent. Data accumulated on the Mallory 4R (Ref. VI-A-20) indicate no loss in capacity at low discharge rates after three years' storage at 70°F. Sixteen percent loss occurred after one year's storage of the 1450R cell at 113°F and a 30-hour discharge.

Mercury cells are rechargeable, contrary to popular opinion. The recommended procedure under repeated recharge service is to discharge them to 50-percent capacity and recharge slowly to 80-percent capacity. Overcharging will destroy the cell, due to gassing. No data are available on cycle life or charging efficiency.

Presently available mercury cells can withstand vibration, shock, or acceleration conditions anticipated in a missile environment. Vacuum conditions do not affect normal operation, nor do zero-g conditions and altitude. Reliability tests on a statistical basis conducted at Signal Corps have indicated that RM-12R and RM-42R (Mallory) have almost absolute reliability. The new low-temperature cells are probably more reliable, since the most advanced manufacturing procedures are used. Special care must be taken in the construction of battery packs, as trouble has been experienced with the ohmic contact between batteries in vibration tests.

5.0 LeCLANCHE, MAGNESIUM AND ORGANIC DEPOLARIZED DRY CELLS

The conventional LeClanche dry cell consists of a cathode of fine manganese dioxide particles mixed with carbon black or graphite, an anode of zinc, and a layer of gelatinous paste or other absorbent material which contains the electrolyte (NH_4Cl-$ZnCl_2$). The container is a drawn zinc cup. At present, the cathode accounts for roughly 1/2 the weight. Theoretical capacity is 140 whr/lb, and 45 whr/lb is achieved at low discharge rates. Nominal open circuit voltage is 1.5 - 1.65v, and opening voltage is 1.25v.

In the last decade, several new developments have resulted in superior performance of dry cells with zinc anodes. For example, cells with potassium hydroxide electrolyte and a manganese dioxide cathode have given superior performance to the LeClanche on heavy continuous discharge rates. This cell contains a powdered zinc anode dispersed in a gel electrolyte and is of an "inside-out" construction.

Theoretically, magnesium is a more attractive anode material for primary cells than is zinc, having a considerably higher reversible electrode potential and more than twice the ampere-hour capacity per unit of weight. The last ten years have seen the coupling of magnesium anodes and aqueous magnesium bromide and magnesium perchlorate electrolytes with such cathode materials as manganese dioxide and a number of organic compounds. Each of the new dry cells has some desirable characteristics and offers the possibility of replacing the conventional dry cells for certain applications. Discharge characteristics for the present LeClanche cell and two new magnesium cells (given in Figures VI-A-16, VI-A-17, and VI-A-18 were obtained by RCA personnel (Ref. VI-A-21).

The capacity in watt hours per unit weight and volume, obtained thus far, is shown by the experimental points of Figure VI-A-16, as a function of discharge time in hours. The manganese dioxide is obtained electrolytically. As shown, with end voltages of 0.9 volts, capacities up to 90 whr/lb have been obtained using M-dinitrobenzine, and capacities up to 70 whr/lb are predicted with MnO_2. The theoretical capacity for these systems is 770 and 193 whr/lb. R.C.A. estimates that the maximum capacity of a practical system will be 130 whr/lb using the organic depolarized system and 90 whr/lb using MnO_2.

Figure VI-A-17 displays typical voltage characteristics of three types of dry cells. The commercial LeClanche cell displays a sloped curve

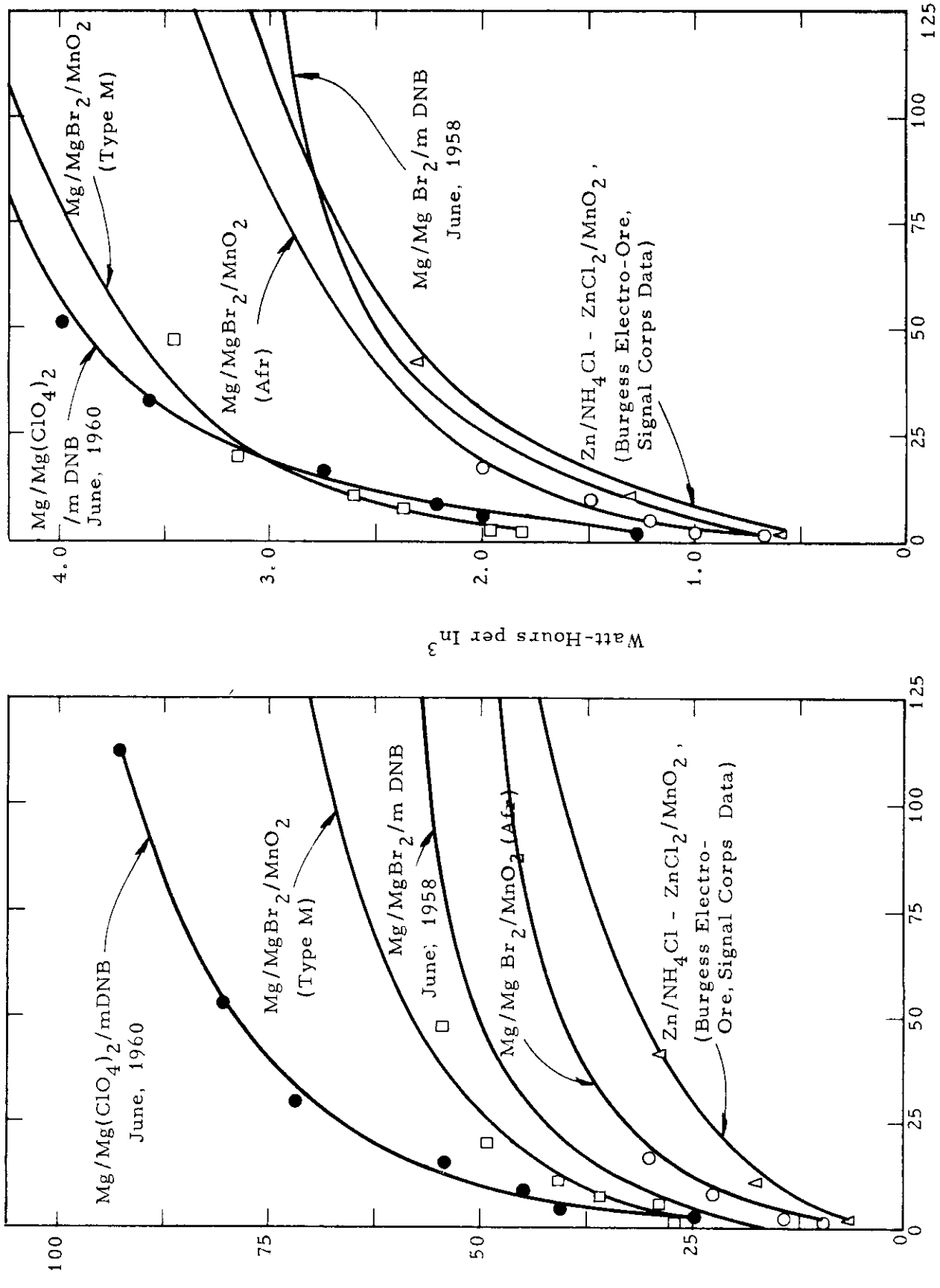

FIG. VI-A-16 CAPACITY IN WATT-HOURS PER UNIT OF WEIGHT AND VOLUME

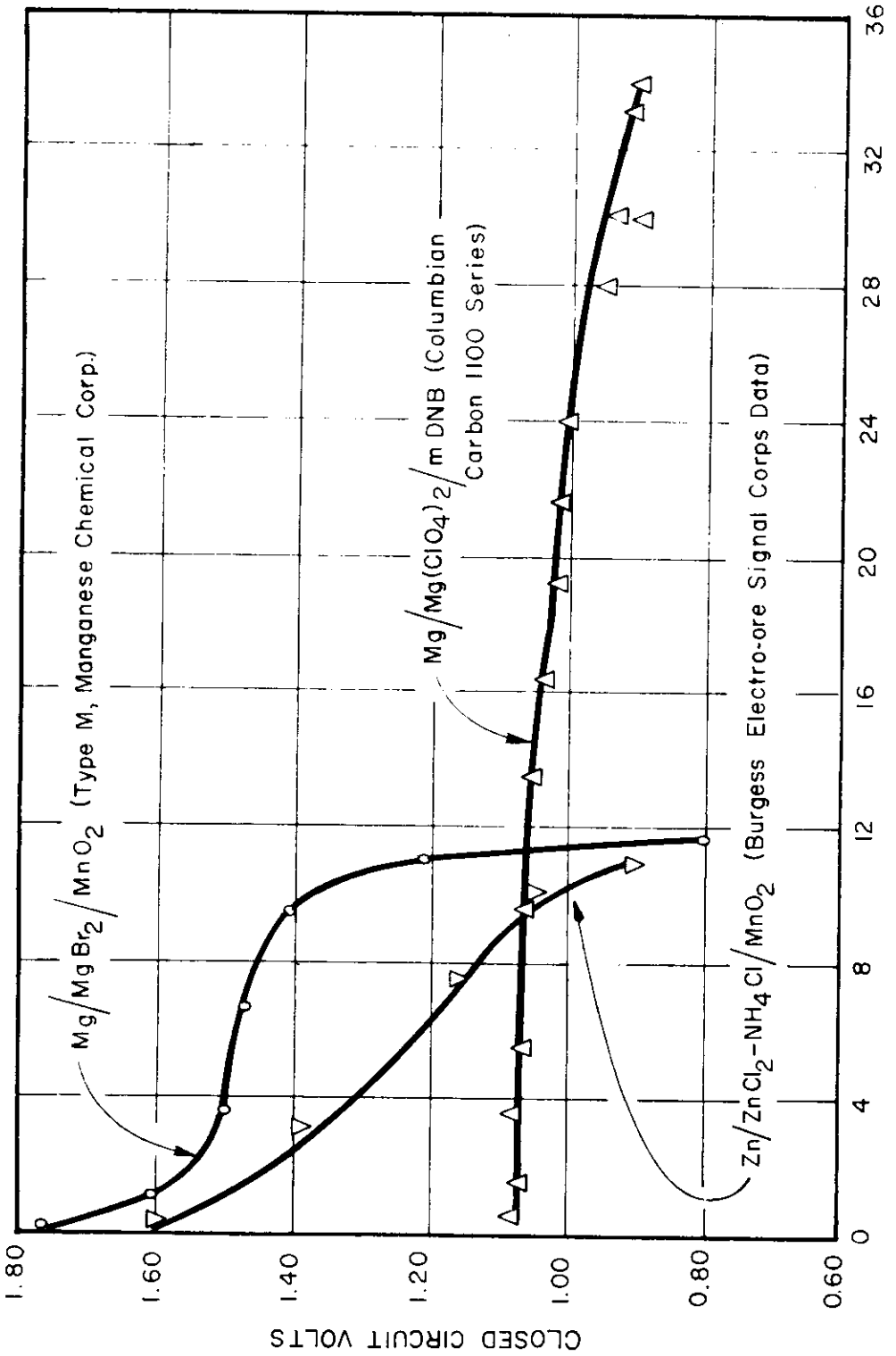

FIGURE VI-A-17 A-SIZE DRY CELLS DISCHARGED CONTINUOUSLY THROUGH 16 2/3 OHMS RESISTANCE

with little or no flat portion and indicates that capacity is a sensitive function of discharge time and required voltage regulation. Capacity of the LeClanche cell increases on intermittent load. Data are incomplete on this aspect of use. The organic depolarized cell displays a relatively flat discharge characteristic, whereas the magnesium cell is intermediate.

Figure VI-A-18 indicates the variation in discharge characteristics with temperature of the organic cell. Conventional LeClanche cells offer the same type of temperature characteristics and will operate in a wide temperature range from -40 to 200°F. At the highest temperature, capacity is almost doubled, but life becomes short.

Although this battery has a slight capability for recharging and cycling, no data in this regard are available. The dry cell is basically a primary or single-cycle battery. It can be operated at any position, and the construction of the commercial cell is such as to provide an inherently high resistance to vibration, shock, and acceleration damage.

The cells using magnesium anodes discussed here are not yet available commercially but are not far from the commercial market.

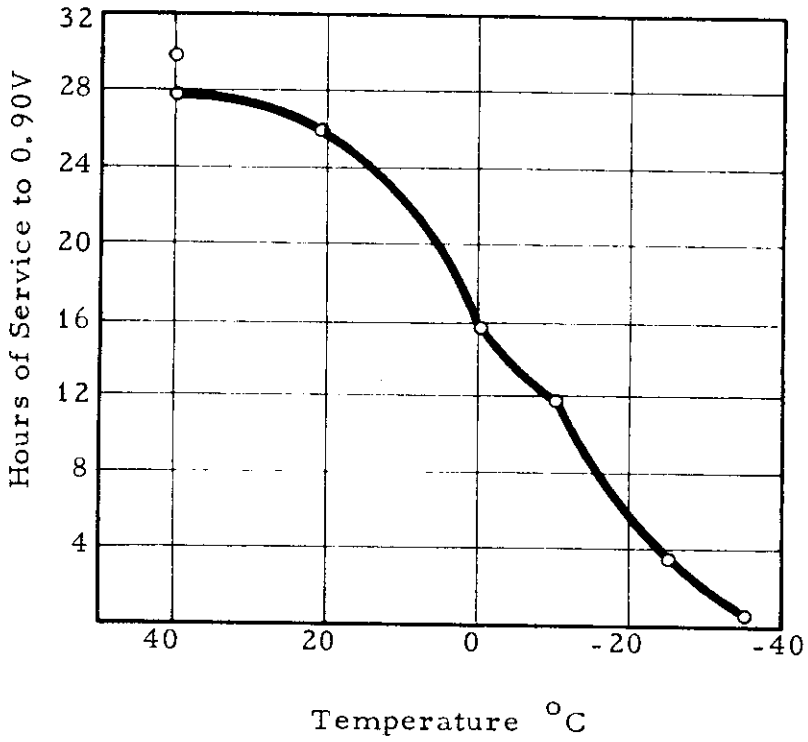

FIGURE VI-A-18 A-SIZE $Mg/MgBr_2$/m-DNB/1:2 DARCO CELLS DISCHARGED CONTINUOUSLY THROUGH 20 OHM RESISTANCE AT VARIOUS TEMPERATURES

REFERENCE LIST

VI-A-1. "An Analysis of Solar Energy Utilization," WADC Technical Report 59-17 Volume II, Sec. 5, February 1959.

VI-A-2. Hamer, Walter J. and Morehouse, Clarence K. "A Review of the State-of-the-Art and Future Trends in Electrochemical Battery Systems," contained in the Proceedings on a Seminar on Advanced Energy Sources and Conversion Techniques, ASTIA AD 209 301, November 1958.

VI-A-3. Proceedings of the Tenth Annual Power Sources Conference, 1956.

VI-A-4. Proceedings of the Eleventh Annual Power Sources Conference, 1957.

VI-A-5. Proceedings of the Twelfth Annual Power Sources Conference, 1958.

VI-A-6. Proceedings of the Thirteenth Annual Power Sources Conference, 1959.

VI-A-7. "Primary Cells Utilizing Organic Compounds as the Active Components," Progress Reports for Signal Corps, Contract No. DA-36-039-SC-78048. Prepared by the Radio Corporation of America, R. Glicksman, Project Director.

VI-A-8. Commercial literature of the Yardney Electric Corporation.

VI-A-9. Commercial literature of P. R. Mallory and Co., Inc.

VI-A-10. Commercial literature of National Carbon Company.

VI-A-11. Commercial literature of Eagle-Picher Company.

VI-A-12. Commercial literature of Sonatone Corporation.

VI-A-13. "The Right Battery for the Job," Electromechanical Design, May 1958.

VI-A-14. Linden, David and Daniel, Arthur F. "New Batteries for the Space Age," Electronics, Engineering Edition, July 18, 1958.

VI-A-15. "Electrochemical Power Moving Fast" Chemical and Engineering News, January 11, 1960.

VI-A-16. Pitzer, E. C. "Higher Energy Batteries," Product Engineering, May 1959.

VI-A-17. Eisenberg, M. "Electrochemical Auxiliary Power Sources for Missiles and Space Flight," Electrical Engineering, January 1960.

VI-A-18. Rappaport, T. J. "Performance Ratings of Secondary Batteries," Electronics, February 19, 1960.

VI-A-19. Daniel, A. F., et al. "Energy in Space: Pounds vs. Power," Chemical and Engineering News, May 18, 1959.

VI-A-20. Clune, R. (Mallory Battery Co.) "Recent Developments in the Mercury Cell." Presented at Fourteenth Annual Power Sources Conference, 1960.

VI-A-21. Lozier, G. S. (R.C.A.) "Organic Depolarized Dry Batteries." Presented at Fourteenth Annual Power Sources Conference, 1960.

VI-A-22. Menard, C. (Gould National Batteries, Inc.) "Electrical Characteristics of Gould Sealed Sintered Plate Nickel Cadmium Batteries."

VI-A-23. "Satellite Auxiliary Power Systems," LMSD-445616, Lockheed Missiles and Space Division, Sunnyvale, California.

VI-A-24. Morse, E. M. (Eagle-Picher Company) "Recent Developments of the Silver Oxide Battery." Presented at Fourteenth Annual Power Sources Conference, 1960.

VI-A-25. Thomas, U. B. (Bell Labs) "Battery Considerations for a Communications Satellite." Presented at A.R.S. Power Sources Conference, September, 1960.

ENERGY CONVERSION SYSTEMS REFERENCE HANDBOOK

Volume VI - Chemical Systems

Section B

PRIMARY AND REGENERATIVE FUEL CELLS

J. Chrisney
Energy Research Division
ELECTRO-OPTICAL SYSTEMS, INC.

Manuscript released by the author
September 1960 for publication in this
Energy Conversion Systems Reference Handbook

WADD Technical Report 60-699

C O N T E N T S

I L L U S T R A T I O N S

TABLES

B PRIMARY AND REGENERATIVE FUEL CELLS

1.0 GENERAL DESCRIPTION

A generally accepted definition of a fuel cell is "an electrochemical device which delivers direct current as a consequence of electrochemical reaction of continuously supplied reactants." In a truly continuous device, reaction products would also be removed continuously rather than allowed to accumulate. Consequently, those fuel cells in which reaction products are absorbed or accumulated in the electrolyte must also have a continuous supply of fresh electrolyte and rejection of spent electrolyte.

Several authors in the past have presented different definitions of fuel cells. For example, W. Ostwald (Ref. VI-B-1) in 1894 defined a fuel cell as a galvanic system producing electrical energy by electrochemical oxidation of carbon with air-oxygen. Such a restriction is rarely accepted today, for even by historical precedence, H. Davy (Ref. VI-B-2) in 1801 and W. R. Grove (Ref. VI-B-3) in 1839 discussed low-temperature hydrogen fuel cells. Some recent authors have applied the term, fuel cell, to devices which would be better classified as batteries, since such devices are self contained and both products and reactants are accumulated or stored in contact with the electrodes.

In view of past definitions of fuel cells and modern usage of the term, it could be enlightening for us to consider some possible variants. Some systems described in recent literature (Ref. VI-B-4) involve incomplete reaction of purified fuel and/or oxidant with product formation on the fuel and/or oxidant side(s) of the electrodes. Consequently, portions of fuel and oxidizer are utilized for transporting product away from the electrodes.

For high efficiency, product separation must be accomplished externally, and separated reactants must be recycled to the electrodes. Other systems (Refs. VI-B-5 and VI-B-6) involve product formation in the electrolyte with external product separation and recycling of electrolyte. Some systems (Refs. VI-B-7, VI-B-8, VI-B-9, and VI-B-10) involve the continuous introduction of one reactant and batch replacement of the other reactant, which may be a metal electrode. Still other systems (Ref. VI-B-11) may involve continuous reaction at electrodes but batch replacement of reactant generators such as potassium or calcium superoxide and lithium hydride or borohydride.

Because of the various combinations of batch and continuous operations in a total system, our definition of a fuel cell as a continuously operated device should be with respect to the immediate vicinity of the electrodes. A further expansion of definition could be made to include the continuous supply of one reactant but batch replacement of the other reactant as long as product removal is accomplished. In this way, we can maintain our definition of a battery as a self-contained, electrochemical device which delivers direct current as a result of electrochemical reaction and in which reactants and/or products are stored in the vicinity of the electrodes.

2.0 PRIMARY FUEL CELLS

Primary fuel cells include all fuel cells in which reaction products are permanently rejected with no attempt at regeneration of fuel or oxidizer from reaction products. Such cells may involve such relatively inexpensive fuels as natural gas (Ref. VI-B-12), other hydrocarbons (Refs. VI-B-13, and VI-B-14), or coal (Refs. VI-B-15, and VI-B-16), which can be supplied more easily from fresh or natural sources than from regeneration. For some applications more expensive primary systems may have merit, i.e., the sodium amalgam-oxygen (Ref. VI-B-17), zinc or magnesium-chlorine

(Refs. VI-B-7 and VI-B-18), or the magnesium-organic oxidizer (Refs. VI-B-8, VI-B-9 and VI-B-10) systems. Naturally, many systems amenable to regenerative operation (discussed in subsection 3.0) may be operated as primary cells.

2.1 Principal Parts

The principal parts of a fuel cell are generally the same as for a battery, i.e. reactants, electrodes, electrolyte, and mechanical encapsulation. In some fuel cells, particularly those with inert electrodes (Ref. VI-B-19), a semipermeable diaphragm will be required for separation of reactants from electrolyte so that chemical reaction can occur only through the electrochemical circuit. In some systems, porous electrodes (Ref. VI-B-20) act as diaphragm separators; in other systems, a reactant (Refs. VI-B-8, VI-B-9, VI-B-10, and VI-B-18) such as magnesium or zinc acts as an electrode. The direct reaction of fuel and oxidant would constitute an internal short-circuit, thereby reducing cell capacity and efficiency. The elimination or minimization of this direct reaction is one requirement for high current efficiency. It is possible that one reactant could diffuse through the electrolyte and reach the wrong electrode but fail to react because of a local polarization or catalytic condition. Such a system could have a current efficiency approaching 100 percent: and, therefore, a semipermeable diaphragm should not be considered a principal part of all fuel cells. To maintain continuously flowing reactant there must also be at least one inlet port and means for replenishment of the second reactant and removal of product.

2.2 Appurtenances

The appurtenances of a fuel cell notably distinguish it from a battery. The continuous operation requirements of product rejection have led to expenditures of much time and effort in different

development programs. In systems with carbonaceous fuel and oxygen with alkaline electrolyte, the carbon dioxide product reacts chemically with the electrolyte, thus requiring spent electrolyte rejection and fresh supply. For gaseous reactants such as hydrogen, oxygen, and chlorine, pressurized cylinders can be used as reactant storage and pressure flow of reactant can be accomplished by proper use of pressure regulators or other control devices. Blowers or compressors may also be used for continuous supply of gaseous reactants to a fuel cell. Liquid reactants or electrolyte may be charged to a fuel cell from collapsible storage chambers by one of three ways: (1) by mechanical drivers to induce collapse, (2) by a piston in cylinder container, or (3) by pumps. For optimum weight and performance, a particular system may include separate control valves on each stream or one control valve for product rejection and pressure balancing devices on storage containers. Those systems involving product formation on the reactant side of electrodes with incomplete reaction require product separators, perhaps centrifugal, and recycling of separated reactant. A fuel cell system may involve product formation and precipitation in a liquid electrolyte, thus requiring an electrolyte pump, filter, scraper, and conveyor for product separation and rejection.

For space applications, fuel cells with high internal resistance must have cooling systems which will maintain the cell within the operating temperature range. For such smaller systems, directly connected radiators are indicated; for rather large systems, coolant loops with cooling channels, pumps, controls, and extended surface radiators may be justifiable. High-temperature fuel cells on intermittent duty may cool below the allowable operating temperature with insufficient mass of insulation.

Start-up heaters may be justifiable with such large high-temperature systems. Naturally, energy for start-up heat would be supplied from another source such as a low-temperature fuel cell which would be too heavy (because of low current density) for scale-up to the full duty cell.

Some fuel cells require phase separation for operation, i.e., gas-liquid, liquid-liquid, solid-liquid, or combinations thereof. For a hydrox cell with water formation on the reactant side of an electrode, the lack of gravity could allow electrode flooding by water. Other cells involve the use of amalgams and aqueous phases with possibilities of amalgam separation and stoppage of electrochemical reaction. For space applications all such bulk multiphase systems would require gravity generation, which could be accomplished by rotation of a cylindrical cell about its longitudinal axis or by tangential injection of a heavy liquid reactant into a cylindrical cell. Consequently, the requirement of gravity generation adds complexities and weight to fuel cells for space applications.

3.0 REGENERABLE FUEL CELLS

Electrolytic batch regeneration of reactants from reaction product indicates the similarity of a regenerable fuel cell to a secondary battery. For space use, thermal and/or electrical energy for regeneration can be supplied by a solar power system when the space vehicle is in an insolation period, and energy must be stored for use in a dark period. For a space vehicle traveling outwards from the earth's orbit, such as a Mars probe, a radioisotope (Po^{210} or Ce^{144}) or nuclear reactor can supply energy continuously to a fuel cell for storage. Thus, the energy stored in the fuel cell can be used intermittently at the rate required for communication, television operation, control devices, etc. Use of the same electrodes for charge and discharge appears,

at first, desirable for a minimum weight design; for some fuel cell designs, such an arrangement is quite possible. However, the use of porous electrodes with gas reactants forming liquid product in the electrolyte may involve a liquid-gas interface within the electrode. On discharge, electrochemical reaction occurs at this interface, and product flows normally into the electrolyte space. Upon attempted charge (regeneration), reactions generating gases can occur on the surface of the electrode, and the regenerated gaseous reactants can remain in the electrolyte space. Consequently, in such regenerable fuel cell systems a second pair of electrodes may be mandatory for acceptable cycle life. The same requirements can also apply to all liquid systems.

3.1 Reactant Separation

In addition to separation from electrolyte, the reactants must be separated from each other and from the electrodes at which they are regenerated. In the absence of gravity, the separation of an immiscible liquid or gaseous reactant from a regeneration electrode can be a severe problem. The separation of a metal anode reactant may be accomplished under conditions yielding a good adherent plate and inhibition of tree growth. Consequently, one could postulate a regenerable fuel cell with a metal anode reactant and an immiscible liquid or gaseous cathode reactant which, upon regeneration, would be separated from a circulated electrolyte by centrifugation or liquid-liquid filtration* The amalgamation process would separate anode reactant from electrolyte upon regeneration in a mercury amalgam fuel cell, for with an alkali metal halide (Ref. VI-B-21) as active ingredient, reduction from aqueous solution would not occur.

In gravity, the separation of a soluble regenerated reactant could be accomplished by fractionation or extraction, but in space,

*Centrifugation theory and design are currently under study (Ref. VI-B-53)

such separation methods appear impractical. In space, use of one electrolyte-soluble reactant could be possible with a circulating system including proper electrical separation. In such a system the reactant would be dissolved in the same solution which holds product in solution in the electrolyte. During discharge, reactant would be depleted during flow past the reactant side of electrodes; product would be formed and dissolved during flow past the electrolyte side of the same electrode. Reactant solution and spent electrolyte solution could be stored in the same cylindrical vessel with a free-moving piston for separation of solutions. Naturally, the other reactant would be easily separable, e.g. an electroplated solid metal.

3.2 Side Reactions

Under regeneration conditions, with a higher applied voltage than that available from fuel cell discharge, the occurrence of side reactions becomes more probable than under discharge conditions. The most probable undesirable side reactions during regeneration are the same as those for many batteries, i.e, hydrogen and/or oxygen formation, commonly called gassing. Local concentration gradients, I-R drops, and chemical polarization (discussed in subsection 4), are causes for high regeneration voltage which may be sufficient for decomposition of water in an aqueous solution. Fortunately, these uncatalyzed gas formation reactions require overvoltages which allow gas-free regeneration at adequate current densities. Side reactions other than electrochemical may also occur, e.g., diffusion of one reactant through a semipermeable membrane separating reactants. With totally different reactant species, such diffusion can cause reduction of capacity, limitation of cycle life, discharge voltage reduction, reduced current density, and possibly catalyst poisoning or overvoltage reduction for a gassing reaction.

3.3 Other Forces for Containment and Separation

For space use, a fuel cell, involving only ionic oxidation and reduction at electrodes, would not require gravity generating equipment but could become diffusion limited, particularly near total discharge. Such a limitation could be more severe if both oxidant and reductant were ions in solution. In a system such as General Electric Redox (Ref. VI-B-19) or Kings College (London) Redox (Ref. VI-B-19), the use of reactant circulating pumps near total discharge could possibly be justified on a weight basis. These circulating pumps might also be used near total charge during the regeneration cycle. Although the withdrawal of extra power near total discharge appears undesirable, the rather high weight of redox solutions could lead to an excessive total weight for a lower depth of discharge and for the same cycle capacity requirement.

The requirement of gravity generation in multifluid fuel cells and rather high weight of aqueous ionic systems leads one to consider use of micro-forces for containment and separation. Such microforces include capillarity and surface tension, interfacial tension, osmosis, adsorption, and barrier diffusion. Although reports of serious development of systems requiring such microforces may not have been published, several intriguing possibilities now present themselves. The use of capillarity appears likely for containment of electrolyte away from porous electrodes for gaseous reactants. A graded porous matrix for absorption of liquid product for gaseous reactants could be much less weighty than gravity generating equipment. Such a matrix, particularly if unsaturated, will act to increase IR drop and charging voltage and decrease current density and discharge voltage. Resistance to bulk flow would also increase for those systems requiring bulk flow now through a porous media instead of an open channel.

Barrier diffusion could be used for separation of mixed regenerated reactant gases in systems designed for missions with long intervals between power demand. By similarity, osmosis could be used for separation of electrolyte from large molecule product, should concentration of product be desirable before regeneration. Reversible adsorption of gases on solids may result in an over-all weight reduction as compared with pressure containers. Electrolytic ion exchange could be used for separate removal of anion and cation product from an electrolyte. Electrolytic oxidation, reduction, and elution of these ions from the ion bed would accomplish the regeneration and separation of reactants for reuse. The sizable number of possibilities and combinations thereof which can effect the required flows, separations, and electrochemical reactions in a gravity-free environment indicates that much research and development remains to be done in the field of fuel cells for space.

3.4 Principal Parts of an Electrolytic Regeneration System

The principal parts of a batch regeneration system consist of an energy source, regeneration electrodes which may be separate from fuel cell electrodes, electrolyte, containers, and controls. The regeneration energy source could be a solar cell system, solar concentrator with thermionic or thermoelectric conversion, radioisotope heat source with thermoelectric conversion, or any sufficient source of direct current at the proper voltage.

The intermittent supply of power from a solar power system necessitates energy storage for use in a dark period. Intermittent power requirements for communication from satellites and space vehicles can best be served by an energy storage device even with a continuous low level power supply such as a radioisotope-thermoelectric converter. The elimination of the energy storage device could lead to excess weight and expense.

Even with a large energy source such as a nuclear reactor, some energy storage would be required for activation and operation of start-up controls if the reactor would be completely shut down during a mission with long intervals between demands for power.

Regeneration electrodes must be operated in a manner allowing separation of regenerated reactants in a sufficiently pure form for adequate electrochemical reaction during discharge of the fuel cell. In a fuel cell with metal anode reactant and a membrane separator the growth of trees during electrode position might be sufficient for puncture of the membrane. Such tree growth can be prevented by rotation of electrodes, a process which has the additional advantage of stirring the solution and thereby reducing diffusional restrictions and concentration polarization. Tree growth can also be inhibited by the addition of large neutral molecules, such as starch or glue, to the electrolysis solution. A poorly adherent or spongy plate of deposited metal reactant could result in physical and electrical separation from the electrode with consequent loss of capacity and the possibility of fouling flow passages and valve seats. A good adherent plate can be promoted by: (1) the proper choice of voltage, current density, and pH (for prevention of hydrogen evolution), (2) choice of complexing anion (which might limit fuel cell voltage), and (3) the addition of a small amount of a large molecule reducing agent such as a substituted hydrazine salt. Other methods of reactant separation may include barrier diffusion, osmosis, adsorption, or ion exchange.

Features of regeneration electrolytes and containers are similar to those of corresponding parts of a primary fuel cell. Some of the regeneration system controls are sufficiently critical to be considered as principal parts. Voltage and current density regulation may be necessary for

prevention of side reactions such as gassing, temperature runaway, possible electrical leakage or other undesirable effects, and for formation of a good adherent coat for electroplating. Circulation or agitation of regenerant solutions near full charge should be accomplished for capacity requirements and alleviation of diffusion limitations.

3.5 Appurtenances of a Regeneration System

Many appurtenances for a regeneration system are also common to the fuel cell, including simple switching devices for reversal of flow from pumps. blowers, compressors, or collapsible storage chambers. For pressure storage of gaseous reactants, the regulators required for fuel cell operation could also serve regeneration. Gravity generating equipment could be a requirement for a regeneration system to be used with a fuel cell which, if primary, would not require gravity. High-pressure storage of gaseous reactants and cryogenic storage of liquified gaseous reactants appear difficult for adoption with regenerable fuel cells for space because of the weight of gravity-generating equipment and refrigeration equipment. Cryogenic storage has the additional disadvantage that, on high power demand, energy must be supplied to the liquified gas reactant for vaporization and heating to reaction temperature.

3.6 Thermally Regenerative Fuel Cells

Another class of fuel cells to be considered are continuously regenerable and therefore operate as energy converters. Operation of experimental calcium and lithium hydride fuel cells with batch regeneration has been described in the literature (Ref. VI-B-20), and designs have been suggested for continuous energy converters. Electrochemical reaction of lithium with hydrogen would occur near 350°C, the product lithium hydride would flow to a regenerator where decomposition would occur near 900°C, and the gravity-separated reactants would return to the fuel cell electrodes for repeated reaction. Other hydrides and some heavy metal iodides may be used in a similar manner but at somewhat different temperatures.

Very recent reports (References VI-B-50, VI-B-51 and VI-B-52) of experimental and theoretical studies of hydride fuel cells indicate numerous difficulties. Materials and methods of construction occasionally induce equipment failures and consequent delays in acquisition of meaningful data. The selection of an electrolyte for fuel cell operation at a reasonably low temperature appears critical. A low (288°C) melting eutectic mixture of the chlorides of lithium, sodium, rubidium, and cesium appears attractive except for the low (0.8 percent) solubility of lithium hydride therein. Consequently, a large mass of electrolyte must be heated to a high temperature in the regenerator, heat exchanged with electrolyte from the fuel cell, and cooled to fuel cell operating temperature. With the simplifying assumptions of equal heat capacities and negligible endothermicity for dissociation of lithium hydride the thermal efficiency of such a system could approach 0.8 percent of the Carnot efficiency. In addition, the metathesis of potassium chloride and lighium hydride would allow

dissociation of potassium hydride and the very small E.M.F. from reaction of potassium metal and hydrogen in the fuel cell. Sodium and cesium hydride formation would also lead to low E.M.F.'s from the fuel cell.

The use of filtration of lithium hydride from such a molten salt electrolyte and subsequent conveyance and regeneration of lithium and hydrogen from this precipitate would add complexity and operational difficulties to this cell. The possibilities of electrode fouling and line plugging by precipitated lithium hydride could limit the reliability for space or military use. An electrolyte of calcium, strontium, and barium salts should not have a severe voltage limiting effect because of the higher decomposition temperatures and free energies of formation of the hydrides but efficiency limitations due to a low lithium hydride solubility could still be severe. A pure lithium hydride electrolyte would require fuel cell operating temperatures above 680°C because of melting point requirements, and would be operable only at a rather low voltage per cell because of the low reaction free energy change at this temperature.

Heavy metal iodide systems are also not free of difficulties. The decomposition mechanism in the regenerator may involve sub-iodide formation with only partial liberation of free iodine for reaction in the fuel cell. One effect of this would be a reduction in efficiency, perhaps to 1/3 of Carnot efficiency, similar to the efficiency reduction in the lithium hydride cell because of the low solubility of lithium hydride in the mixed chloride electrolyte. Materials of construction and limited voltages combined with high equivalent weights are also sources of difficulty for these heavy metal iodide systems.

Perhaps the only conclusion to be drawn from such brief qualitative analyses is that more research and development is needed before judgement of any kind should be expressed. Our knowledge of non-aqueous chemical systems is quite limited at best, and many systems with hard-to-handle

or expensive materials yield meaningful data only to the most persistent investigators.

A concentration cell can also be postulated as thermally regenerative for the circumstance in which a current-carrying ion would have a vast change in chemical activity through an operable temperature interval. Such thermally regenerable fuel cells naturally must compete with other thermal energy converters such as thermionic and thermoelectric devices. The optimization of an overall system design for a Venus or Mercury space probe would include consideration of solar concentrator weight with temperature and heat availability so that with future developments any one of these systems could be indicated by specifications.

3.7 Photochemical Regenerative Fuel Cells

A continuously regenerable photochemical fuel cell may be available for distant future use. A non-toxic fuel cell for normal temperature use in a manned space vehicle might be satisfied by the ferrous ion-thionine system (Ref. VI-B-21). Under solar radiation, the thionine is reduced to leukothionine, and ferrous ions are oxidized to ferric. Separation of reactants is accomplished by diffusion of small ferric ions out of a starch paste electrolyte. The reverse reaction occurs electrochemically in the dark. Another system under investigation is the nitric oxide-chlorine system (Ref. VI-B-22) in which the product nitrosyl chloride is decomposed photochemically and reactants recombine electrochemically. Investigation of photochemical synthesis of H_2O_2 and combined thermo-photochemical decomposition of sulfur trioxide is also underway (Ref. VI-B-54). Today, photochemical systems have low efficiency, but future development combined with particular specifications may offer use for photochemical fuel cells.

4.0 THEORY OF ELECTROCHEMICAL REACTIONS

4.1 Thermodynamics

In any chemical reaction proceeding spontaneously, a decrease in free energy must occur. From an isothermal reaction this free energy change is related to the enthalpy change, temperature, and entropy change by the equation:

$$\Delta F = \Delta H - T\Delta S$$

which is most useful for isobaric reactions. Since enthalpy, H, is related to internal energy, E, by

$$H = E + PV$$

the free energy change may be expressed by

$$\Delta F = \Delta E + \Delta PV - T\Delta S$$

For electrochemical application, the work content is a main concern. The isothermal change in work content (Helmholtz Free Energy) is

$$\Delta A = \Delta E - T\Delta S$$

so that

$$\Delta F = \Delta A + \Delta PV$$

From the first law of thermodynamics the change in internal energy for a process, whether it proceeds reversibly or irreversibly, is

$\Delta E = Q - W$ and $\Delta A = Q - W - T\Delta S$ for reversible conditions,

but since

$$Q = T\Delta S$$

it follows that

$$-\Delta A = W_r$$

For the isothermal process, therefore, the maximum work from a process is the decrease in work content, A. Such is the case for a reaction carried out reversibly at constant volume as in many fuel cells. The relation of free energy change to total reversible work may be expressed as

$$-\Delta F = W_r - \Delta PV$$

This relation becomes useful under isobaric conditions so that

$\Delta PV = P\Delta V = W_p$, the reversible work of expansion

against a constant external pressure, P. Thus, under isobaric conditions the maximum net useful work of the system becomes $W_r - W_p = -\Delta F_p$. For a fuel cell with no volume change at constant pressure, e.g., a redox cell, the work of expansion becomes zero so the work equation in ΔF reduces to the work equation in ΔA.

Because of widespread use of combustion processes and internal combustion engines, it has become common for thermal efficiencies to be based on the ΔH rather than ΔF or ΔA. A comparison of fuel cell efficiencies based on ΔH could be somewhat misleading,because the maximum useful work is limited to $-\Delta F$ upon which fuel cell efficiencies should be based for comparison.

In a galvanic device such as a battery or fuel cell, the electrical work is represented by

$$W_e = nFE$$

Where E is the electromotive force of the cell, F is Faraday's equivalent, and n the number of gram equivalents reacting. With application of a back emf such that current flow is negligible, the reaction is carried out reversibly, the work is at a maximum, and therefore E is also a maximum, E^o. For

an isothermal and isobaric reaction the decrease in free energy is

$$-\Delta F = nFE^{o}$$

while at constant volume, the decrease in Helmholtz free energy is

$$-\Delta A = nFE^{o}$$

So far, all ΔF's, ΔA's, and ΔH's, have been used in reference to reaction with unit chemical activity of products and reactants at all times but at isothermal reaction at the temperature of the reaction. Since thermodynamic functions are tabulated for specific temperatures and pressures, the variations of some functions should be mentioned. For the constant volume process

$$\left(\frac{\partial A}{\partial T} \right)_V = -S = \frac{A - E}{T} ,$$

For the isobaric process

$$\left(\frac{\partial F}{\partial T} \right)_p = -S = \frac{F - H}{T} ,$$

and for the isothermal process

$$\left(\frac{\partial A}{\partial T} \right)_T = -P \text{ and } \left(\frac{\partial F}{\partial P} \right)_T = V ,$$

4.2 Chemical Activity

Thus, for evaluation of the fuel cell emf from thermodynamic data the proper function should first be evaluated for the temperature and pressure of reaction. The variation in emf with chemical activities should next be evaluated from the Nernst equation,

$$E = E^{o} - \frac{RT}{nF} \ln Q$$

where Q is the product of the activities (or fugacities) of products divided by the product of activities of reacting substances, each activity raised to that power whose exponent is the coefficient of the corresponding substance in the balanced chemical equation. Thus Q has the form of the equilibrium constant, but the selected activities are not necessarily at equilibrium conditions. The number of chemical equivalents or Faraday's of electricity involved in the chemical equation is represented as n. The occurrence of absolute temperature in the Nernst equation compensates in no way for the change of emf with temperature for the ΔF or ΔA should first be established at reaction temperature.

In a practical fuel cell with flowing reactants, a concentration change may exist across each electrode. Thus, the applicability of theoretical equations could be limited to point conditions. However, it is usual for inlet and outlet concentrations (activities) to be used in the Nernst equations for establishment of an ideal emf for use in efficiency determinations. For some cells, effectively pure reactants (as gases) will flow through porous electrodes, or plated metal anodes will be present so that chemical activity across an electrode surface or cross section will be effectively constant.

The estimation of chemical activities for use in thermodynamic calculations can be accomplished through the medium of activity coefficients, defined as the ratio of chemical activity to molality, $\gamma = \frac{a_+}{m_+}$. It has been observed as an empirical fact that, in a mixture of conducting salts, the activity coefficient of a salt is affected by the average ionic strength, μ, of positive and negative ions. The ionic strength is defined as

$$\mu = \frac{Z_+^2 \, m_+ + Z_-^2 \, m_-}{2} \qquad \text{or} \quad \mu = 1/2 \, \Sigma \, m_i \, Z_i^2$$

where Z is the charge on the ion in question and m_i is its molar concentration. The Dehye-Hiickel theory (Rev. VI-B-25) supplies the limiting relationship for dilute solutions. For a single ion in dilute solution

$$\log \gamma_i = -0.505 \, Z_i^2 \, \mu^{1/2}$$

and for the mean chemical activity of a salt

$$\log \gamma = -0.505 \, Z_+ \, Z_- \, \mu^{1/2}$$

The activity coefficient, γ, becomes equal to unity at infinite dilution for all types of salts, and different authors have used different extrapolation methods. Thus, an alternate relation (Ref. VI-B-26) is

$$\log \gamma = -0.505 \, Z^2 \quad \frac{\mu^{1/2}}{1 + \gamma^{1/2}}$$

which corresponds to an approximate average of curves for several salts at low ionic strength. Thus, the variation in potential as a function of ionic strength becomes

$$E = E^{\circ} + 0.05914 \, \Delta Z^2 \, (0.505 \quad \frac{\mu^{1/2}}{1 + \mu^{1/2}})$$

for which E° is the thermodynamic potential without regard to solution ionic strength. For more concentrated solutions, as is usual in fuel cells, the mean activity coefficients are almost invariably much higher than predicted by the limiting law, particularly for non-associating species. The well-known exception of sulfuric acid to the limiting law can be explained by associated complex ions, even in dilute solution. For these concentrated solutions, therefore, empirical tabulations of activity coefficients are most

useful even if data are supplied for different salt systems, for by theory, activity coefficients of an active species will remain constant in different salts of the same ionic strength.

For non-ionizing species, as those present in a hydrocarbon fuel cell, the activity coefficients may be estimated from an integrated form of the Gibbs-Duhem equation (Ref. VI-B-26a).

$$N_1 \left(\frac{\partial \ln \gamma_1}{\partial N_1} \right)_{T,P} + N_2 \left(\frac{\partial \ln \gamma_2}{\partial N_2} \right)_{T,P.} + \ldots = 0$$

For non-electrolytes which do not associate or interact (i.e., do not form hydrogen bonds), the Van Laar (Ref. VI-B-27) equation is an acceptable integrated form of the Gibbs-Duhem equation

$$\log \gamma_1 = \frac{A_{1-2}}{\left(1 + \frac{A_{1-2} N_1}{A_{2-1} N_2} \right)^2}$$

$$\log \gamma_2 = \frac{A_{2-1}}{\left(1 + \frac{A_{2-1} N_2}{A_{1-2} N_1} \right)^2}$$

for binary systems. For non-regular solutions, the Margules equations should be used since they are the integrated form of the Gibbs-Duhem equation for the more general case. (Ref. VI-B-28). The Margules equations for binaries are a pair of exponential series of unlimited numbers of terms. Fortunately,

two terms are sufficient for most applications and can be expressed as:

$$\log \gamma_1 = N_2^2 \quad A_{1-2} + 2N_1 (A_{2-1} - A_{1-2})$$

$$\log \gamma_2 = N_1^2 \quad A_{2-1} + 2N_2 (A_{1-2} - A_{2-1})$$

where N's are mole fractions and A's are the end values of the activity coefficient curves and therefore not independent. For symmetrical systems $A_{1-2} = A_{2-1}$ and the Margules equations may be simplified to

$$\log \gamma_1 = AN_2^2 \text{ and}$$

$$\log \gamma_2 = AN_1^2$$

From these relationships the whole equilibrium diagram can theoretically be constructed from one reliable equilibrium measurement. Actually, several points of data should be available so that an investigator can choose the integrated form best suited to the system in question. Margules relationships for ternary (Ref. VI-B-29) and quaternary systems have been published and, as expected, are much more complex than the binary equations.

4.3 Polarizations

There are several polarizations which restrict an operating cell E. M. F. to a value less than the theoretical value as calculated from thermodynamic functions and the Nernst equation. First, a true open circuit E. M. F. can be less than theoretical because of a reaction mechanism polarization. This is exemplified by limitations of oxygen electrodes to a peroxide potential rather than the full oxygen potential. Presumably, an ozone electrode would exhibit similar behavior if reduction past oxygen were attempted.

Although many authors have included reaction mechanism polarization with activation polarization, a quantitative comparison of different cells with and without reaction mechanism polarization would require unrealistic values of exchange current density, I_o'. The exchange current is the current flowing across unit area of electrode in each direction at the reversible potential where activation polarization becomes zero.

The general quantitative expression for current density as a function of activation polarization is, (Ref. VI-B-30)

$$I'_{As} = I_o' e^{\frac{\xi\eta F}{RT}} - I_o' e^{\frac{(\xi-1)\eta F}{RT}}$$

where η is the activation polarization, volts, and ξ is the fraction of overpotential assisting the direction of the overall reaction. For the special case of a small activation polarization ($\eta < 0.02$ volt), simplification will yield

$$I_{As}' = \frac{I_o'\eta F}{RT}$$

and the neglect of reaction mechanism polarization could be misleading. For a higher activation polarization ($\eta > 0.05$ volt), the well-known Tafel equation applies

$$\eta = a + b \log I_{As}'$$

where a is $\pm$ (2.303 RT/ξF) log I_o' and b is 2.303 RT/ξF. The exchange current, I_o', thus can be determined for an electrode system without reaction mechanism polarization.

For a high polarization over a short range of current density, the activation polarization is approximately linear with current density,

$$\eta = a' + b' I_o'$$

where a' and b' are empirical constants. This third case is the equivalent of expressing any curve as a series of short straight lines; therefore, theoretical significance should be nil. In all cases the true, rather than projected, area has been considered for current densities so that direct application to physical cells should be made only for equivalent roughness and porosity.

Ohmic polarization in a cell is due to the internal resistance of the electrolyte and is generally linear with current density. High concentrations, thinness, and high temperature usually contribute to reduction of ohmic polarization. However, those fuel cells which must carry product from the electrolyte vicinity must have sufficient electrode spacing that precipitation or excessive dilution does not occur. Also, at high current densities, concentration polarization can be limiting if internal ohmic resistance is too low.

From the foregoing principles and relationships and with minimal data, the performance of a fuel cell can be theoretically estimated. First the ΔF^o for an isobaric process or ΔA^o for a constant volume process can be selected for the cell reaction from tables of thermodynamic functions. Then the selected function should be corrected for the desired steady-state operating temperature and pressure of the cell. The activity coefficients of reactants and products should next be ascertained. An experimental activity coefficient will be required but the extrapolation

to operating conditions is possible by proper consideration of ionic strength. Activity coefficients with concentrations should next be inserted in the Nernst equation for estimation of the reversible E. M. F. of the cell. Reaction mechanism polarization can be estimated from thermodynamic functions for intermediate reaction steps. From knowledge or estimates for exchange current, I_o, and reaction assistance, ξ, the activation polarization can be estimated. Ohmic polarization can be estimated from electrolyte resistivity and cell geometry.

The foregoing procedure is obviously simplified and is also dependent on a few points of data which may not be available. Consequently, empirical test results must remain as an acceptance criterion. The occurrence of side reactions, overvoltage, catalysis, poisons, promoters, and, at high current densities, concentration polarization, all add complexities to this simplified procedure.

Concentration polarization is the result of rapid electrode reaction with depletion of active species in the immediate electrode vicinity. As reactant molecules diffuse to the electrode surface, steady state reactant and product concentrations limit cell potential as predicted by the Nernst equation. For fuel cells with gas flow through porous electrodes, diffusion of gas reactants may be limiting or dilution of electrolyte with product may be the limiting feature.

These polarizations are presented graphically in Figure VI-B-1 (Ref. VI-B-31), ion membrane cell, Figure VI-B-2 (Ref. VI-B-32), stannous ion-bromine cell, and Figure VI-B-3 (Ref. VI-B-32), general.

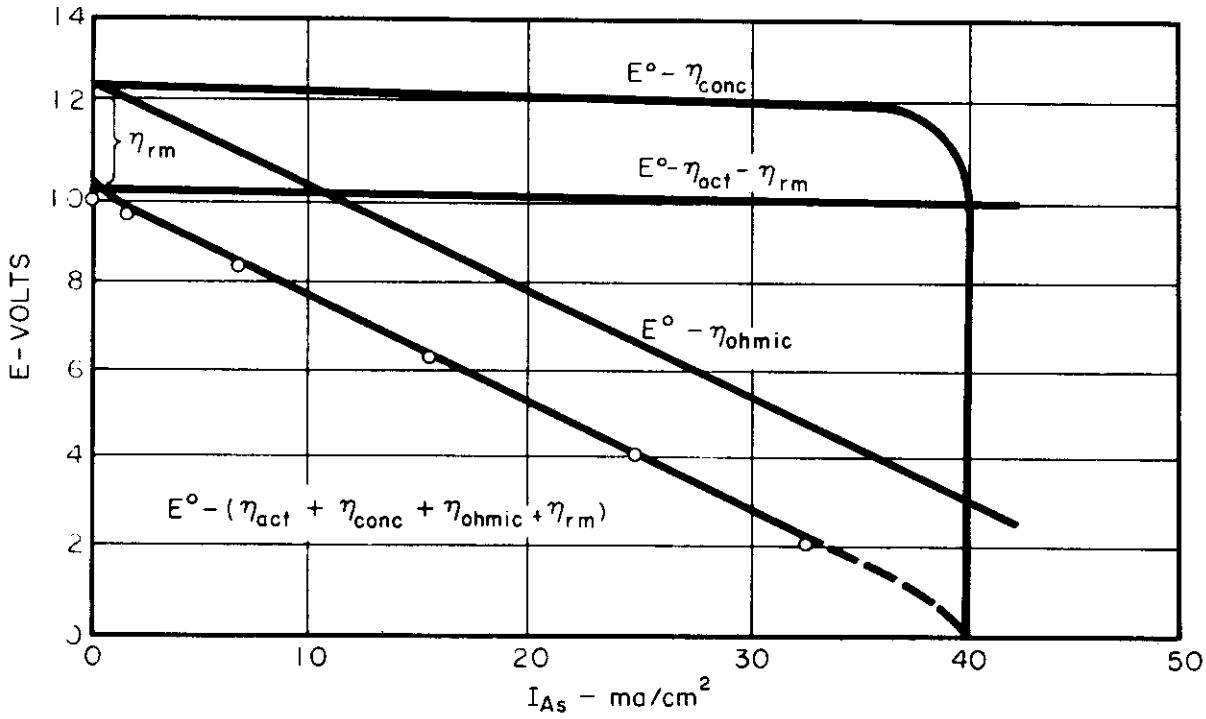

FIGURE VI-B-1 POLARIZATION CURVES - ION MEMBRANE CELL

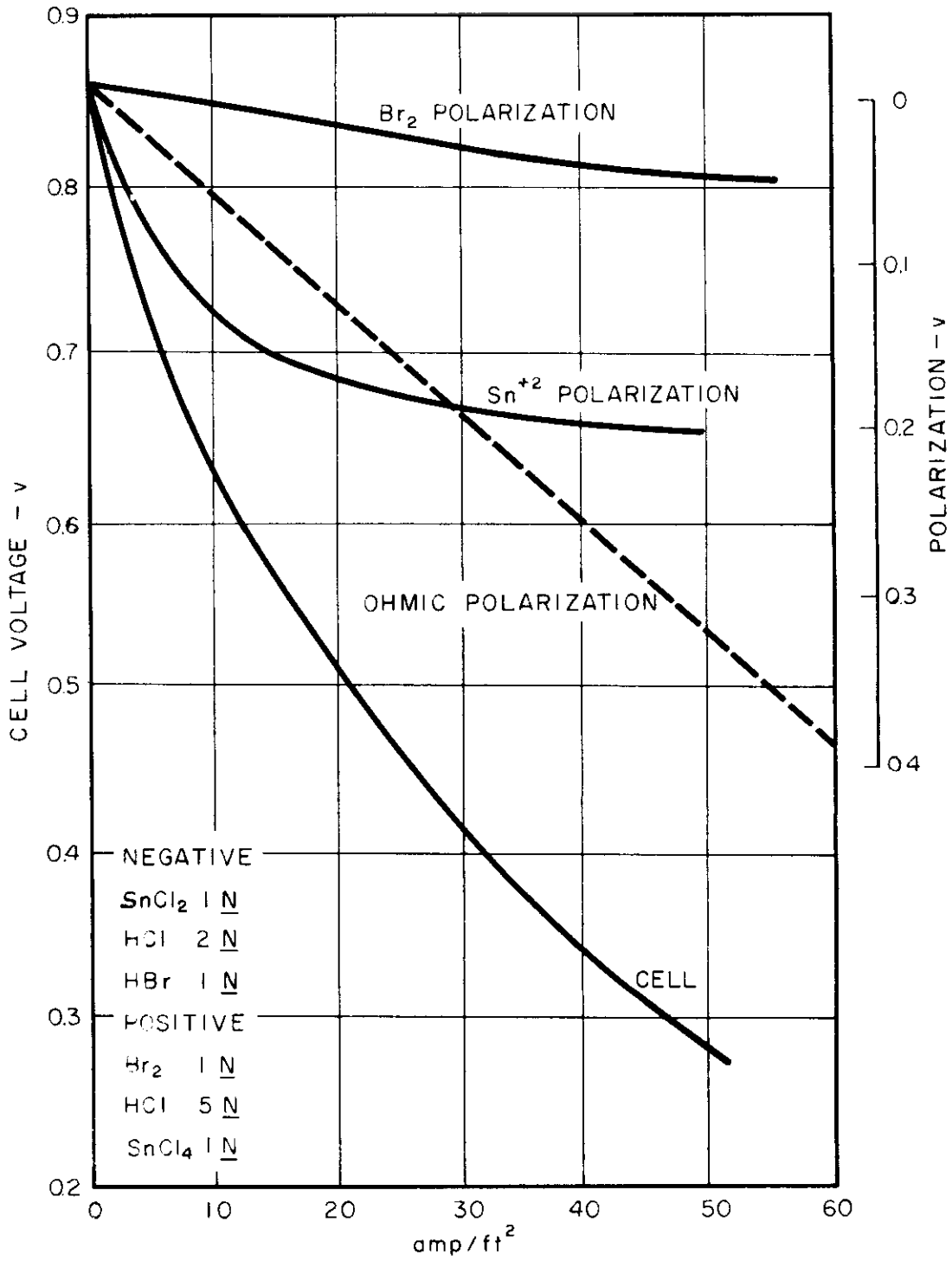

FIGURE VI-B-2 POLARIZATIONS IN STANNOUS ION - BROMINE CELL

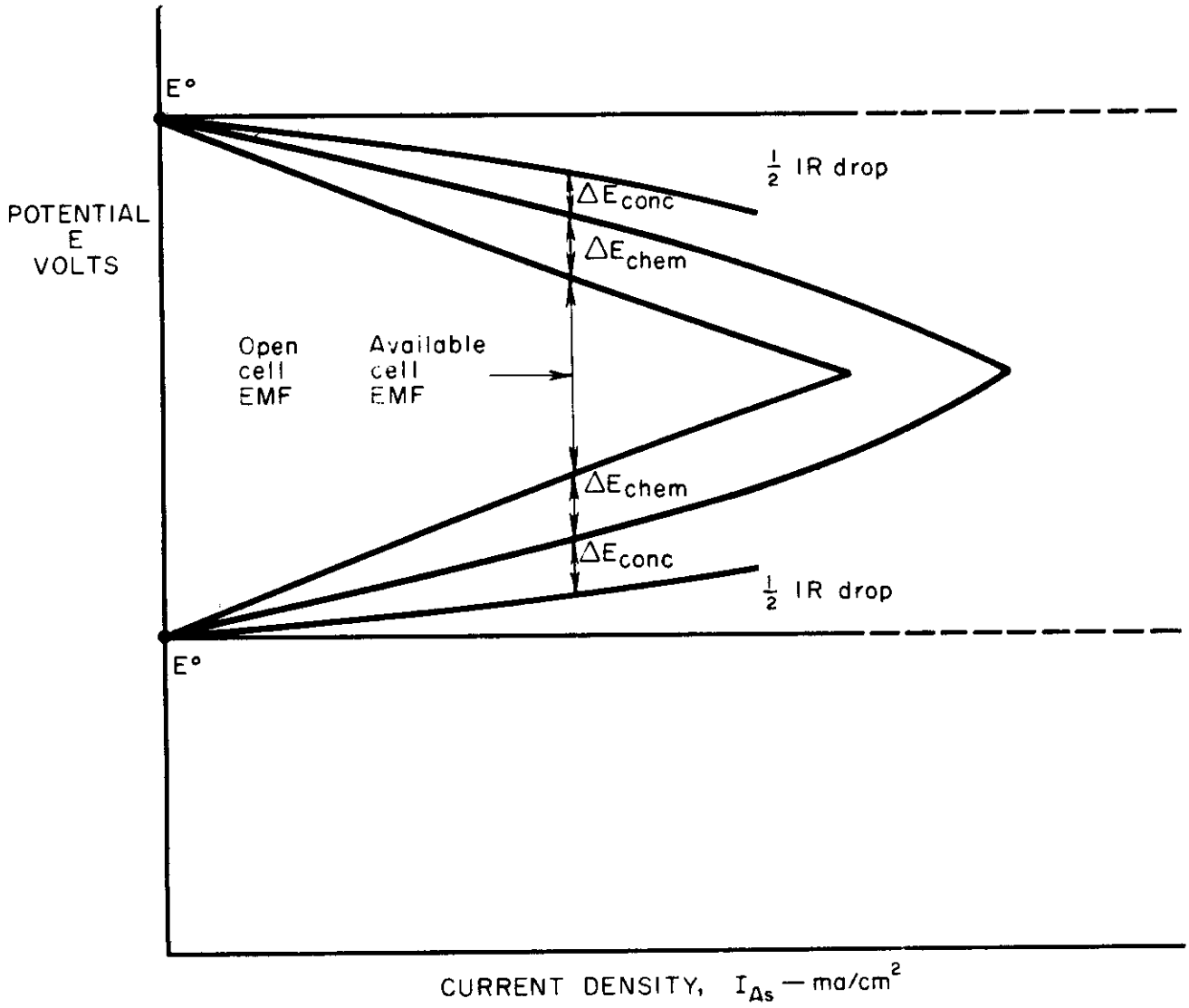

FIGURE VI-B-3 FUEL CELL POLARIZATIONS

4.4 Overvoltage

The form of activation polarization known as overvoltage occurs in heterogeneous electrochemical reactions involving a gas, solid electrode, and generally a liquid electrolyte. An excess voltage (over the equilibrium value) is required for the electrolysis of hydrogen from acidic solutions. The overvoltage depends on the element used as cathode, its physical condition, and the current density. For example, at 100 ma/cm^2 in 1M sulfuric acid, the overvoltages of hydrogen on aluminum, shiny platinum, and platinum black are 1.0 volt, 0.29 volt, and 0.04 volt, respectively. Hydrogen overvoltage increases with current density and decreases with rising temperature, the change being 0.02 to 0.03 volts per 10°C rise.

Reaction mechanism can help explain the slowness of many hydrogen reactions. The reduction of a single hydrogen ion must result in a single hydrogen atom, the standard potential for which is

$$H^+ + e^- \rightarrow H \qquad E^\circ = -2.10 \text{ volts.}$$

This high potential barrier has been subjected (Ref. VI-B-33) to quantum mechanical treatment for probability of leakage of an electron across the potential barrier. The possibility of surface reaction of atomic hydrogen with the metal electrode leads to the conclusion that greater stability of the surface hydride will reduce both the equilibrium potential and also the overvoltage. Thus, the advantages of a hydride-forming electrode for overvoltage reduction appear to be cancelled by simultaneous reduction of equilibrium potential. However, for a regenerable fuel cell, the reduction of discharge potential is balanced by the reduction of charge potential (for weight of regeneration system), so the reduction of overvoltage is a substantial net gain. The decrease of hydrogen ion concentration has little effect on over-

voltage until preponderance of hydroxide ion changes the surface compound, perhaps to hydroxide.

Overvoltages are high for pure metal electrodes in electrolysis of oxygen even from 1M potassium hydroxide. Even with platinum black electrodes, best for pure metals, oxygen overvoltage is 0.64 volts at 100 ma/cm^2 in 1 M KOH. Explanations of such high overvoltages include formation of free hydroxyl, OH, (Ref. VI-B-34), hydrogen peroxide formation from free hydroxyl (References VI-B-35 and VI-B-36), or formation of atomic oxygen (Ref. VI-B-37). The possibility of hydroxide, oxide, or peroxide formation with the metal electrode adds complexity, particularly if competing or parallel mechanisms occur simultaneously. The formation of perhydroxyl (Ref. VI-B-38), HO_2, probably occurs away from the electrode so would not contribute to overvoltage but could affect reaction rate in alkaline solution.

4.5 Catalysis

Catalysis is the usual weapon against inefficiencies caused by overvoltage. Experimentally determined rate equations (Ref. VI-B-39) demonstrate that two active sites are needed for chemisorption by hydrogen in catalyzed porous carbon electrodes. Similar results are presented for an oxygen electrode. Other investigators (Ref. VI-B-40) have considered activation polarization and chemisorption in more detail. Theory and reasons for selection of a particular catalyst have also been published (Ref. VI-B-41).

The dependence on catalysis for long-term fuel cell operation can be unfortunate because of poisoning. An amount of a poison too small for formation of a monomolecular layer can make an electrode completely inoperable because of inactivation of active centers. The presence of minute amounts of sulfides, for example, can completely poison platinum black catalysts for chemical or electrochemical reactions. Consequently, the selection of a fuel cell with difficulty poisoned catalysts for electrodes

could be better than the selection of easily poisoned electrodes. Absence of catalyst dependence, of course, would contribute to a high reliability.

Catalyst promoters increase the activity of a catalyst, perhaps by formation of active centers, by intensifying the activity of existing active centers, by shortening time of occupation of active centers by reaction mechanism products, or by some combination thereof. Thus can be predicted a fuel cell to which is supplied reactants with minute amounts of promoters for absorption by catalyzed electrodes for improved operation over the unpromoted reaction.

For continuously regenerable fuel cells, the addition of a homogeneous catalyst would be desirable because of the resulting reduction of activation energy for both fuel cell and regeneration reactions. The consequent reduction in weight of both the fuel cell and the regenerator and the possible slight reduction of regeneration temperature would increase efficiency. Since equilibrium is not affected by catalysis the regenerator temperature could not be reduced below the temperature required by equilibrium for regeneration.

5.0 EXAMPLES OF PRIMARY FUEL CELLS FOR SPACE

For space use, fuel cells must be selected primarily on the basis of weight and reliability. Low equivalent weights and the state of development of hydrogen oxygen fuel cells essentially restrict consideration to these cells for primary use as contrasted to other fuel cells. F. T. Bacon has published (Ref. VI-B-5) analyses of the Bacon fuel cell in comparison with other energy sources. His comparison is presented as Figure VI-B-4. The low weight of the Diesel engine is explained by the supposition of atmospheric oxygen.

G. E. Evans, of the National Carbon Company, has published (Ref. VI-B-20) weight-time analyses of the N. C. C. hydrogen-oxygen cell, as shown in Figs. VI-B-5 through VI-B-7. His demonstration of current density influence on weight is illuminating but the examples of "fairly flat" current density curves may apply only to longer operating periods, particularly for other fuel cells.

From assumptions similar to those of Evans, optimum current densities can be estimated for minimum system weight at any cell endurance requirement. In reference to plots of cell voltage versus current density (with IR drop included), it can be noticed that many fuel cells exhibit linear relationships over a fairly broad operating range. Thus, within limits, the voltage-current density equation becomes

$$E = C - b I_{As}$$

where C and b are empirical constants and I_{As} is the current density in milliamperes per square centimeter. For multicell systems of reasonable size the assumption of a constant weight (constant gravity) per unit of

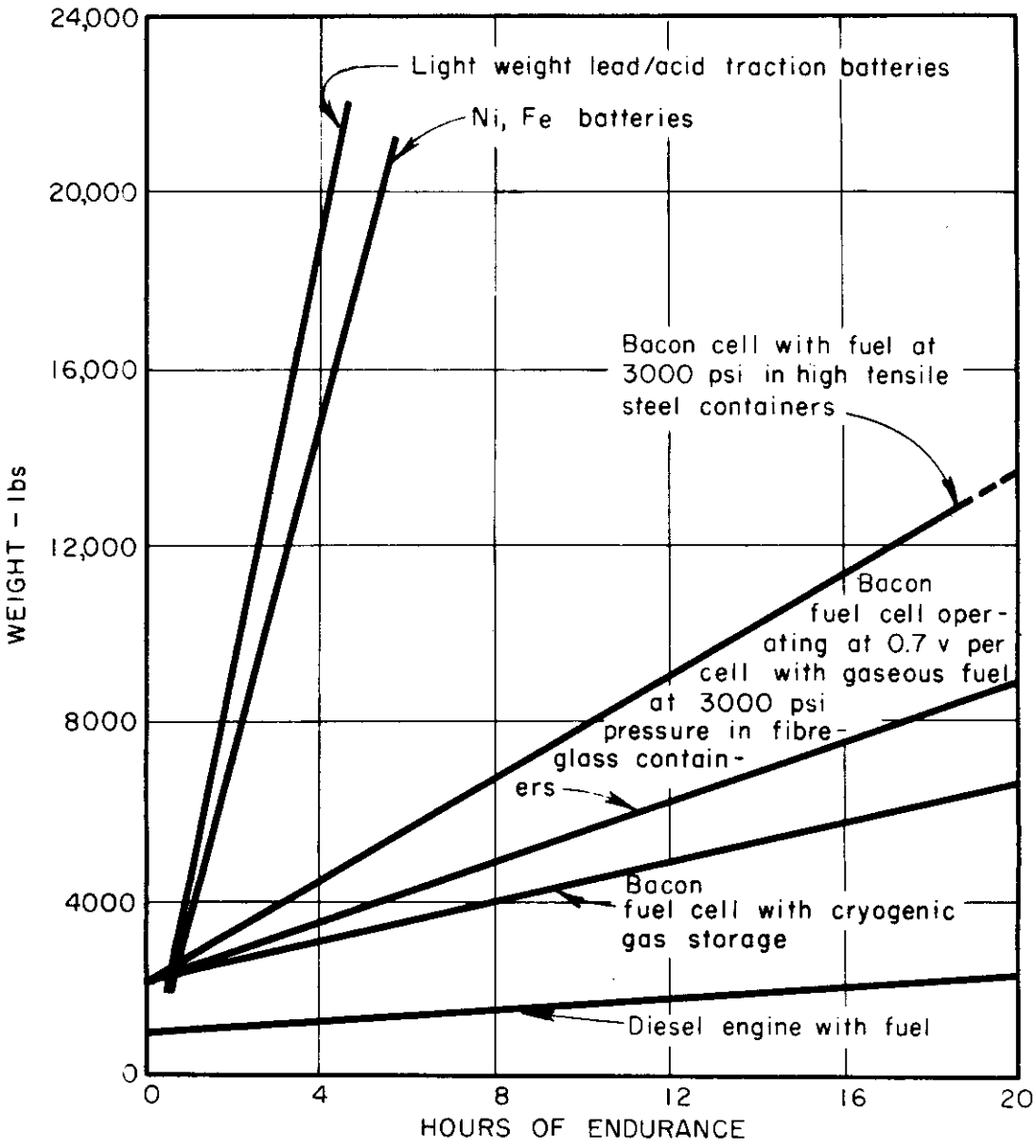

FIGURE VI-B-4 SYSTEM WEIGHT FOR 44KW BACON CELL

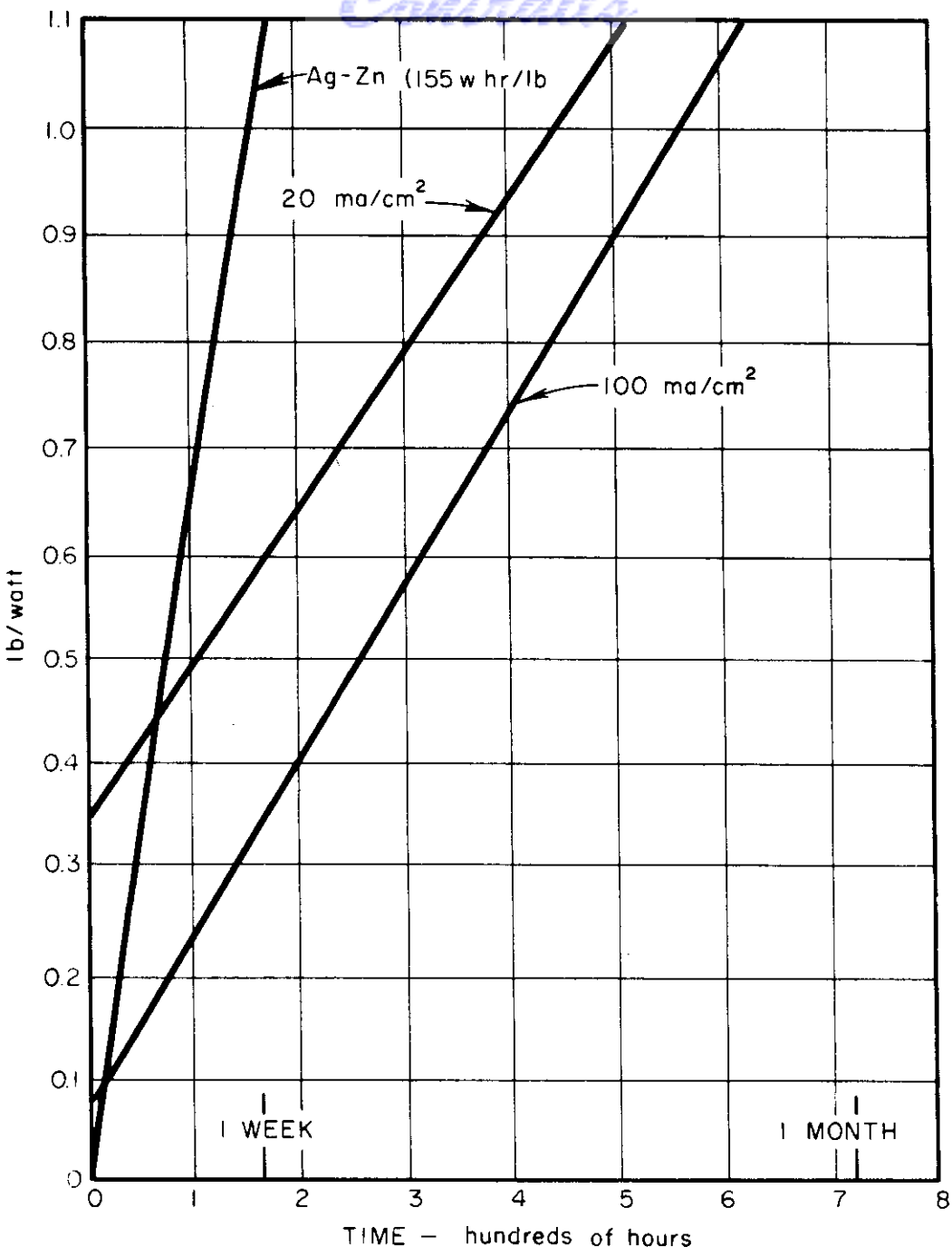

FIGURE VI-B-5 SYSTEM UNIT WEIGHT - SHORT ENDURANCE: N. C. C. HYDROGEN-OXYGEN CELL - ACCORDING TO EVANS

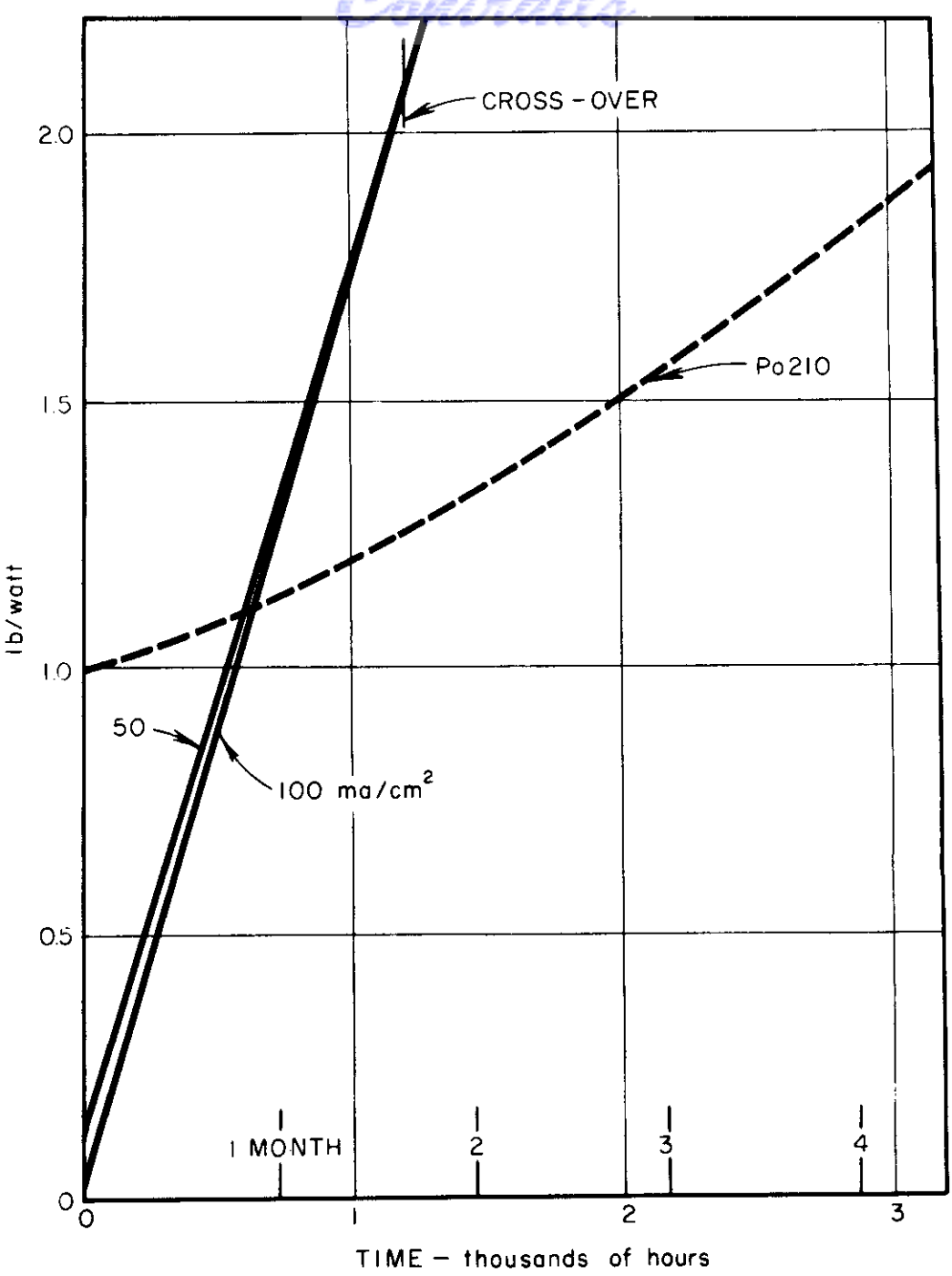

FIGURE VI-B-6 SYSTEM UNIT WEIGHT - INTERMEDIATE ENDURANCE: N. C. C. HYDROGEN-OXYGEN CELL - ACCORDING TO EVANS

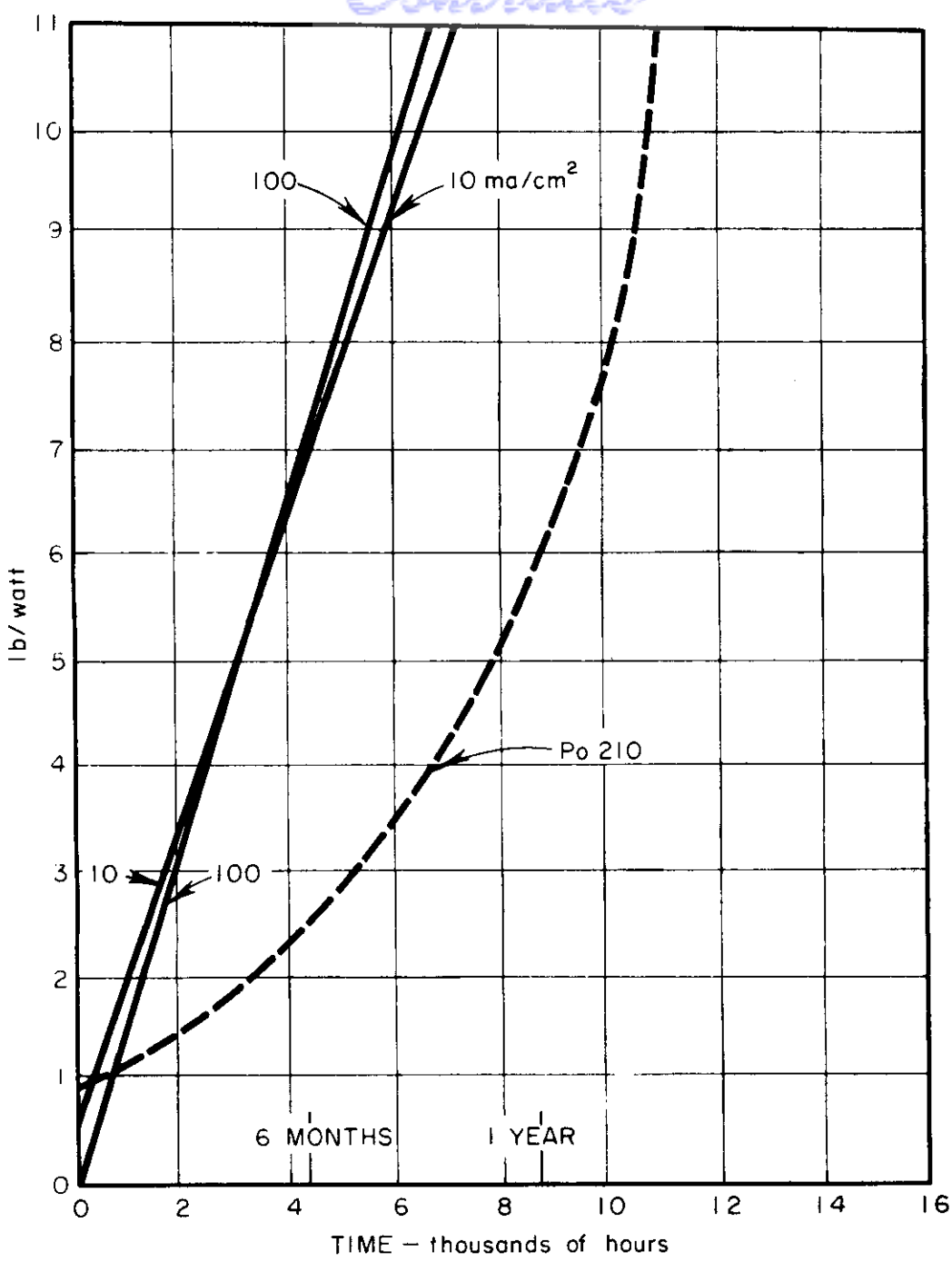

FIGURE VI-B-7 SYSTEM UNIT WEIGHT - LONG ENDURANCE: N. C. C. HYDROGEN-OXYGEN CELL - ACCORDING TO EVANS

electrode area is made. Thus, characteristic of cell construction, a equals the cell weight in pounds per 1000 cm^2 electrode area. Then

$$\frac{a}{CI_{As} - b I^2 As}$$ weight cell, encapsulation, and fixed electrolyte per watt

In consideration of equivalent weight of reactants, storage vessels, and appurtenances and with Faraday's constant and current efficiency, a new cell constant is defined.

Γ = ampere hour per gram of reactants, storage, and appurtenances, and for weight unit conversion β = lb/g = 0.002206.

With cryogenic storage of hydrogen and oxygen the use of two pounds total weight per pound of reactants by G. E. Evans was admittedly better than existing cryogenic storage weights, so the assumption of 2-1/2 pounds total weight per pound of reactants is used here. From mission specifications we can select

θ = hours of fuel cell operation

and therefore:

$$\frac{\beta \theta}{C\Gamma - b\Gamma I_{As}}$$ = weight of reactants, storage, and appurtenances per watt

and

$$\frac{\text{Weight of total system, lbs}}{\text{Watt}} = \frac{a}{CI_{As} - b I^2 As} + \frac{\beta \theta}{C\Gamma - b\Gamma I_{As}}$$

$$= \frac{a}{E I_{As}} + \frac{\beta \theta}{\Gamma E}$$

From this equation it is observed that the total system weight per watt is divided between the cell exclusive of reactants and the reactant system

exclusive of the mechanical cell. By differentiation with respect to current density and setting of the derivative equal to zero, the solution for I_{As} is

$$I_{As} = \frac{-a\,\Gamma\,b + \sqrt{a^2\Gamma^2b^2 + a\,\beta\,F b\,\theta\,C}}{\beta\,b\,\theta} = \frac{1-a\Gamma}{\beta\theta} + \sqrt{\left(\frac{a\Gamma}{\beta\theta}\right)^2 + \frac{a\Gamma}{\beta\,\theta}\;\frac{C}{b}}$$

where I_{As} is now optimum with respect to the total weight of the fuel cell system including cell, reactants, and storage. For a minimum weight cell, without regard to reactants and storage, the optimum current density expression reduces to zero over zero. Subsequent use of differentiation results in

$$I_{As} \longrightarrow \frac{C}{2b} \text{ as } \theta \longrightarrow 0$$

and

$$E \longrightarrow \frac{C}{2} \text{ as } \theta \longrightarrow 0$$

Since C is the linearly extrapolated open circuit voltage the use of the experimental open circuit voltage approaches exactitude only for a cell with negligible activation polarization. For practical applications the use of minimum cell weight would lead to excess weight because of inefficient consumption of reactants at reduced voltage even with constant current efficiency. As the time of operation increases without limit, the weight must also increase without limit, but weight per watt-hour approaches a finite limit. By algebraic manipulation

$$\frac{lb}{watt\ hr} = \frac{a}{EI_{As}\,\theta} + \frac{\beta}{E\Gamma}$$

and as θ increases without limit

$$\frac{lb}{watt\ hr} \rightarrow \frac{\beta}{E_{oc}\Gamma} \text{ and } \frac{watt\ hr}{lb} \rightarrow \frac{E_{oc}\Gamma}{\beta}$$

where E_{oc} is now the experimental open circuit voltage. With the concept of constant wattage requirement, only the reactant system weight would

decrease as the required operating time decreased and the lower limit of zero is set for watt hours per pound. With both upper and lower limits now established, a few graphs of watt hours per pound are presented in Figure VI-B-8. Each point along each weight curve is estimated from use of the optimum current density for the particular operating time for each fuel cell. However, particularly for short operating periods, a calculated optimum current density was higher than published values would allow because of concentration polarization. For such cases, the maximum published current density was used.

For a few points at very long operating periods, the calculated current densities would allow a higher cell E. M. F. than predicted from the linear relationship because of decreased activation polarization. For these few points judgment was exercised for choice of E and I_{As}, values for which fell between constant current density at higher E. M. F. and constant E. M. F. at higher current density.

Such a simplified analysis as this could be severely misleading without qualifications. Reliability and cost have been ignored; and, indeed, such considerations could completely nullify the choice of a particular fuel cell system otherwise appearing best. The assumptions of constant weight per unit electrode area and constant storage weight per unit reactant weight become worse for smaller units, and even the values chosen could be altered appreciably for a particular design. No attempt was made for selection of standard sizes or standard voltages although such selections could alter conclusions, particularly for smaller cells or short operating periods. The effect of a weight allowance for phase separation is assumed to be similar for all three primary cells so that qualitative comparison could remain valid.

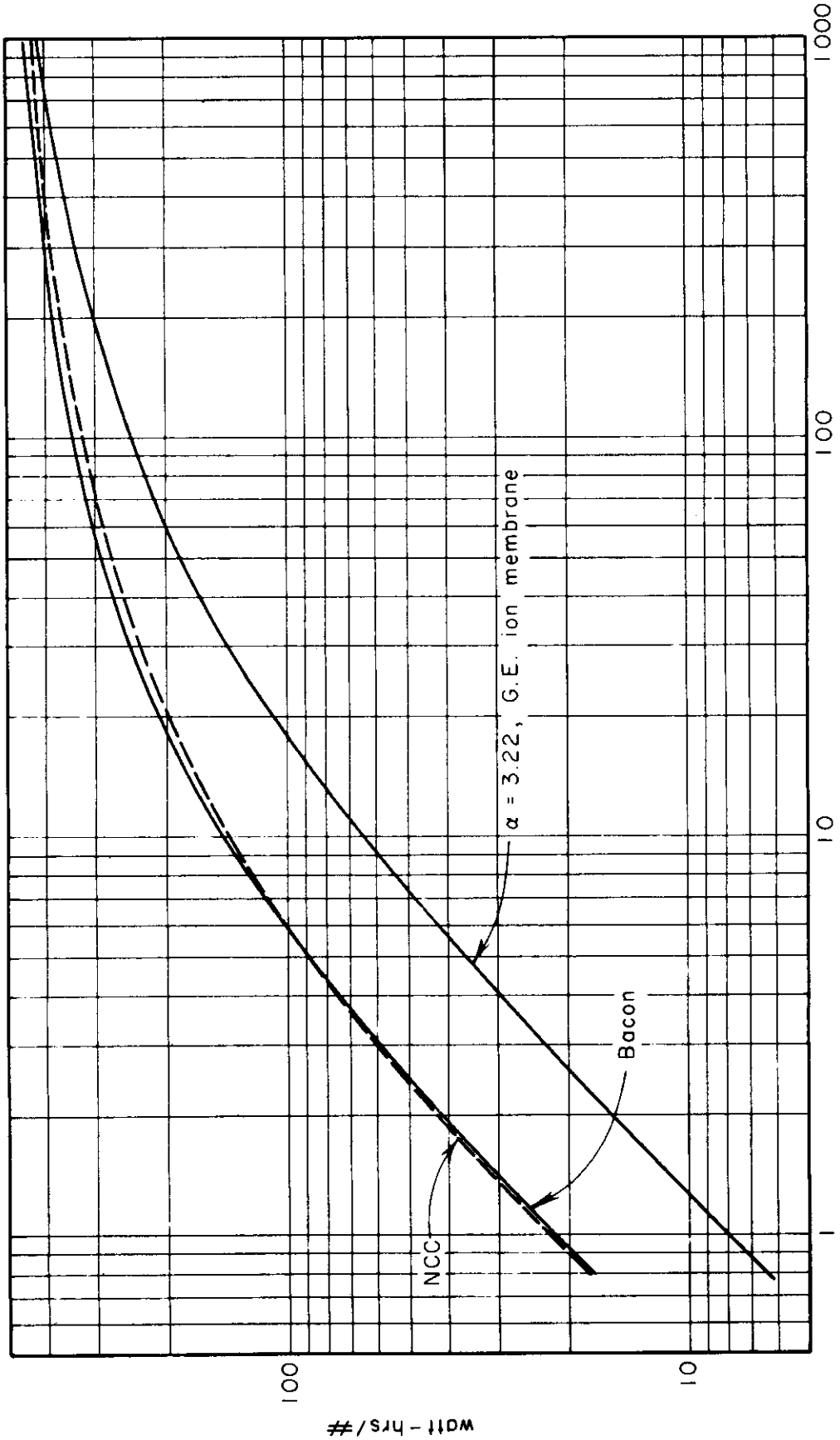

FIGURE VI-B-8 UNIT WEIGHT CHARACTERISTICS OF PRIMARY FUEL CELLS FOR SPACE

5.1 Evaluation of Constants for Primary Fuel Cells

Hydrogen-Oxygen Cells

$$1/2\ H_2 + 1/4\ O_2 \longrightarrow 1/2\ H_2O$$

Equivalent Weight = $1 + 8 = 9 = \frac{\Sigma MW}{n}$,

$$\frac{96,494}{3,600} = \text{26.8 amp. hr./g. eq. at 100 percent current efficiency}$$

$$\frac{26.8}{9} \longrightarrow \frac{\text{amp hr}}{\text{g. reactants}}$$

With the assumption of 2.5 g. total weight of reactants + cryogenic storage + appurtenances per g. reactants.

$$F = \frac{2.98}{2.5} = 1.19\ \frac{\text{amp.-hr}}{\text{gram}_{\text{total}}}$$

$$\beta = \text{lb/g} = 0.002206$$

From the equation for operating voltage within the linear limits

$$E = C - b\,I_{As}$$

$$\frac{\text{watts}}{1000\ \text{cm}^2} = \frac{\text{milli watts}}{\text{cm}^2} = CI_{As} - b\,I_{As}^2$$

With the assumption that the weight of cell is proportional to surface area of electrodes

$$\alpha = \frac{\text{pounds total cell}}{1000\ \text{cm}^2\ \text{electrode area}}$$

For a Bacon cell $E = 0.92 - 0.00045\ I_{As}$, $I_{As\ Min} = \frac{0.92}{0.0009} = 1022\ \text{ma/cm}^2$

Published zero time weight is 0.05 lb./watt at 0.7v, $I_{As} = 490\ \text{ma/cm}^2$

For optimum I_{As}, weight $= \frac{490}{1022}(0.05) = 0.024$ lb/watt for zero time extrapolation

For evaluation of a for the Bacon cell

$$0.024 \text{ lb/watt} = \frac{a}{0.92\,(1022) - 0.00045\,(1022)^2} = \frac{a}{470}$$

Bacon a = 12.9 lb/1000 cm^2 electrode area

National Carbon Company Hydrogen-Oxygen Cell

$$E = C - bI_{As} = 0.936 - 0.00244\, I_{As}$$

$$I_{As(max)} = \frac{0.936}{0.00488} = 192 \text{ ma/cm}^2$$

Published zero time weight = 0.35 lb/watt at 20 ma/cm^2

For optimum I_{As}

$$\text{Zero time wt/watt} = \frac{20}{192}\ 0.35 = 0.0365$$

For evaluation of a

$$0.0365 \text{ lb/watt} = \frac{a}{0.936(192) - 0.00244\,(192)^2} = \frac{1000\,a}{90}$$

N.C.C. $$a = \frac{90\,(0.0365)}{1000} = 3.28 \text{ lb/1000 cm}^2$$

General Electric Company Ion Membrane Cell

$$E = 1.0 - 0.00931\, I_{As},\ I_{As\ Min} = \frac{C}{2b} = 53.7 \text{ ma/cm}^2 \text{ at } 0.5 \text{ v.}$$

$$a = \frac{3.22 \text{ lb}}{1000 \text{ cm}^2},\quad C = 1.0,\quad b = 0.00931$$

5.2 Summary of Cell Constants

	α	β	Γ	b	C	Limits
Bacon Cell	12.9	0.002206	1.19	0.00045	0.92	90-400 ma/cm^2
N. C. C. Cell	3.28	0.002206	1.19	0.00244	0.936	20-200
G. E. Ion Membrane Cell	3.22	0.002206	1.19	0.00931	1.00	1.5 - 54

BACON HYDROX CELL — SUMMARY OF CALCULATIONS

Discharge Period (hr.)	Volts	Current Density ma/cm^2	lb. /watt	watt hr. /lb.
0	0.74*	400*	0.0436	0
1	0.74*	400*	0.0461	21.7
5	0.74*	400*	0.0561	89.1
10	0.74*	400*	0.0687	145.5
50	0.74*	400*	0.1688	296.
100	0.78	314	0.2907	344.
400	0.84	171	0.971	412.
700	0.8605	132.3	1.613	434.
1000	0.8896	112	2.213	452.
∞	1.1	nil	∞	593.

*Limit of experimental data

NATIONAL CARBON H_2 - O_2 CELL

Discharge Period (hr.)	Volts	Current Density ma/cm^2	lb/watt	watt hr. /lb.
0	0.448*	200*	0.0364	0
1	0.494	181	0.0406	22.6
5	0.533	165	0.0549	91.0
10	0.602	137	0.0699	142.7
50	0.726	86	0.1804	277.2
100	0.771	67.5	0.3038	329.3
400	0.846	36.8	0.981	408.
700	0.866	28.5	1.631	429.
1000	0.877	24.2	2.264	441.
∞	1.1	nil	∞	593.

*Limit of data

G.E. ION MEMBRANE CELL (a = 3.22)

Discharge Period (hrs.)	Volts	Current Density ma/cm^2	lb/watt	watt hrs. /lb
0	0.5001	53.7	0.120	0
1	0.5075	52.9	0.124	8.06
5	0.5336	50.1	0.137	36.50
10	0.5596	47.3	0.153	65.36
50	0.6714	35.3	0.263	190.1
100	0.7291	29.1	0.406	246
200	0.7849	23.1	0.650	308
400	0.8371	17.5	1.107	361
600	0.8600	15.0	1.544	389
700	0.8725	13.7	1.756	399
800	0.8771	13.2	1.986	407
1000	0.8883	12.0	2.388	419
∞	1.03	nil	∞	555

It should be recognized that additional weight must be charged to each system involving phase separation, because of the added complexities of gravity generation or other separation method. Although a spinning body in space may continue to spin without added energy, the precession induced by a required directional change can add difficulties and weight. Reaction at bearings can also add difficulties of uncertain magnitude; the weight of gravity generation has been ignored so far.

6.0 EXAMPLES OF REGENERABLE FUEL CELLS FOR SPACE

There are a few fuel cells which do not require gravity generation. Although apparently restricted from primary utilization by weight or predicted operational difficulties for long period operation, these cells could serve for regenerable applications. The two redox cells (with meager publication of operating conditions) involve reaction of aqueous ions without phase change. The EOS cell involves the use of capillarity and adsorption for phase separation control. For purposes of comparison, operating conditions of the ion membrane cell were obtained privately, and added weight was assumed for gravity generation or an equivalent method of phase separation.

The catholyte solution for both General Electric Company and Kings College Redox cells can be selected from published equilibrium and solubility relationships. The basis for establishment of solution concentrations is chosen as 70 percent of saturation of bromine at 50°C and full charge or 70 percent of saturation of sodium bromide at 0°C and full discharge, whichever is limiting. The 70 percent of saturation is selected as a safety factor which will allow simplifying assumptions for expediency. A handbook listing for sodium bromide solubility is 79.5 g per 100 ml of water

at 0°C. The expedient assumption of 100 ml of resulting solution leads to a solubility product of 59.8 for molar concentrations. A handbook listing for bromine solubility is 3.5 g per 100 ml of water at 50°C. A published (Ref. VI-B-42) association constant for the Br_3^- ion is 17: a published (Ref. VI-B-43) dissociation constant for the Br_5^- ion is 0.055. A further specification of negligible hydrogen ion concentration at full charge allows estimation of added water for catholyte weight. Simultaneous solution of all equations leads to the following saturation concentrations at full charge.

$Br_{2\ (Aq)}$ - 0.219 M	Br_5^- - 2.85 M
Br^- - 0.191 M	Na^+ - 3.75 M
Br_3^- - 0.714 M	Total oxidant Br_2 - 6.63 M

The unit weight characteristics of regenerable fuel cells for space are summarized in Figure VI-B-10 following calculations and tables.

6.1 Evaluation of Constants for Gravity Free Cells

G. E. Redox Cell

$$1/2\ Br_2 + Ti^{+++} + H_2O \rightarrow Br^- + TiO^{++} + 2H^+$$ Discharge Reaction

Basis: Regenerable cell, charged to 95 percent and discharged to 10 percent of capacity

1.0 g. - equivalent reactants $\rightarrow$ 26.8 (0.95 - 0.10) = 22.8 amp. hr

Catholyte		Anolyte	
Br_2	79.9 g.	$TiCl_3$	154.3 g.
H_2O	71.9	H_2O	1000.0
HBr	1.2	HCl 4M	145.7
NaBr	29.0		1300.0 g
	182.0	Storage	700.0
Storage 1 atm	98.0		2000.0
	280.0 g		280.0
			2280.0 g. Total

Γ = Amp. hr./g. = $\frac{22.8}{2280}$ = 0.01

Cell α = 8.0 lb/1000 cm^2 incl. pump β = 0.002206 lb./g.

$E = C - b I_{As}$

Eoc = 0.96, E at 43 ma/cm^2 = 0.8 say $E = 0.92 - 0.0028\ I_{As}$

Allowance for pump energy = 0.21_{As}

For Net I_{As} $E = 0.92 - \frac{0.0028}{0.8} I_{As} = 0.92 - 0.0035\ I_{As}$

Kings College Redox Cell

$$Br_2 + Sn^{++} \rightarrow Sn^{++++} + 2Br^-$$

Basis: Regenerable cell, charged to 95 percent and discharged to 10 percent capacity

1.0 g equivalent of reactants 26.8 (0.85) = 22.8 amp.hr/g. eq.

Catholyte		Anolyte	
Br_2	79.9 g	$SnCl_2$	95 g
H_2O	71.9	H_2O	2000
H Br	1.2	HCl	438
NaBr	29.0	Chemicals	2533 g
Chemicals	182.0 g	Storage	767
Storage	98.0		3300 g
	280.0 g		280
			3580 g Total

$$\Gamma = \frac{22.8}{3580} = 0.00637$$

Cell α = 8.0 lb/1000 cm^2 incl. pump β = 0.002206 lb/g

$E = C - b I_{As}$ Data $0.62 = C - 8.37\ b$

$0.29 = C - 42.8\ b$

$E = 0.70 - 0.0096\ I_{As}$, $C = 0.7$

Allowance for pump energy = $0.2\ I_{As}$

For Net I_{As}, $E = 0.70 - \frac{0.0096}{0.8} I_{As} = 0.70 - 0.012\ I_{As}$

Electro-Optical Systems, Inc. Porous Matrix $H_2 - O_2$ Cell

$E = 0.65 - 0.000452\ I_{As}$ Limits 12 to 150 ma/cm^2 (From Figure VI-B-9)

C = 0.65, b = 0.000452

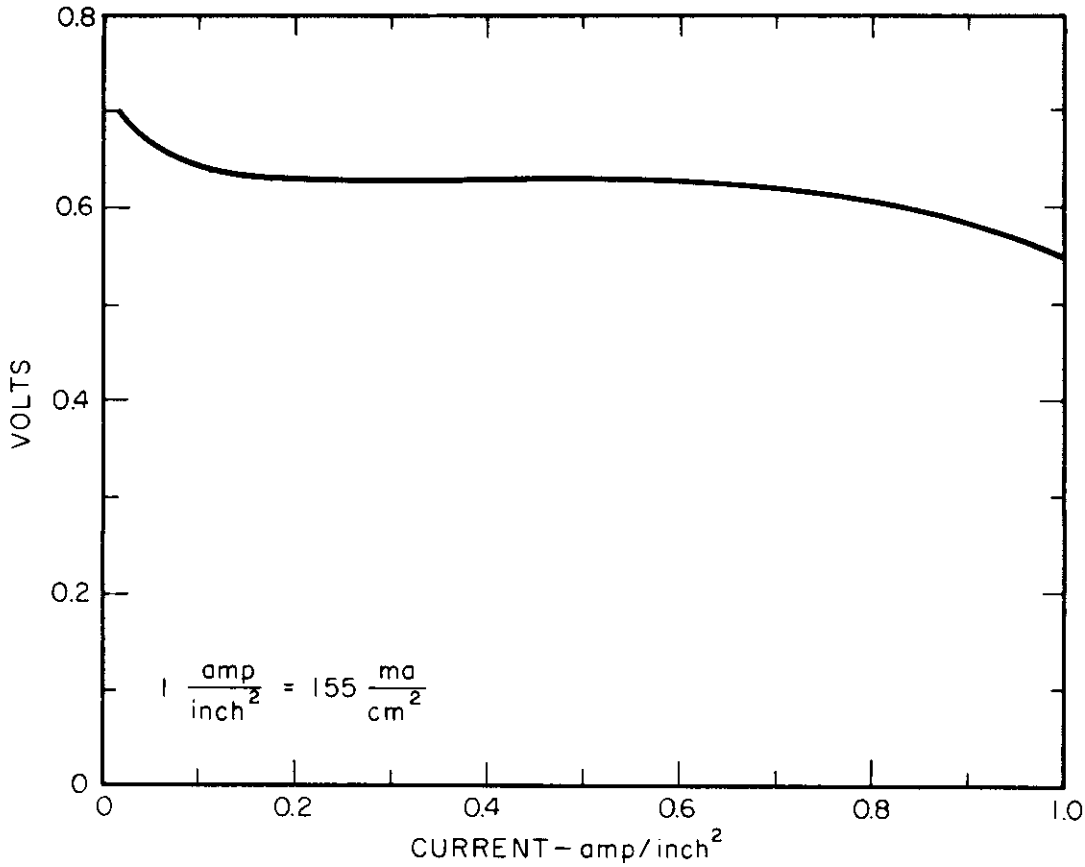

FIGURE VI-B-9 EOS POROUS CELL
CURRENT VOLTAGE CURVE AFTER ELECTROLYSIS AT 1.00 VOLT AND 1.13 AMPS/INCH^2 FOR 4 MINUTES (71st CYCLE)

For optimum pressure storage in fiberglas containers we allow 3.5 pounds total/pound reactant. With the assumption of 95 percent charge to 10 percent discharge

$$\Gamma \rightarrow \frac{26.8(0.85)}{9(3.5)} = 0.723 \text{ amp. hr./gram as } \theta \text{ increases without limit.}$$

However, the minimum hydrogen electrode, porous nickel, will store enough hydrogen for approximately 10 hours. Consequently, for the first 10 hours of operation, only the weight of the oxygen storage system should contribute to Γ. As an approximation, Γ is set at 1.446 for $0 < \theta < 10$ hours. For simplification a linear relationship for Γ vs. θ is selected for the reciprocals so that Γ equals 0.723 when $1/\theta$ equals zero. The resulting equation is

$$\frac{1}{\Gamma} = 1.384 - \frac{6.92}{\theta} \qquad \text{for } \theta > 10 \text{ hours}$$

The unit weight of the cell is conservatively estimated as α = 6 lb/1000 cm^2 electrode area and β = 0.002206 lb./g.

Ion Membrane Cell (General Electric Company)

The equation relating current density and voltage was obtained by private communication.

$$E = 1.00 - 0.00931\, I_{As}, \quad C = 1.00, \quad b = 0.00931$$

The value of Γ in amp. hr/g. is the same as the limiting value for the EOS cell computation, Γ = 0.723. With gravity generation or acceptable equivalent for phase separation, we allow 5.0 lb. cell per 1000 cm^2 of electrode area for α.

SUMMARY OF CELL PARAMETERS

	α	β	Γ	b	C	Assumed Limits
G. E. Redox	8.0	0.002206	0.01	0.0035	0.92	5-130ma/cm^2
Kings College Redox	8.0	0.002206	0.00637	0.012	0.70	10-37 ma/cm^2
EOS Porous Cell	6.0	0.002206	*	0.000452	0.65	12-150ma/cm^2
Ion Membrane Cell	5.0	0.002206	0.723	0.00931	1.0	1.5-55ma/cm^2

* 0 to 10 hr. $\Gamma = 1.446$, for $\theta > 10$ hr. $\frac{1}{\Gamma} = 1.384 - \frac{6.92}{\theta}$

SUMMARY OF CALCULATIONS - KINGS COLLEGE REDOX

Discharge Period (Hr.)	Volts	Current Density ma/cm^2	lb./watt	watt hrs./lb.
0	0.353	29.1	0.784	0
1	0.414	23.76	1.647	0.608
5	0.513	15.5	4.377	1.142
10	0.556	11.13	7.38	1.356
50	0.67	7.0	27.17	1.845
100	0.73	4.0	50.2	1.99
∞	0.91	nil	∞	2.63

G.E. REDOX

Discharge Period (hrs.)	Volts	Current Density ma/cm^2	lb./watt	watt hr./lb.
0	0.46	131.4	0.1325	0.
1	0.66	70.0	0.498	2.005
5	0.79	36.4	1.674	2.99
10	0.82	27.5	3.043	3.29
50	0.88	13.1	13.24	3.74
100	0.89	9.42	25.76	3.88
200	0.90	6.73	50.3	3.98
∞	0.96	nil	∞	4.36

SUMMARY OF CALCULATIONS

EOS POROUS MATRIX CELL

a = 6 lb./1000 cm^2 electrode area

Discharge Period (hrs.)	Volts	Current Density ma/cm^2	lb./watt	watt hr./lb.
0	0.54 *	160 *	0.0694	0.
1	0.54 *	160 *	0.0722	13.85
5	0.54 *	160 *	0.0835	59.8
10	0.54*	160 *	0.0976	102.5
50	0.54*	160 *	0.323	155
1100	0.58*	155.5 *	0.567	176
200	0.60	113.0	1.083	184
400	0.61	81.2	2.10	190
600	0.62	66.7	3.09	194
800	0.62	58.1	4.08	196
1000	0.63	52.2	5.02	199
∞	0.72	nil	∞	236

* Extrapolated data

G.E. ION MEMBRANE CELL

a = 5 lb./1000 cm^2 electrode area

Discharge Period (hr.)	Volts	Current Density ma/cm^2	lb./watt	watt hr./lb.
0	0.5001	53.7	0.186	0.
1	0.5084	52.8	0.192	5.21
5	0.5354	49.9	0.215	23.26
10	0.5624	47.0	0.243	41.1
50	0.6732	35.1	0.440	114
100	0.7337	28.6	0.654	153
200	0.7896	22.6	1.053	190
400	0.8389	17.3	1.80	222
600	0.8641	14.6	2.51	239
800	0.8799	12.9	3.21	249
1000	0.8911	11.7	3.90	256
∞	1.03	nil	∞	338

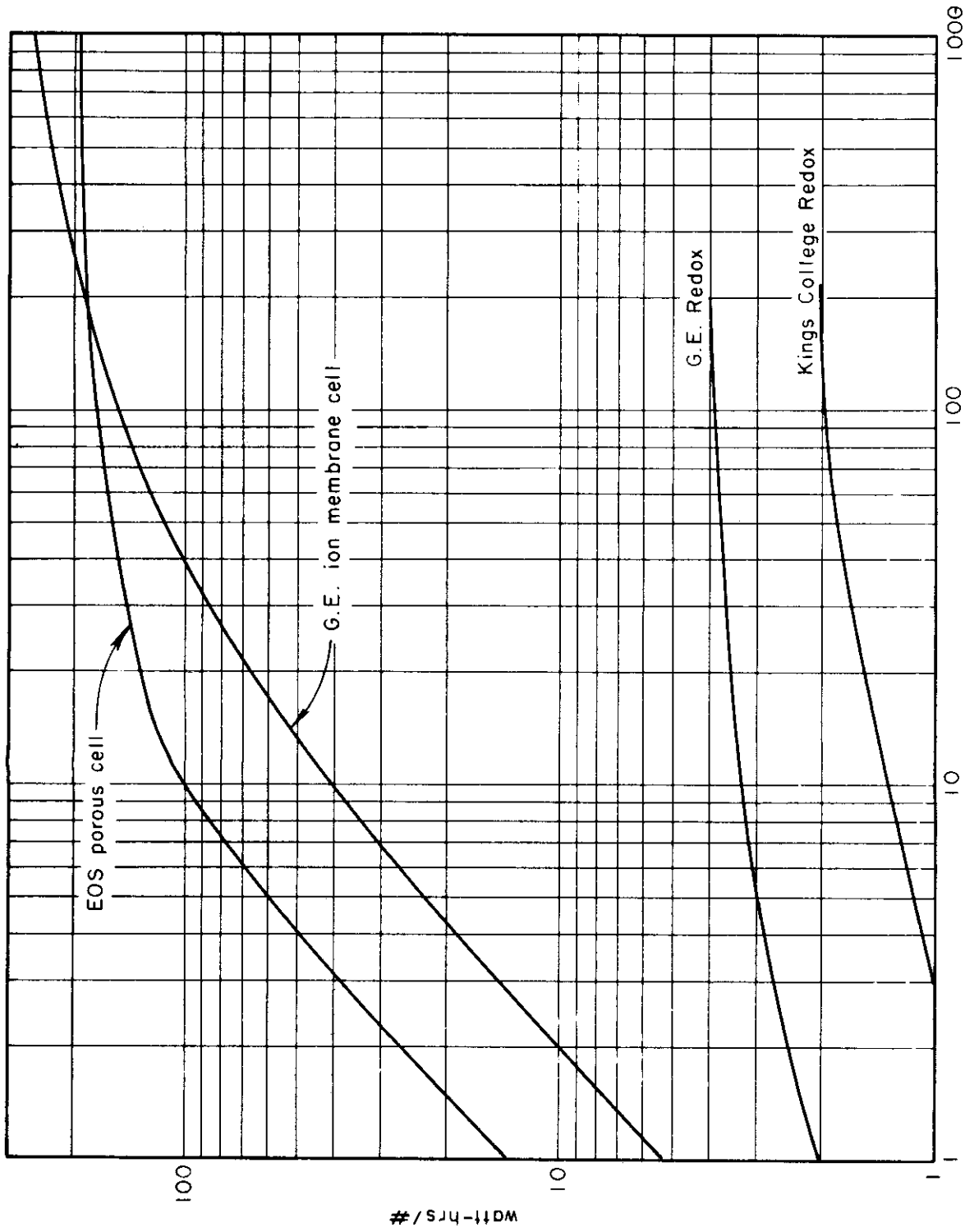

FIGURE VI-B-10 UNIT WEIGHT CHARACTERISTICS OF REGENERABLE FUEL CELLS FOR SPACE

So far, only the weight of the fuel cell system has been considered. Of far greater importance because of the unit weight in pounds per watt will be the regeneration system and, therefore, the regeneration efficiency. From published data on an older ion membrane cell and preliminary data from Electro-Optical Systems, Inc., the graph in Figure VI-B-11 was constructed. The negative current densities refer to the charge cycle and the ratio of charge voltage may approximate the weight ratio of the regenration systems. With the present state-of-the-art of solar cell systems, such a system will weigh much more than the fuel cell system, particularly for short operating periods. The required current density on charge will be determined by the length of the insolation period although competing cells will most probably be designed for different current densities for weight minimization. Different methods of regeneration will probably lead to similar conclusions except, possibly, nuclear regeneration from which an exceedingly small fraction of available power would be withdrawn.

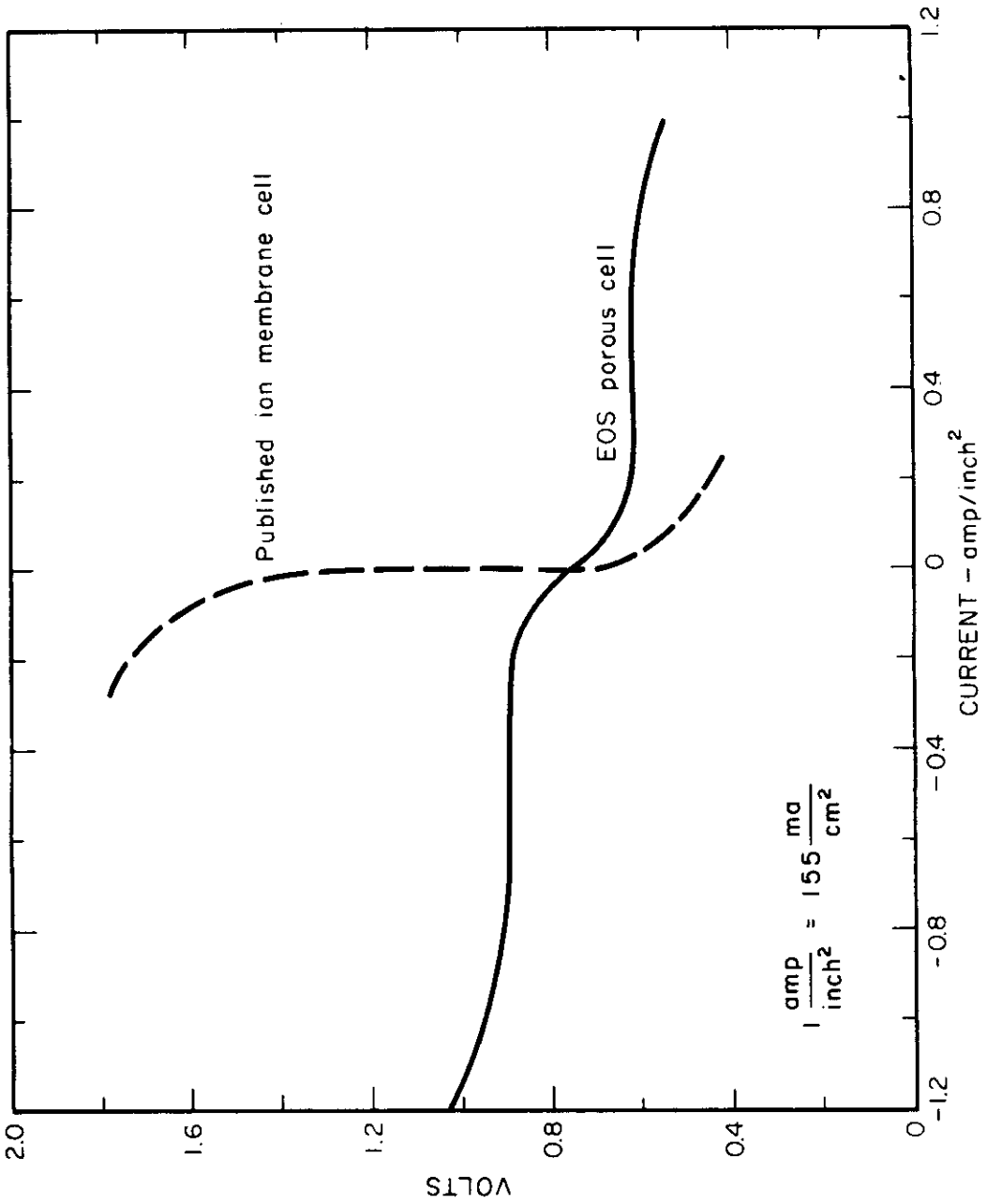

FIG. VI-B-11 CHARGE-DISCHARGE DATA COMPARISON OF THE EOS REGENERATIVE CELL WITH THE STATE-OF-THE-ART (GE ION MEMBRANE CELL)

7.0 APPENDIX TABLES

TABLE VI-B-I

IDENTIFICATIONS OF COMPANIES ENGAGED IN FUEL CELL DEVELOPMENT

	Status	No. Persons	Stage	Gov't Contract	Person in Charge Telephone No.
Aerojet General Corp. 6352 N. Irwindale Ave. Azusa, California	W	4	Lab	None	L. R. Rapp, Head CU 3- 6111
Anderson Physical Lab. 609 So. Sixth St. Champaign, Illinois	W	1	Lab	None	Mr. Scott Anderson Director FL 6- 1347
Chrysler Corp. Engr. Division P. O. Box 1118 Detroit 31, Michigan	W		Study	None	Dr. C. R. Lewis Chief Engineer TU 3- 4500
Consolidation Coal Co. Library, Pennsylvania	C			DA-36-039 SC 7-4941	Dr. E. Gorin
Curtiss-Wright Corp. Research Division Quehanna, Pennsylvania	C		Model	Yes	Dr. Egon DeZubay AM 3-4711
Dow Metal Products Co. Midland, Michigan	C		Model	No	Dr. R. C. Kirk Chief Chem. Dev. Sec. ME 6-5604
Electric Storage Battery Co. Research Center 19 West College Ave. Yardley, Pennsylvania	W	10	Model	No	Capt. C. G. Grimes Director HI 3-3601

TABLE VI-B-I (Continued)

	Status	No. Persons	Stage	Gov't Contract	Persons in Charge Telephone No.
Electro-Optical Systems, Inc. 125 N. Vinedo Pasadena, California	W	2	Study	DA-36-039 SC-85270	Frank A. Ludwig Project Supervisor SY 5-9961
Electro-Optical Systems, Inc. 125 N. Vinedo Pasadena, California	W	2	Lab	AF33(616)-6546	John J. Rowlette Project Supervisor SY 5-9961
Esso Research and Engr. Co. P. O. Box 121 Linden, New Jersey	W	4	Model	No	Dr. C. E. Heath WA 5-0100
General Electric Co. 930 Western Ave. West Lynn 3, Massachusetts	C	20	Production	DA-44-009 Eng-3771	Dr. D. L. Douglas Mgr. Fuel Cell Engr. LYnn 8-6000
General Motors Corp. Delco Remy Division Anderson, Indiana	W	Many	Lab	None	Dr. J. J. Lander
Institute of Gas Technology State and 34th St. Chicago 16, Illinois	W	4	Lab	No	Dr. H. R. Linden Research Director CA 59600, Ext. 600
MSA Research Corp. Callery, Pennsylvania	W	3	Lab	DA-36-039 SC 78955	Dr. C. B. Jackson Vice President Evans City 3510
North American Aviation, Inc. 12214 Lakewood Blvd. Downey, California	W	1	Study	No	Mr. George E. Ellis Sr. Engineer SP 3-0610, Ext. 8661
Patterson Moos Research Leesona Corporation 90-28 Van Wyck Expressway Jamaica 18, New York AX 7-4400	W		Model	AF-33(600) 34709	Chief of Mil. Sales Pratt and Whitney Aircraft Division 400 Main St. E. Hartford 8, Conn. JA 8-4811

TABLE VI-B-I (Continued)

	Status	No. Persons	Stage	Gov't Contract	Person in Charge Telephone No.
Pennsylvania State Univ. University Park, Pa.	W	1	Lab	No	Prof. L. G. Austin UN 5-2481
Radio Corp. of America Semiconductor and Materials Div. Somerville, New Jersey	C	9	Lab	DA-36-039 SC-78048	Dr. G. S. Lozier Group Leader RA 2-3200, Ext. 403
Resin Research Lab. Inc. 406 Adams St. Newark 5, New Jersey	W	5	Lab	AF 33(616) 6399	Dr. Gerald A. Baum Senior Chemist MA 2-5251
Sundstrand Turbo Div. Sundstrand Corp. 10445 Glenoaks Blvd. Pacoima, California	W	5	Lab	AF 33(616) 6585	Mr. R. H. Olson Vice President EM 6-8121
Union Carbide Consumer Products Co. P. O. Box 6116 Cleveland 1, Ohio	W			NONR 1785(00)	Dr. G. E. Evans Director, Research TU 4-8000
Western Reserve University Morley Chemical Laboratory Cleveland 6, Ohio	C		Mdod	NONR 2391(00)	Prof. Ernest Yeager CE-1-7700, Ext. 753
Westinghouse Electric Corp. Research Laboratories Beulah Road, Churchill Boro Pittsburgh 35, Pennsylvania	W		Lab	No	Mr. W. W. Auxier Manager, Chemistry Dept. PH 2-1500

W - Working

C - Complete

TABLE VI-B-II

FUEL CELL SUMMARY

0- 100 Watt Power Level

Company	Type	Reactants	Electrolyte	Diaphragm	Catalyst	Thermodynamic Efficiency
Aerojet General Corp.	Thermally Regenerable	Bismuth-Iodine	Fused Salt	Ceramic in some models	None	
Dow Metal Products Company	Consumable Electrode	Magnesium-Air	Sea Water	None	--	60 per cent
Hoffman Electronics Corp.	Electrically Regenerable	Alkali Amalgam-Halogen	Aqueous Alkali Halide	Yes	Possible	--
MSA Research Corp.	Thermally Regenerable	Lithium-Hydrogen	Fused Salt	Yes	--	to 30 per cent
Radio Corp. of America	Consumable Electrode	Magnesium Nitro-Organic	Aqueous $MgBr_2$	--	No	--
Electro-Optical Systems	Electrically Regeneral	Hydrogen Oxygen	KOH in Porous Matrix	No	Yes	--

TABLE VI-B-III

FUEL CELL SUMMARY

100 - 2000 Watt Power Level

Company	Type	Reactants	Electrolyte	Diaphragm	Catalyst	Thermodynamic Efficiency
Curtiss-Wright Corp.	Fused Electrolyte	Propane Air	Fused Salt	--	Yes	--
Electric Storage Battery Co.	Regenerable	--	--	Microporous Polyethylene	Yes	60 per cent
General Electric Company	Ion Membrane	Hydrogen Oxygen	Ionic Membrane	Ionic Membrane	Platinum Black	62 per cent
Hoffman Electronics Corp.	Electrically Regenerable	Alkali Amalgam-Halogen	Aqueous Alkali Halide	Yes	Possible	--
National Carbon Co.	Hydrox	Hydrogen-Oxygen	Aqueous KOH		Yes	--
Sunstrand Turbo	Photochemically Regenerable	Nitric Oxide-Chlorine	Nitrosyl Chloride Metallic Chloride	No	No	Low
Western Reserve University	Consumable Electrode	Sodium Amalgam-Oxygen	4N NaOH	No	Yes	50 per cent

TABLE VI-B-IV

FUEL CELL SUMMARY

2- 15 Kilowatt Power Level

Company	Type	Reactants	Electrolyte	Diaphragm	Catalyst	Thermodynamic Efficiency
Allis Chalmers Mfg. Co.	Hydrocarbon	Propane-Additive-Air	--	--	Yes	60 per cent
General Electric Co.	Redox	Aqueous Ti+++ -Br_2	Aqueous Salt	Yes	--	to 80 per cent
National Carbon Co.	Hydrox	Hydrogen Oxygen	Aqueous KOH	--	Yes	--
Resin Research Labs., Inc.	Consumable Electrode	Metal-Nitro-Organic		Yes	No	--

TABLE VI-B-V

FUEL CELL SUMMARY

Unspecified Power Level

Company	Type	Reactants	Electrolyte	Diaphragm	Catalyst	Thermodynamic Efficiency
Consolidation Coal Co.	Fused Electrolyte	Hydrogen-Air	Fused Carbonates	--	--	--
Esso Research and Engr. Co.	Hydrocarbon	Ethane-Air	Aqueous KOH	No	Yes	--
Institute of Gas Technology	Redox	Cuprous Ion Bromine	Aqueous	Yes	No	8 per cent
Penn. State University	Indirect Coal	Water-Gas-Air	10 per cent	--	Yes	--
Pratt and Whitney	Bacon Hydrox	Hydrogen-Oxygen	Aqueous Koh	--	Yes	to 61 per cent

Other companies include: Chrysler Corp., General Motors Corp., Lockheed Aircraft Co., North American Aviation, and Westinghouse.

REFERENCE LIST

VI-B-1. Ostwald, W. Direct Fuel Cells. Z. Elektrochem. 1:122 (1894).

VI-B-2. Davy, H. Low Temperature Hydrogen Fuel Cell. Ann. Phys. 8:301 (1801).

VI-B-3. Grove, W. R. Low Temperature Hydrogen Fuel Cell. Phil. Mag. (3) 14:129 (1839).

VI-B-4. Kordesch, K. The Hydrogen-Oxygen (Air) Fuel Cell with Carbon Electrodes. Symposium on Fuel Cells. ACS Meeting, Atlantic City, N. J. (1959).

VI-B-5. Bacon, F. T. The High Pressure Hydrogen-Oxygen Fuel Cell. Symposium on Fuel Cells. ACS Meeting, Atlantic City, N. J. (1959).

VI-B-6. Garin, E., and Recht, H. L. The High Temperature Fuel Cell and the Nature of the Electrode Process. Symposium on Fuel Cells. ACS Meeting, Atlantic City, N. J. (1959).

VI-B-7. Langworthy, E. M., et al. Chlorine Depolarized Battery. Proceedings of the Eleventh Annual Battery Research and Development Conference. (Power Sources Division, U. S. Army Signal Engineering Laboratories, Fort Monmouth, N. J.) (1957).

VI-B-8. Glicksman, R. Organic Depolarized Batteries. Proceedings of the Thirteenth Annual Power Sources Conference. (Power Sources Division, U. S. Army Signal Research and Development Laboratory, Fort Monmouth, N. J.) (1959).

Glicksman, R., and Morehouse, C. K., J. Electrochem. Soc. 105:299, 613 (1958).

Glicksman, R., and Morehouse, C. K. J. Electrochem. Soc. 106:288 (1959).

VI-B-9. Morehouse, C. K., and Glicksman, R., J. Electrochem. Soc. 104:467 (1957).

Morehouse, C. K., and Glicksman, R., J. Electrochem. Soc. 105:306, 519 (1958).

VI-B-10. Lozier, G. S., et al. J. Electrochem. Soc. 104:52 (1957).

VI-B-11. New Entry in Fuel-cell Race. Chem. Week 76:73 (April 30, 1960).

VI-B-12. Linden, H. R., and Rosenberg, R. Institute of Gas Technology, Chicago, Illinois. Private Communication (1959).

VI-B-13 Heath, C., and Sage, R. W. Esso Research and Engineering, Linden, N. J.,Private Communication (1959).

VI-B-14 Fuel Cell Paces Power, Allis-Chalmers Sales News (1959).

VI-B-15 Bischoff, K., and Justi, E., Direct Carbon Fuel Cell. Ann. Min. Belg. 52: 381 (1953).

VI-B-16 Spengler, H. Direct Carbon Fuel Cell. Angew. Chem. 6:822, 689 (1956).

VI-B-17 Yeager, E., et al. Continuous Feed Primary Battery of the Sodium Amalgam-Oxygen Type. Report, National Carbon Co., Cleveland, Ohio ONR Contract Nonr. 1785(00) (April 1958).

VI-B-18 Kirk, R. C. Dow Chemical Co., Midland, Michigan., Private Communication (1959).

VI-B-19 Stein, B. R., Status Report on Fuel Cells, Army Research Office Report No. 1, Department of the Army (1959).

VI-B-20 Evans, G. E., Low Temperature Type (Fuel Cell). Proceedings, Thirteenth Annual Power Sources Conference (Power Sources Division, U. S. Army Signal Research and Development Laboratory, Fort Monmouth, N. J.) (1959).

VI-B-21 Smatko, J. S., Hoffman Electronics Corp., Los Angeles, California, Private Communication (1960).

VI-B-22 Werner, R. C., et al. Regenerative Type (Fuel Cell). Proceedings, Thirteenth Annual Power Sources Conference (Power Sources Division, U. S. Army Signal Research and Development Laboratory, Fort Monmouth, N. J. (1959).

VI-B-23 Anderson, S. Some Possibilities for Solar Energy Utilization by Means of the Photogalvanic Effect. Transactions of the Conference on the use of Solar Energy. Volume IV, Photochemical Processes, University of Arizona Press (1955).

VI-B-24 Pitts, Jr., J. N., et al. Photochemistry and Space Power Generation. American Rocket Society Meeting, Los Angeles, California (May 1960).

VI-B-25 Debye, P., and Huckel, E., Phys. Z. 24: 185 (1923).

VI-B-26 Schumb, W. C., et al. J. Am. Chem. Soc. 59: 2360 (1937).

VI-B-26a Lewis, G. N., and Randall, M., Thermodynamics and Free Energy of Chemical Substances (New York: McGraw-Hill), 1923.

VI-B-27 Carlson and Colburn, Ind. Eng. Chem. 34: 581 (1942).

VI-B-28 Wohl, Trans. Am. Onst. Chem. Engrs. 42: 215 (1946).

VI-B-29 Benedict, et al. Trans. Am. Inst. Chem. Engrs. 41:371 (1945).

VI-B-30 Kimball, G. E. J. Chem. Phys. 8: 199 (1940).

VI-B-31 Niedrach, L. W., The Ion Exchange Membrane Fuel Cell. Proceedings of the Thirteenth Annual Power Sources Conference (Power Sources Division, U. S. Army Signal Research and Development Laboratory, Fort Monmouth, New Jersey) (1959).

VI-B-32 Eisenberg, M., A Second Redox Type (Fuel Cell). Proceedings of the Thirteenth Annual Power Sources Conference (Power Sources Division, U. S. Army Signal Research and Development Laboratory, Fort Monmouth, New Jersey) (1959).

VI-B-33 Gurney, R. W., Proc. Roy. Soc. A134: 137 (1931).

VI-B-34 Berl, W. G., Trans. Electrochem. Soc. 83: 253 (1943).

VI-B-35 Noyes, A. A., et al. J. Am. Chem. Soc. 59: 1316 (1937)

VI-B-36 Glasstone, S., and Hickling, A. Trans. Faraday Soc. 31: 1656 (1935).

VI-B-37 Walker, O. J. and Weiss, J. Trans. Faraday Soc. 31: 1011 (1935).

VI-B-38 Weiss, J., Trans. Faraday Soc. 31: 668 (1935).

VI-B-39 Austin, L. G.,"Electrode Kinetics of Low Temperature Hydrogen-Oxygen Fuel Cells." Fuel Cells, Young, G. J. (Editor) Reinhold Publishing Corp. New York (1960).

VI-B-40 Parsons, R. Trans. Faraday Soc. 54: 1053 (1958).

VI-B-41 Young, G. J., and Roselle, R. B., Catalysis of Fuel Cell Electrode Reactions, Symposium on Fuel Cells, ACS Meeting, Atlantic City, New Jersey (1959).

VI-B-42 Griffith, R. O. et al. Trans. Faraday Soc. 28: 101 (1932).

VI-B-43 Liebhafsky, H. A, J. Am. Chem. Soc. 56: 1500 (1934)

VI-B-44 Smolak, G. R., and Knoll, R. H. "Cryogenic Propellant Storage for Round Trips to Mars and Venus," Aero/Space Engr. 42 (June 1960).

VI-B-45 Layton, P. L, Fiberglass Filament Winding Technique for Aircraft and Guided Missile Applications. Owens-Corning Fiberglas Corp. Report (April 1959).

VI-B-46 Bockris, J. O'M., and Potter, E. C, J. Electrochem. Soc. 99:169 (1952).

VI-B-47 Moore, W. T, Physical Chemistry, 3rd Ed. (London: Longmans, Green and Company), 1957.

VI-B-48 Baker, et al. Trans. Faraday Soc. 51:1592 (1955).

VI-B-49 Armbruster, M., "The Solubility of Hydrogen at Low Pressure in Iron, Nickel, and Certain Steels at 400 to 600°," J. Am. Chem. Soc. 65:1050 (1943).

VI-B-50 Shearer, R. E., "Study of Energy Conversion Device," Report No. 1, Contract DA-36-039-SC-78955, October 31, 1959.

VI-B-51 Shearer, R. E., "Study of Energy Conversion Devices," Report No. 2, Contract DA-36-039-SC-78955, January 31, 1959.

VI-B-52 Shearer, R. E., Ciarlariello, T. A., and Vaccharella, S. J., "Study of Energy Conversion Devices," Report No. 3, Contract DA-36-039-SC-78955, April 29, 1960.

VI-B-53 Lee, J.M., First Semi-Annual Report, "Research on a 500 Watt Solar Regenerative H_2-O_2 Fuel Cell Power Supply System". PWA 1782, Contract DA 36-039-SC-85259 (Oct. - Dec. 1959).

VI-B-54 Rowlette, J.J., Fourth Quarterly Progress Report, "Research on Chemical Reactions Capable of Converting Solar Energy into Forms Which Can be Used as Power Sources," Contract No. AF 33(616)-6546 (Aug. 1960).

NOMENCLATURE

A = Surface Area, Helmboltz Free Energy
End value activity coefficient

A_s = Cross sectional area available for flow

C = Empirical constant

D_v = Diffusivity, Area/Time

E = Energy
Cell E. M. F. volts

F = Free Energy

$\mathcal{F}$ = Faraday Equivalent

H = Enthalpy

I = Current, amperes

I_{AS} = Current density $^{ma}/_{cm^2}$

J = Mechanical equivalent of heat

K = Equilibrium constant

L = Length

MW = Molecular weight

$\underline{M}$ = Molar concentration

N = Mole fraction

$\underline{N}$ = Normality (concentration)

P = Total pressure

Q = Quantity of heat transferred, BTU

R = Gas constant

S = Entropy

T = Absolute temperature

a = chemical activity
empirical constant

b = empirical constant

d = differential operator

e = base of natural logs

e^- = electron

f = fugacity

g = acceleration of gravity

i = current, local

k , thermal conductivity

m = mass

m = molar concentration

ma = milliamperes

n = number, as of moles in PV = nRT

p = partial pressure

q = Rate of heat transfer BTU/hr

s = surface tension

t = ^oF or ^oC

NOMENCLATURE (cont)

V = Volume

W = Work

w = mass flow rate

x, y = coordinates

Z = Charge on an ion

α = empirical

β = empirical constant

γ = activity coefficient

Γ = empirical constant

Δ = finite increment operator

∂ = partial differential operator

ϵ = emissivity (for thermal radiation)

η = electrode polarization, volts

θ = time (period)

ξ = fraction of overpotential assisting direction of reaction

π = 3.1416

ρ = density

Σ = summation of

ψ = function

ENERGY CONVERSION SYSTEMS REFERENCE HANDBOOK

Volume VI - Chemical Systems

Section C

COMBUSTION CYCLES

W. R. Menetrey
Energy Research Division
ELECTRO-OPTICAL SYSTEMS, INC.

Manuscript released by the author
September 1960 for publication in this
Energy Conversion Systems Reference Handbook

WADD Technical Report 60-699

C O N T E N T S

I L L U S T R A T I O N S

TABLES

C. COMBUSTION CYCLES

Thermal energy from combustion products of a monopropellant or bipropellant fuel may be converted to useful power by a variety of gas turbine systems. Thus far, these systems have been used in nonrecoverable boosters with power requirements that vary between .5 to 50 kw for durations of .5 to 5 minutes. Usually both electrical and hydraulic power are required.

In the near future, chemical systems of slightly longer duration, perhaps .5 to 5 hours, will find use in such applications as "Dynasoar" type military vehicles, recoverable boosters, and re-entry of space vehicles in general. Electrical and hydraulic power requirements might vary in the range of 5 to 50 kw, with combined peak loads exceeding these values. The combustion devices discussed here may show weight advantages over those systems in the duration of range a few minutes to 24 - 100 hours, depending on power level. Only systems with durations of greater than roughly one hour will be considered.

Based on duration changes, the optimum design characteristics for turbine systems are shown in Table VI-C-1. The three main categories of systems to be considered are as follows: (1) turbine systems which use liquid monopropellant or hydrogen-oxygen bipropellant fuel, (2) the hydrogen-oxygen bipropellant reciprocating engine, and (3) a static converter system which uses hot combustion products as a heat source.

Only open cycle systems will be considered here since for short term applications, the closed cycle has obvious disadvantages arising from (1) the complexities of handling another fluid and (2) the radiator weight required

TABLE VI-C-1

TYPICAL OPTIMUM TURBINE SYSTEM CONFIGURATION DESIGN CHARACTERISTICS

(Ref. VI-C-1)

	Short Duration	Medium Duration	Long Duration*
Energy Source	Solid Propellants	Liquid Monopropellants	Bipropellants
Heat Sink	Thermal Lag	Expendable Evaporants	Propellants of Expendable Evaporants
Type of Turbine	Modified Terry	Axial Flow Impulse	Re-Entry
Lube System	Grease Pack or Splash	Splash	Pressure
Fuel System	Solid Propellant Gas Generator	Direct-Pressurized Monofuel Tank	Fuel Pump(s)
Turbine Design Criteria	Minimum Fixed Weight or Diameter Limitation Imposed by Envelope	Limiting Tip Speed	Minimum SPC and Long Operating Life
Fuels	Ammonium Nitrate Composite or Double Base Solid Propellants	Ethylene Oxide, Hydrazine or N-Propyl Nitrate	Hydrogen-Oxygen or Nitrogen Tetroxide-Hydrazine

*The time bracket is somewhat flexible, in that higher power levels shorten the minimum duration for which a hydrogen-oxygen system becomes applicable.

to reject waste heat from the cycle. Another disadvantage of the closed cycle is the Carnot efficiency imposed by maximum cycle temperature and minimum radiator temperature. The open cycle, on the other hand, rejects waste heat into the exhaust gas and is limited only by the pressure ratio and engine efficiency. As an example, the crossover point in time where a closed cycle (using high-pressure gas storage) became lighter than an open cycle system varied from 15 to 200 hours, depending on power level, length of time that fuel is stored, and other factors.

The merit of these chemical systems is enhanced by their possible utilization in supplementary functions. For example, the oxygen or steam from the decomposition of hydrogen peroxide can be used in vehicle life support systems. The liquid propellant can also be used as a coolant or heat sink before being ducted into the gas generator portion of the secondary power system. Another example is the use of combustion products in an attitude control system, where nozzles are used to change the direction of gas flow.

Over-all system weight will be determined by the supplementary functions of fuel and decomposition products. A detailed examination of system weight savings is excluded here but must be considered by the vehicle designer.

AiResearch cites the following three potential advantages which may result from the "Integrated Power and Environmental Control System":

a. Optimum Utilization of the Cooling Media

The various components to be cooled have greatly varying temperature tolerances. In integrated systems, the coolant, which may be an expendable evaporant, can often be used sequentially to cool different components at increasing

temperature levels. The total heat rejection capacity of the coolant is increased, thereby reducing the heat sink requirements, regardless of the type of heat sink used.

b. Combined Power Cycle Working Fluid and Heat Sink

If waste heat is rejected to the power cycle working fluid, part of the waste energy can be recovered in the form of useful output power, thus improving the power cycle specific fuel consumption. The available cooling capacity in the power unit propellant flow may, in some designs to be considered, be adequate to meet the entire cooling load, eliminating the need for a separate expendable evaporant.

c. System Simplification

When the various fluid loops (APU propellants, expendable evaporants, intermediate heat transfer fluids, etc.), the associated components (reservoirs, heat exchangers, pumps, valves, controls, etc.), and the power conversion equipment are integrated into a single system, maximum use can be made of advanced packaging techniques whereby structure is combined with manifolding and mounting provisions. This results in rugged systems which have a minimum of external fittings and lines and which can be tested for performance as a unit. Installation within the vehicle is also simplified, since the number of components requiring attachment to the vehicle structure is reduced.

1.0 OPEN CYCLE TURBINE

A wide variety of monopropellant and bipropellant fuels have been used successfully in operation of gas generators and turbines. Propellants considered for open cycle secondary power systems have included solid propellants, ethylene oxide, propyl nitrate, hydrogen peroxide, hydrogen-peroxide-hydrazine, hydrogen-peroxide-diesel fuel, etc. Because of their evident superiority and likelihood of being used, only hydrazine and hydrogen-oxygen propellant systems will be discussed here -- their use and performance characteristics applying in general to future superior propellants. The performance of some typical propellants is summarized in Table VI-C-2.

As is characteristic of bipropellant systems, high impulses and available energies are achieved at gas temperatures too high for use in uncooled prime movers that operate continuously. This is indicated in Figure VI-C-1, which plots a number of test points of various bipropellant systems. In order to reduce this temperature to the design region of 1,600 - 1,900°F, it is necessary to operate at nonstoichiometric conditions with a consequent reduced impulse to a level showing little advantage over a good monopropellant such as hydrazine.

In the case of the hydrogen-oxygen system, the energy available from the stoichiometric reaction results in an impulse of roughly 350 seconds (pressure ratio 20/1) at a temperature of approximately 5,900°F which can be reduced by adding excess fuel or oxidizer. A more satisfactory method is the addition of excess hydrogen, which results in a peak impulse of 380 seconds at 4,000°F and 340 seconds at 1,800°F. This reaction is about twice that available from hydrazine and more than twice that available

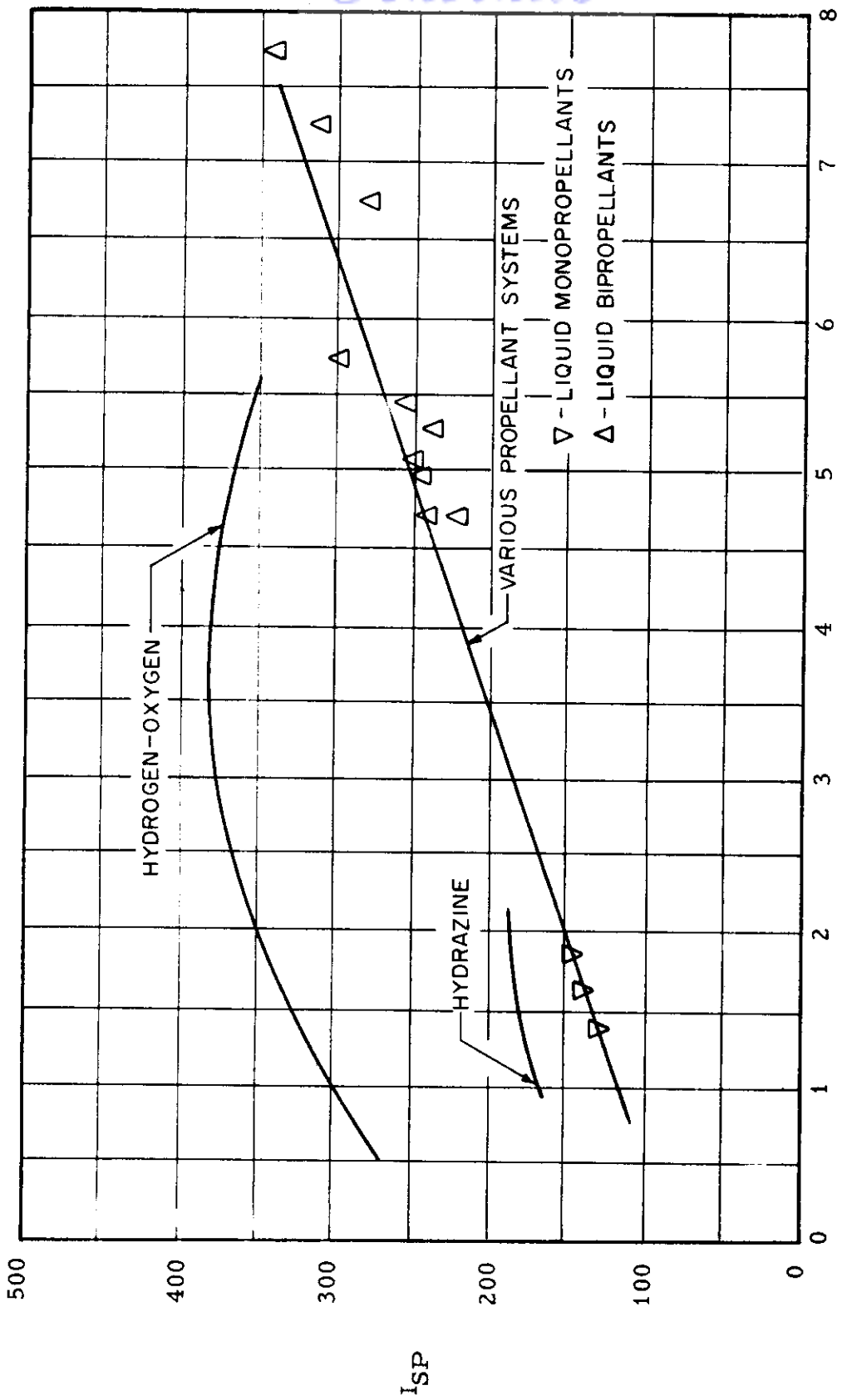

FIGURE VI-C-1 SPECIFIC IMPULSE OF PROPELLANT SYSTEMS (PRESSURE RATIO-20:1)

TABLE VI-C-2

PERFORMANCE OF TYPICAL APU PROPELLANTS

(Ref. VI-C-1)

	Ethylene Oxide	95 Percent Hydrazine	N-Propyl Nitrate	Solid Propellant	H_2-O_2 Bipropellant
Gas Temperature, deg F	1,860	1,900[1]	1,940	1,830	1,840°F
Gas Molecular Weight, M_w	20.5	15.2	16.8	20.4	3.84
Specific Heat Ratio, γ	1.180	1.260	1.325	1.300	1.4
Propellant Density, lb/ft^3	49.9[2]	60.1[2]	62.0[2]	96.7	6.8
Oxidizer/Fuel Ratio	-	-	-	1.78[3]	1.0[4]
Adiabatic Heat,[5] ft x 10^{-5}, H_{ad}	11.47	11.60	9.0	7.53	41.8
Melting Point, deg F	-171	34	-150	-	-
Normal Boiling Point, deg F	51	236	232	-	-

(1) Controllable by Gas Generator Design Over the Range from 1,400-2,300°F.

(2) At 160°F.

(3) Stoichiometric O/F = 9.0, T_p = 3,500°F.

(4) Stoichiometric O/F = 7.94, T_p = 5,920°F at 600 psia.

(5) Infinite Pressure Ratio.

from other propellant systems. The specific output of the cycle is a function of the thermodynamic properties of the gas, the pressure ratio, and prime mover efficiency. The available work is expressed by:

$$\frac{\text{ft lb f}}{\text{lb m}} = \frac{\gamma}{(\gamma - 1)} \frac{R T_p}{M_w} \cdot \eta_e \left[1 - \left(\frac{P_e}{P_c} \right)^{\frac{\gamma - 1}{\gamma}} \right] \qquad \text{(C-1)}$$

where

γ = specific heat ratio

M_w = molecular weight

T_p = gas temperature

P_c = inlet pressure

P_e = exhaust pressure

η_e = engine efficiency

R = gas constant.

Optimum design of turbines and the design compromises necessary due to temperature, tip speeds, and other factors are discussed in Volume III, Section B.

Using Equation C-1, the theoretical specific fuel consumption for the hydrazine and hydrogen-oxygen systems can be shown as a function of engine efficiency, as in Figure VI-C-2. These curves--combined with expected engine efficiency under various pressures, temperatures, etc--lead to the optimum design for long-term secondary power systems.

The very high adiabatic heats of the propellant gases suggest the use of pressure staging to achieve more nearly optimum velocity ratios and higher over-all efficiency. However, the theoretical thermodynamic gain

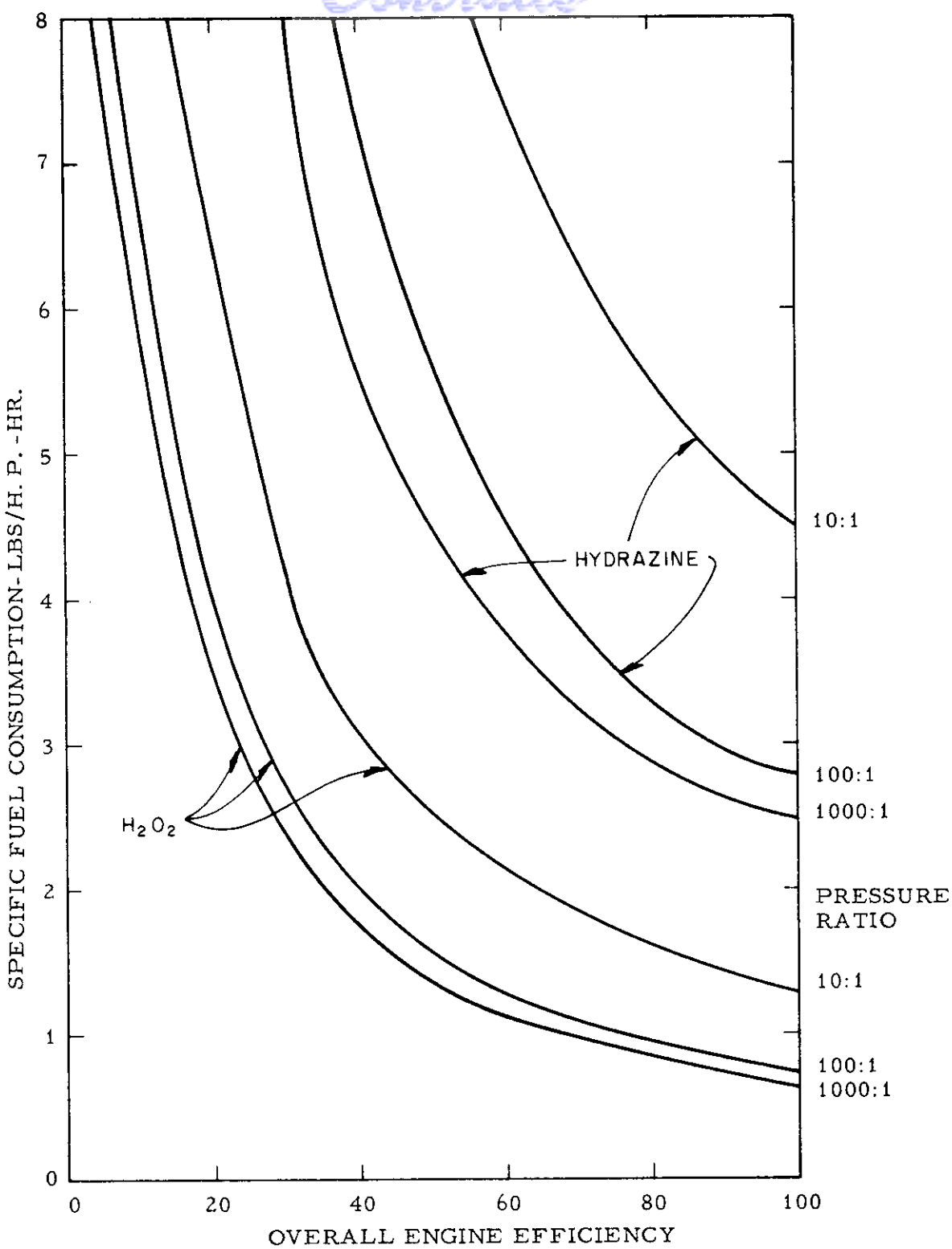

FIGURE VI-C-2

THEORETICAL ENGINE PERFORMANCE AT VARIOUS PRESSURE RATIOS USING HYDROGEN-OXYGEN AND HYDRAZINE FUEL (95 % N_2H_y, 4% H_2O)

(BASED UPON HYDROGEN AND OXYGEN FED INTO A GAS GENERATOR AT A TEMPERATURE OF 77°F)

(REF. VI-C-7)

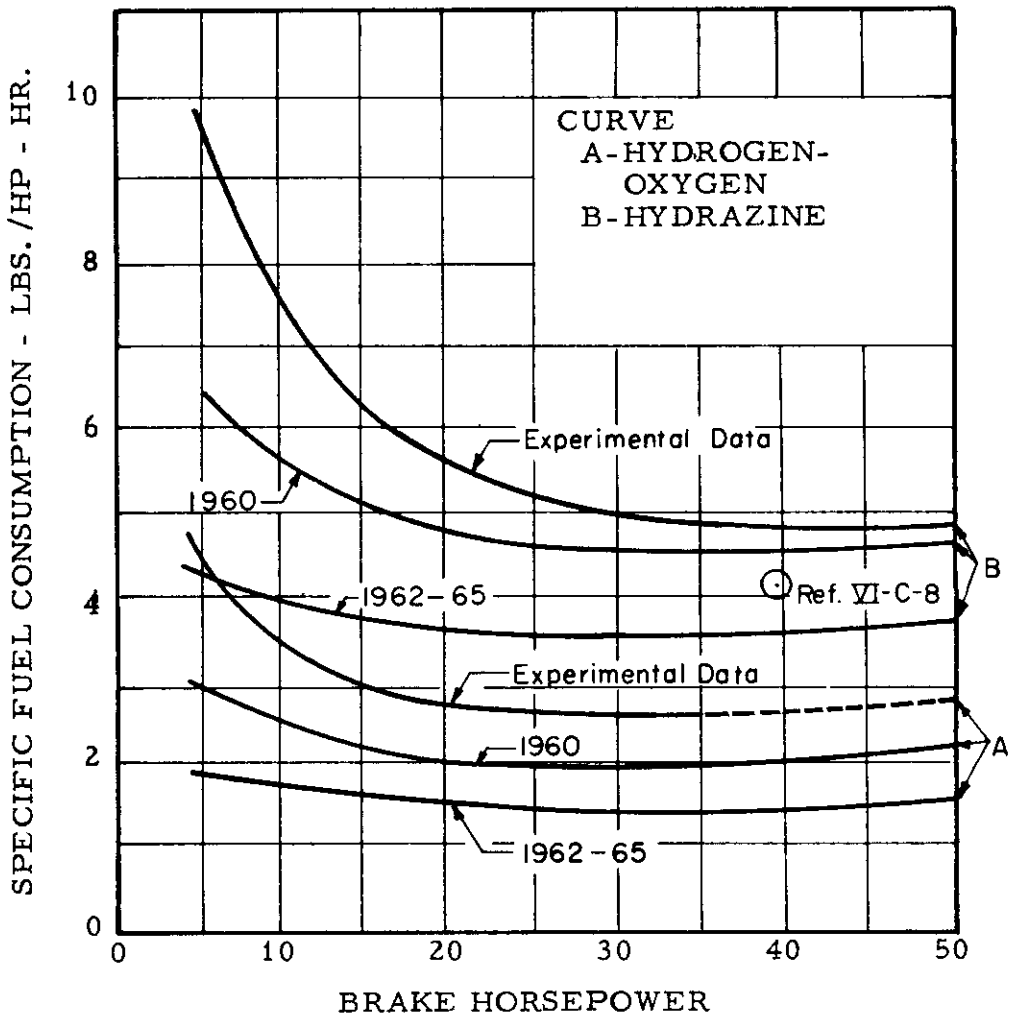

FIGURE VI-C-3 MEASURED PERFORMANCE 2 STAGE AXIAL FLOW TURBINE CURRENT AND PREDICTED TEST RESULTS (REF. VI-C-7)

with increasing number of stages is offset by increasing disc friction loss and increasing turbine weight. The optimum turbine design depends on the power level and length of duty cycle. In general, use of a single-stage turbine will be optimum for energy outputs of less than about 1 kw/hr.

An example of the specific fuel consumption of a two-stage axial flow turbine is shown in Figure VI-C-3, which presents actual performance of equipment available in 1959 (Ref. VI-C-7) operating on hydrazine and hydrogen-oxygen at 1,800°F and at a pressure ratio of 150:1 at 25 hp output. As shown, fuel consumption increases with a decrease in power output (based on power out of the gear box at 12,000 rpm). At the 30 hp point, the efficiency of this turbine ranged from 30 percent for oxygen-hydrogen to 55 percent for hydrazine. Also shown are Orsini's estimates of 1960 performance and possible improvements in 1962-65 if serious effort is expended. An additional data point, shown from Ref. VI-C-8, represents performance of a hydrazine two-stage, re-entry turbine (Sundstrand-Turbo) with a flame temperature of 2,500°R and a pressure ratio of 960.

Weights for many of the turbine APU systems which have reached hardware status have been plotted by McJones and Howard and are shown in Figure VI-C-4 (Ref. VI-C-2). The wide scatter in system weight is not surprising in view of the differences in duty cycle, speed control accuracy, etc. Average values of fixed weight for the turbine and the hydraulic and electric drive are shown. For short duration missions, the lightest APU's would be chosen at the expense of specific fuel consumption. Figure VI-C-5 summarizes the expected

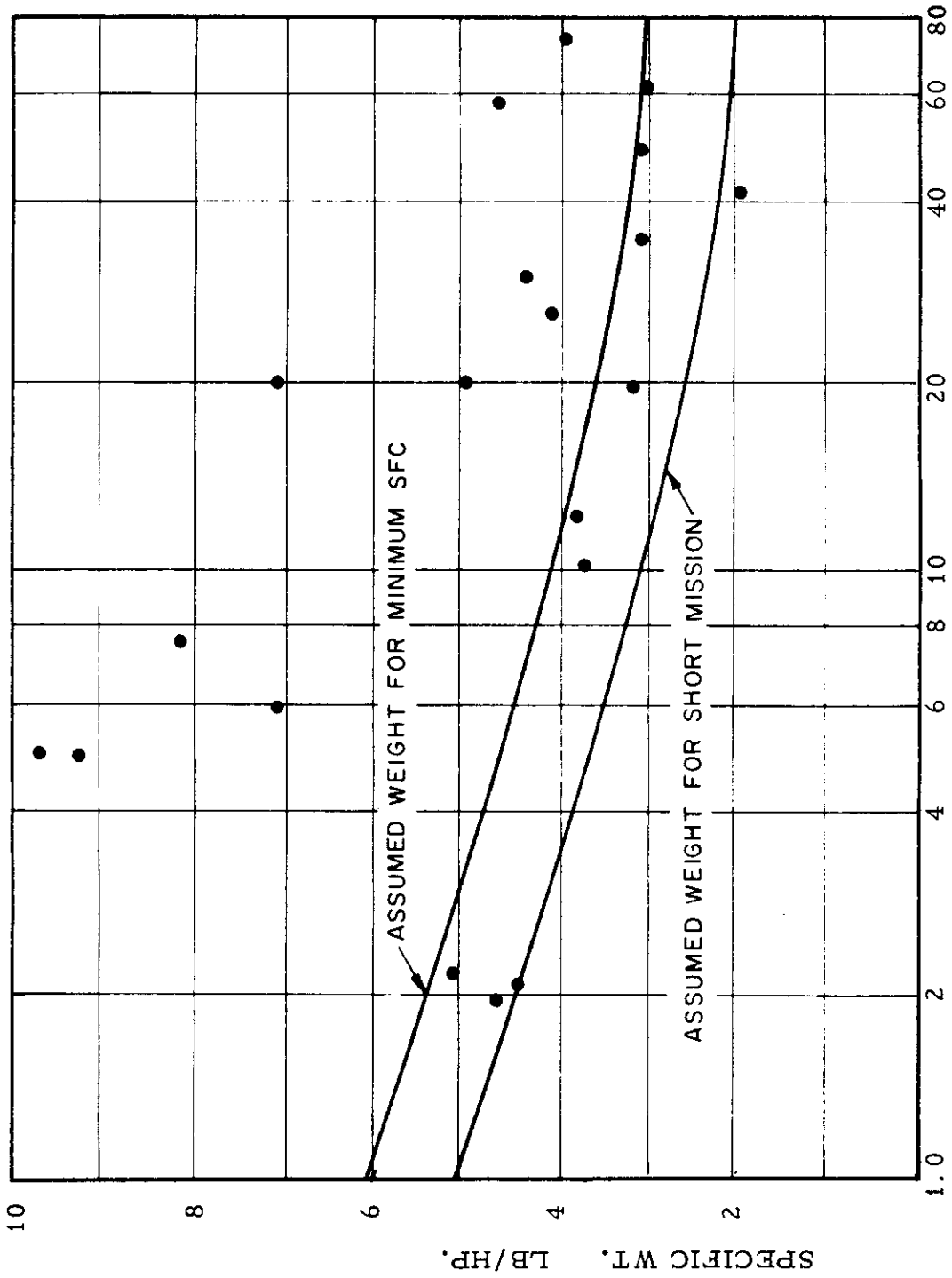

FIGURE VI-C-4 FIXED WEIGHT OF TURBINE DRIVES INCLUDES HYD. AND/OR ELECTRIC OUTPUT (REF. VI-C-2)

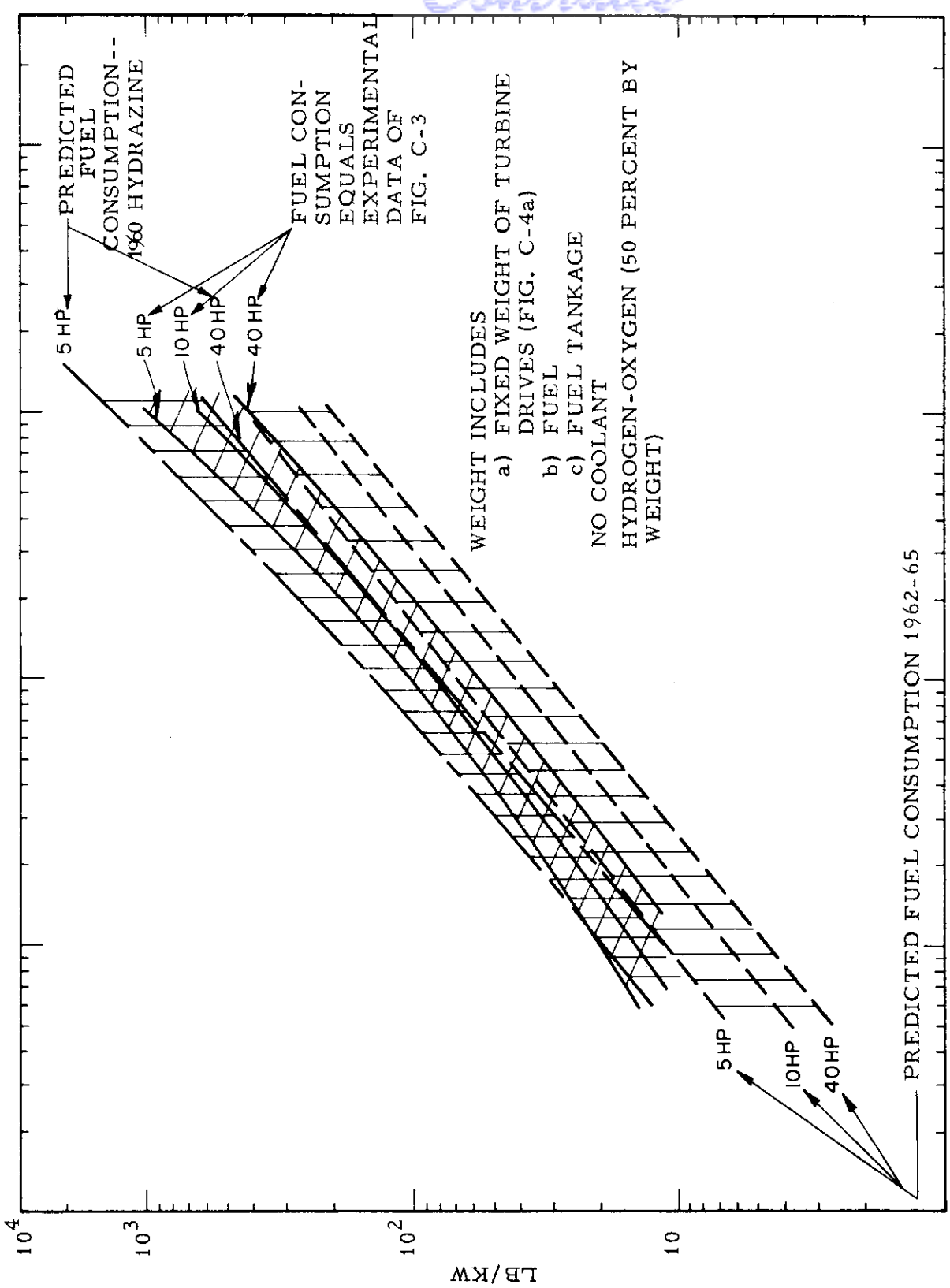

FIGURE VI-C-5 SPECIFIC WEIGHT OF OPEN CYCLE TURBINE SYSTEMS

weight of an open cycle turbine system using the experimental data and predicted performance curves of Figure VI-C-3 for hydrazine and hydrogen-oxygen. As shown, the use of hydrogen-oxygen has a weight advantage over hydrazine for the short durations considered here. For long-term operation (e.g., weeks) the hydrogen and oxygen losses incurred in long storage may shift the weight advantage to the hydrazine unit.

In addition to specific fuel consumption, other factors will influence the choice of propellant system. If possible, the fuel system should provide heat sink capabilities for the space vehicle. The temperature rise required of the propellants prior to utilization can conceivably come from the waste heat dissipated in the vehicle capsule. For example, hydrazine stored at 40°F and allowed to reach 200°F before entering the gas generator will absorb about 120 Btu/lb and provide a useful power of about 730 Btu/lb. As an additional coolant, approximately .61 pounds of water would be required for every pound of propellant in order to dissipate the additional energy of the fuel. For the hydrogen-oxygen system, the difference between useful power and possible heat absorption would be about 920 Btu/lb, requiring .92 pounds of water for every pound of propellant. The vehicle system designer must consider the fact that although less fuel is required by a highly efficient power system, more coolant in the form of water or other fluid might be required. Figure VI-C-6 shows predicted system weights including the necessary coolant water and an additional loss due to the generator losses.

Although hydrogen-oxygen gas generators and turbines have been operated on a basis suitable for space application, extensive experience has not been accumulated. Problems remain in the areas of integration

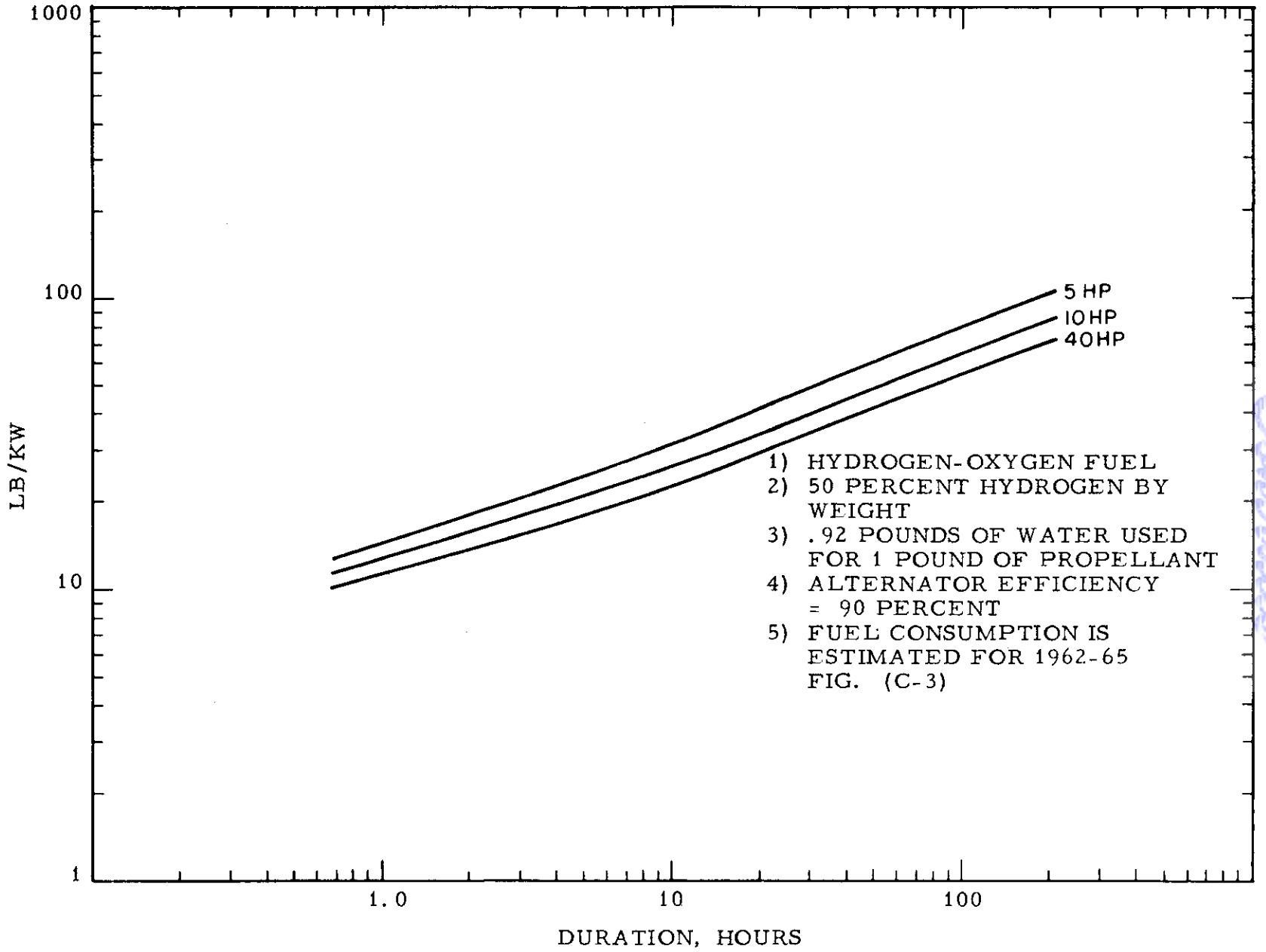

FIGURE VI-C-6 SPECIFIC WEIGHT OF OPEN CYCLE TURBINE 1962-65

with a vehicle and development of containers, heat exchangers, and controls compatible with dual requirements of heat sink and power generation functions. In general, chemically fueled open cycle power systems have thousands of actual running hours of experience to support design criteria. The basic design of much of the mechanical energy conversion equipment does not change radically with the use of a new fuel system such as the hydrogen-oxygen system. Therefore, present and predicted future performance characteristics can be used with some confidence.

The use of hydrogen-oxygen bipropellant fuel as a supplementary heat sink is determined by the oxygen/hydrogen ratio. For the turbine system, this ratio is about 50 percent by weight. As explained in Section 2.0, the ratio for the positive displacement engine becomes about .4 lb of oxygen to 1 lb of hydrogen--this large amount of hydrogen negating the requirement for cooling water by absorbing the waste heat. At the other end of the spectrum, a fuel cell is poorly suited to do joint work as a cooling system because of its high oxygen/hydrogen ratio.

The high reliability of open cycle turbine systems has been demonstrated over short periods of operation. For long durations, reliability will be increased by lower temperatures of operation, heavier construction, and other factors which tend to decrease efficiency and increase over-all system weight. When properly designed, these systems may have reliabilities greater than .95, with individual component reliabilities of greater than .99 proven in tests to date.

Figure VI-C-7 illustrates the block diagram associated with a typical hydrogen-oxygen integrated power and environmental control system.

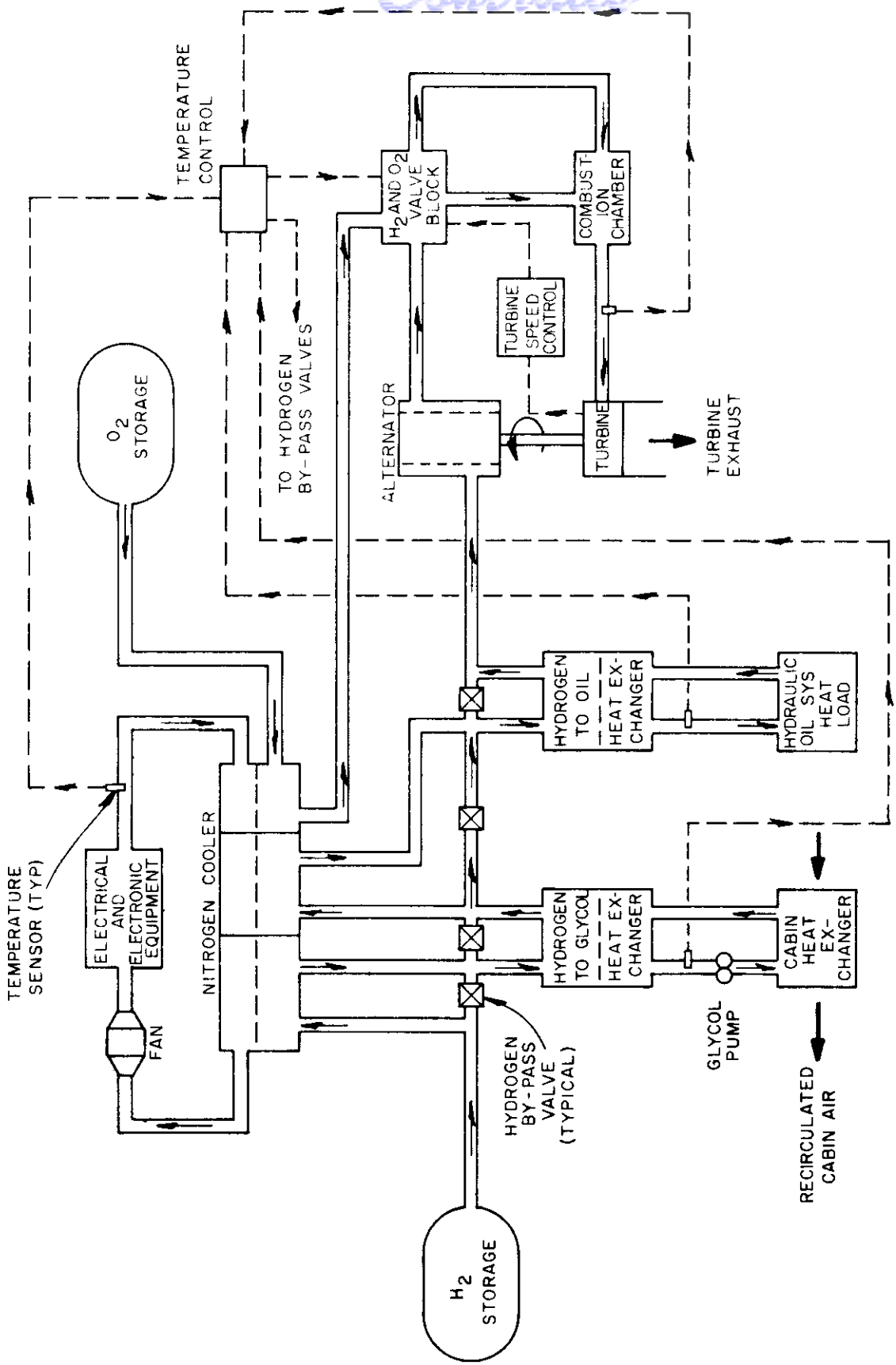

FIGURE VI-C-7 SCHEMATIC DIAGRAM OF A TYPICAL HYDROGEN-OXYGEN IPECS (AIRESEARCH MFG. CO.)

2.0 RECIPROCATING ENGINE

Another possibility for the use of hydrogen-oxygen bipropellant fuel is a positive displacement engine operating on an Otto cycle. At present, these engines using hydrogen are characterized by efficiencies of approximately 80 percent, inlet pressure of 765 psia, and inlet temperatures on the order of 850°F. These characteristics result in a specific propellant consumption of 1.5 lb/hp at an oxygen/hydrogen ratio of about .4 to 1 (at a 3 hp level).

The efficiency of the positive displacement engine makes it well suited for use in a combined power and cooling system. The large hydrogen consumption negates the need for cooling water, as the hydrogen can absorb all of the excess heat.

The weight breakdown for a simple system is typically illustrated in Table VI-C-3 below:

TABLE VI-C-3

ESTIMATED COMPONENT WEIGHTS

	Pounds
H_2 tank (with insulation)	120
Pump	4
Pressurization system	30
Hydrogen (167 lb usable)	172
Hydrogen supply	326
Tank	25
Oxygen	61
Oxygen supply	86
Helium to hydrogen	3.5
Hydraulic oil to hydrogen	8.2
Manned-compartment hydrogen	4.1
Circulation blow	3.2
Heat exchangers	19
Combustor	3
Expansion engine	24
Alternator	75
Hydraulic pump	7
Speed control	21
Power generators	127
Total	558

For longer missions, the engine would be modified to reduce the rate of fuel consumption at the expense of increasing weight. The estimated weight of a hydrogen-oxygen reciprocating unit for various durations, as shown in Figure VI-C-8, includes the machinery, hydrogen-oxygen, and fuel tanks.

The positive displacement engine is attractive because it will operate efficiently at all power levels on hydrogen, whereas turbines are not readily adaptable to low horsepower, low specific propellant consumption applications. The positive displacement engine, with a variable "cutoff" point where the gas inlet valve closes, gives minimum propellant consumption at any load--a characteristic desirable for space missions necessitating many hours of operation at a reduced load and a brief spurt of power at peak load. A wide range of power operation is obtainable in a turbine only through the added complexity of variable geometry or the additional loss of efficiency through throttling. The predicted engine performance is shown in Figure VI-C-9. Figure VI-C-10 illustrates the three-cylinder engine.

Vickers made several detailed design studies of positive displacement expansion engines before settling on a three-cylinder design (Figure VI-C-10). In-line as well as radial-cylinder arrangements were considered.

A cam-actuated, coaxial or concentric, double-poppet-valve design was chosen to control the gas intake. In effect, a variable-opening poppet valve is used, operated by the differential action of a cam driven by the engine shaft and another cam driven by the governor mechanism. The valves are actuated through concentric push rods from the rocker arms with

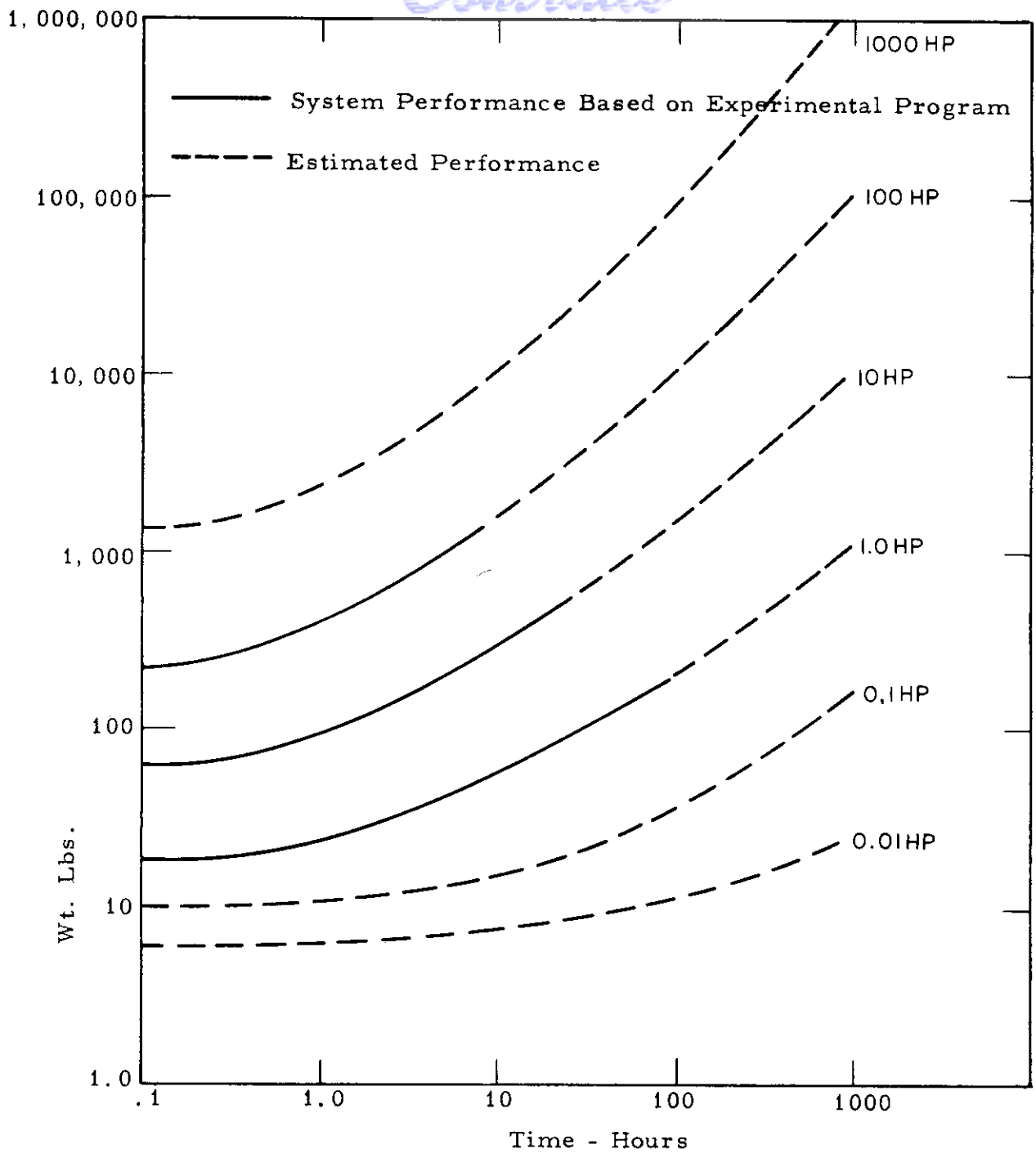

FIG. VI-C-8 HYDROGEN-OXYGEN EXPANSION SYSTEM INCLUDES: ENGINE, FUEL, TANKAGE, ELECTRIC GENERATOR AND CONTROLS (Vickers, Inc.)

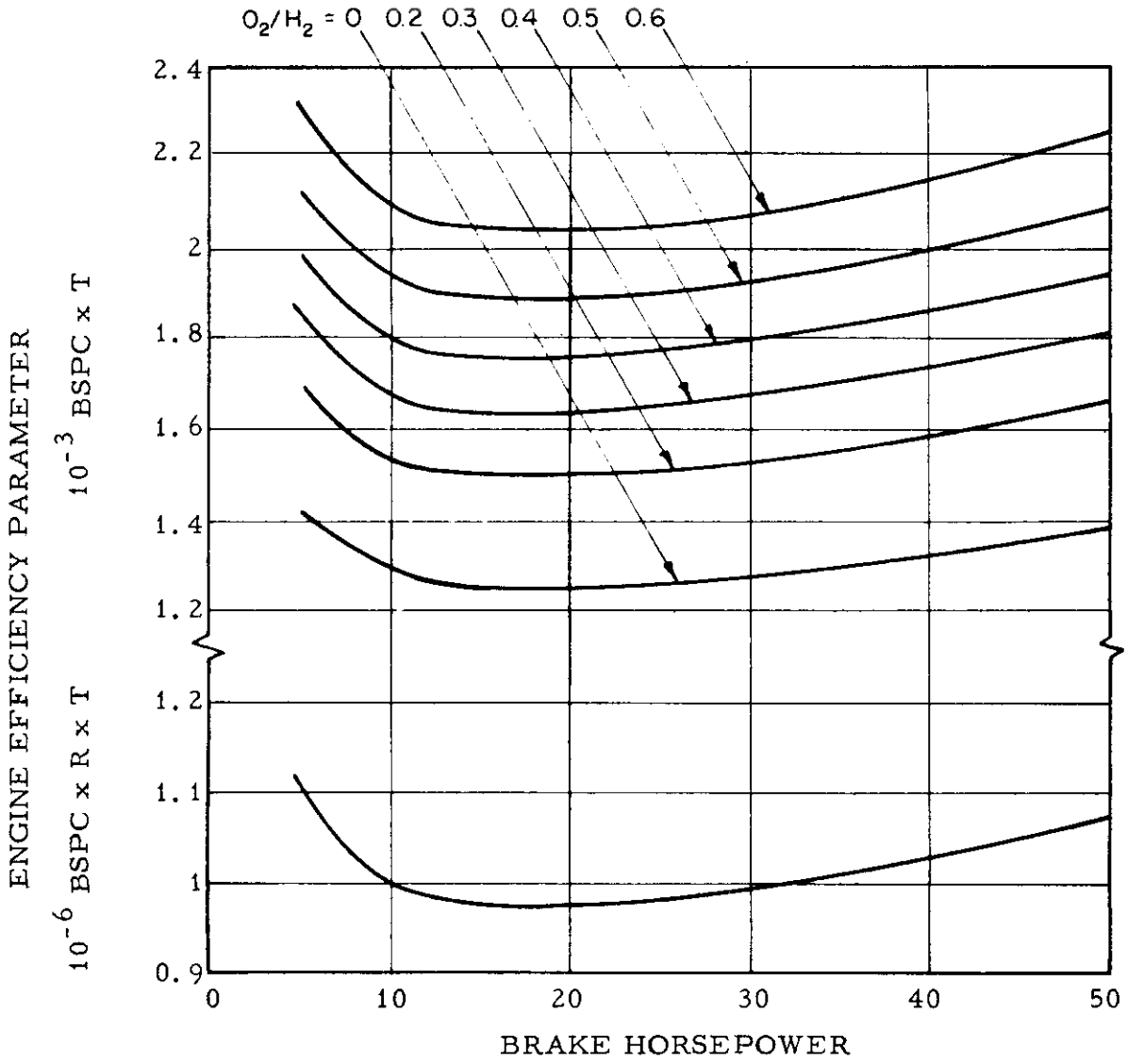

FIGURE VI-C-9

PREDICTED PERFORMANCE of three-cylinder hydrogen engine designed for 3.5 per cent clearance volume, eight cubic inches piston displacement, 8000 rpm, 1000 psia inlet pressure, and 10 psia exhaust pressure at various inlet temperatures (T) and oxidizer-fuel ratios (where BSPC is brake specific propellant consumption). The gas constant (R) and (T) are used in plotting engine efficiency so that comparisons can be made for different gases and temperatures.

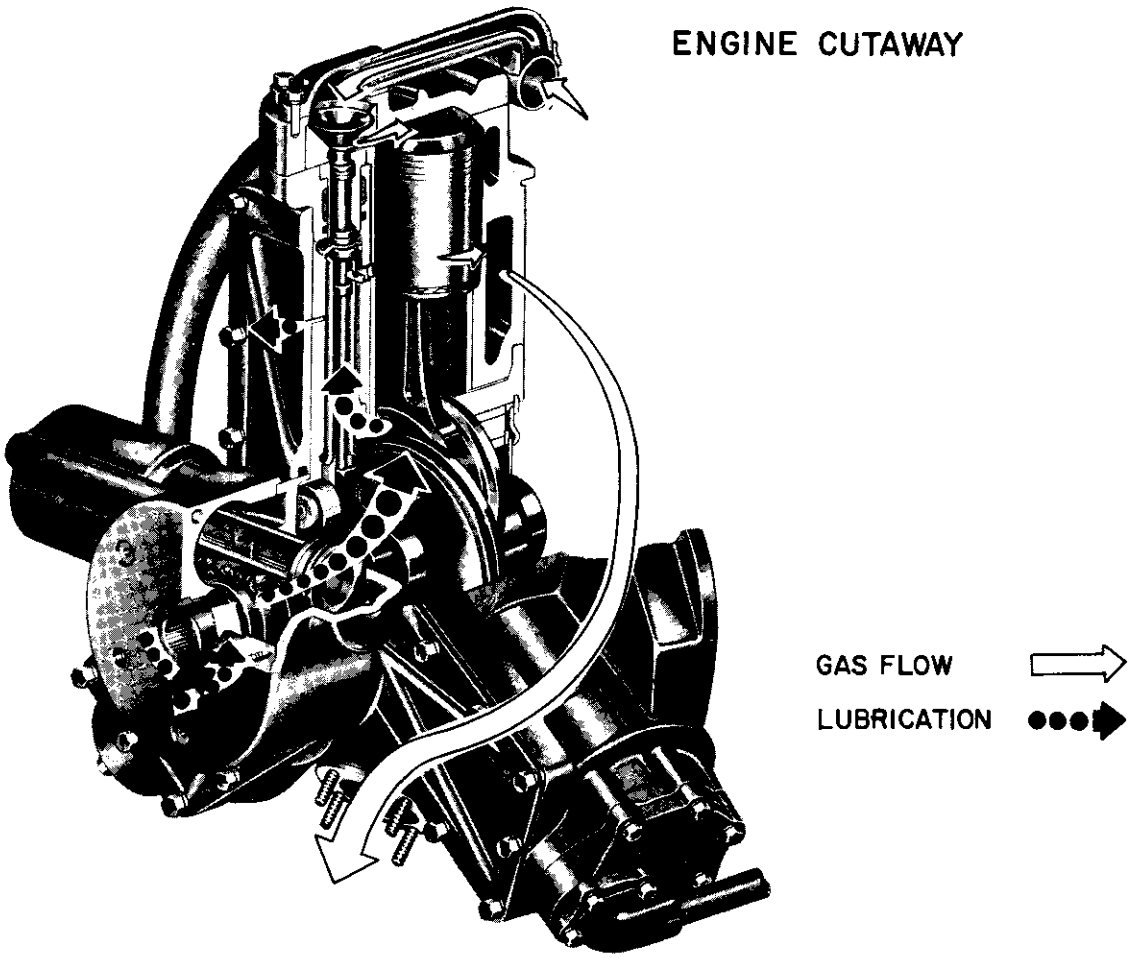

FIGURE VI-C-10 THREE-CYLINDER HYDROGEN ENGINE BEING DEVELOPED BY VICKERS. It weighs 15 lb., has 1.25-inch bore and stroke, and a 10-inch diameter. It will deliver 40 horsepower at 8000 rpm and is designed for most efficient operation at an inlet pressure of 750 psia and an inlet gas temperature of 850 degrees F.

roller cam followers.

A mist oil lubrication system is used in which oil from a gear pump is metered into the crankshaft and reaches the connecting rod bearings through drilled passages. It is then thrown out in the form of a mist, or spray, which lubricates crankshaft bearings, cylinder walls, piston pin, valve mechanism, and other areas. Oil mist is removed from the crankshaft through three relief valves in the valve chamber and is eventually dumped overboard by the exhaust system. Vickers expects the engine oil consumption to be considerably less than 0.05 lb/hp-hr.

For over a year now, Vickers has been running an experimental single-cylinder test engine supplied by a small combustor to collect data for a full-fledged development program devoted to a three-cylinder engine. The results have been most encouraging. So far, Vickers has accomplished the following: (1) shown by test that a positive displacement engine can operate at very low specific propellant consumption and low horsepower levels, (2) proved that its new variable-cutoff-valve concept is practical for high-speed operation, and (3) built and tested a hydrogen-oxygen combustor to operate over a wide range of mixture ratios and flow rates.

Vickers has piled up over 75 hours of running time on two engines that, it reports, have caused very few mechanical headaches. The engines have been operated at inlet pressures up to 765 psia and inlet temperatures ranging from 70 to 850 degrees F. Although they have been operated at as much as 8,000 rpm, most of the testing has been done at 6,000 rpm or less. Inlet valve cutoff has been varied from 4 to 30 percent of the piston stroke.

The combustor, to which the liquid hydrogen is delivered after passing through the heat exchangers, is designed to handle fuel-rich mixture ratios. The flow of hydrogen depends primarily on the total heat that has to be absorbed. No more oxidizer is mixed with the fuel than is needed to meet vehicle power demands. To insure reliable combustion at fuel-rich mixtures, the basic, or primary, hydrogen flow (needed for power) is injected along with the oxygen into a central combustion zone. The rest of the hydrogen (needed for cooling) is then injected into a mixing zone.

In tests of an experimental combustor, exit gas temperatures have varied from 200 to 935 degrees F (depending on the mixture ratio and the hydrogen injection temperature). Vickers' results show that the combustor will operate at pressure levels up to 1,000 psi even at very low oxidizer-fuel ratios and at low flow rates.

The power package consists of engine, alternator, hydraulic pump, and speed control--with both the alternator and the pump being driven at engine speed. The alternator is a six-pole, brushless, 400-cps unit similar in design to the alternators of current high performance aircraft. Its operating efficiency should approach 90 percent in a helium atmosphere.

The variable-displacement pump is a typical aircraft hydraulic-piston type, with nine axial pistons reciprocated in a cylinder block. Displacement is automatically controlled to maintain a constant hydraulic pressure output.

The speed control consists of a centrifugal governor driven directly by the engine shaft. The governor controls the speed to within 1 percent

by varying the phasing of an inlet cutoff valve on the engine, thereby regulating gas flow and engine power.

The weight and performance values of Figure VI-C-8 are based upon design studies and experimental work described above. The extended duration of performance shown in this figure can be improved by the use of a compound expansion engine, wherein the heat addition and expansion processes are repeated two or more times before the working fluid is finally exhausted overboard. Vickers estimates this process can lower the over-all consumption of hydrogen and oxygen to values well below 1.0 lb/hp-hr and increase the oxygen-hydrogen ratio toward stoichiometric, minimizing both propellant volume and tankage weight. Future performance curves are plotted where a fuel consumption of 1.1 lb/hp-hr is assumed at the longest durations.

3.0 STATIC HEAT ENGINES

Units which burn hydrocarbon fuels (i.e., propane) to heat a thermopile have been recently developed for commercial power generators by several companies (i.e., General Instrument Corporation and Westinghouse Corporation). The units are constructed in a manner quite similar to commercial waste heat recovery units. The thermocouples are placed on the perimeter of a stack designed to entrap the combustion products, and the stack walls are maintained at a temperature designed for optimum fuel utilization.

The over-all efficiency of the device may be roughly approximated by the following equation:

$$\eta_{system} = \eta_{converter}\ \eta_{burner}\ \eta_{stack}$$

In the thermoelectric units built to date, burner efficiency when using air is approximately 85 percent. Thermoelectric efficiency, using lead telluride thermal elements, is on the order of 7 to 8 percent--the remaining losses resulting from combustion gas energy still contained in the stack. In current units, the stack losses are about 40 to 50 percent. Over-all unit efficiencies of 2.5 to 3 percent have been reported.

For ground application, the radiator is a finned structure which maintains cold temperatures of about 150°F. For space application, where radiation is the mode of heat loss, the optimum cold temperature will be about 250°F, with a resultant drop in thermoelectric efficiency from roughly 8 to 7 percent.

Present devices emphasize ruggedness and reliability rather than light weight. Small 5-watt units weigh on the order of 2 lb/watt, whereas

large 100-watt units weigh about 1 lb/watt. The reliability of these devices is extremely high. Cost is currently about $1,000 per watt but will drop to $100 per watt in large-scale quantities.

The performance of this type of device will undoubtedly improve with better design and increased converter efficiency. Advanced static converters will operate at higher source temperatures and higher efficiencies, as discussed in Volume IV. Burner efficiencies will also improve. Stack losses will decrease due to better stack design but will increase at higher temperatures due to the increased energy of the exhaust.

Table VI-C-4 below presents an estimate of the possible performance of a combustive-fueled static converter system using thermocouples and thermionic emitters available at present and in 1970. Two types of fuel are considered, propane and hydrogen, each used with oxygen. Hydrogen and oxygen would probably be stored cryogenically. The theoretical whr/lb capacity of the fuel at a stoichiometric ratio with oxygen is shown. In practice, this capacity would drop when a fuel-rich mixture is used to lower the flame temperature.

As shown in Table VI-C-4, the possible specific energy provided by the fuel is relatively low. To fuel weight must be added the weight of the storage tanks and the power sources.

As indicated, the combustive-fueled static converter unit is much heavier at present than primary batteries and, in the future, than primary fuel cells. It would not appear that this type of system is at all suitable for space application.

TABLE VI-C-4

PERFORMANCE OF FUEL-FIRED STATIC CONVERTER GENERATOR

Year	Converter	Fuel	T_h	T_c	$\eta_{converter}$	η_{burner}	η_{stack}	Theoretical whr/lb (Stoichiometric)	$\eta_{overall}$	Possible whr/lb from fuel
1960	Thermocouple	Propane	1,100°F	250	.075	.85	.45	1,250	.029	36.2
		H_2	1,100	250	.075	.85	.45	1,650	.029	47.9
	Thermionic	Propane	1,700	1,100	.05	.85	.40	1,250	.017	
		H_2	1,700	1,100	.05	.85	.39	1,650	.0166	21.2 27.4
1970	Thermocouple	Propane	2,000	900	.25	.95	.45	1,250	.107	134
		H_2	2,000	900	.25	.95	.45	1,650	.107	176
	Thermionic	Propane	2,800	1,400	.3	.95	.4	1,250	.114	142.5
		H_2	2,800	1,400	.3	.95	.4	1,650	.114	188

REFERENCE LIST

VI-C-1 Burriss, W. L. "Integrated Power and Environmental Cooling Systems," July 8, 1960.

VI-C-2 Howard, Harris J., and McJones, Robert W. (Vickers, Inc.). "Available Power Systems for Space Vehicles," ARS Paper No. 1032-59, November 16, 1959.

VI-C-3 Wayman, W. E., and Mills, A. W. (Sundstrand-Turbo). "An Advanced Chemically Fueled Power Supply for Space Vehicles," ASME Paper 60-AV-29, June 5, 1960.

VI-C-4 Wood, Homer J. (H. J. Wood and Associates) and Morgan, Normand E. (Vickers, Inc.) "Comparative Rating of Positive-Displacement Engines and Turbines for Cryogenic Power Systems," August 1960.

VI-C-5 Howard, H. J., and Laughlin, R. M. (Vickers, Inc.) "The Use of Chemical Power Systems in the Construction, Servicing and Operation of Manned Space Stations." Presented at IAS Manned Space Stations Symposium, April 20-22, 1960.

VI-C-6 Deacon, W. K. (Vickers, Inc.) "Available Power Systems for Space Vehicles." Presented at Hydraulic Conference, November 1959.

VI-C-7 Orsini, A. (Walter Kidde and Co., Inc.) "Propellant Type Open Cycle Secondary Power Systems for Manned Space Vehicles," ARS Paper No. 1035-59, November 16, 1959.

VI-C-8 Linhardt, Hans D., and Silvern, D. H. (Sundstrand-Turbo) "Analysis of Partial Admission Axial Impulse Turbines," ARS Paper No. 1202-60.

VI-C-9 Basi, Victor de. (Space Aeronautics) "Cryogenic Accessory Package Looks Feasible," 1960 R and D Handbook.

VI-C-10 Somers, E. V., and Swanson, B. W. "Optimization of a Conventional Fuel Fired Thermoelectric Generator." Contained in "Direct Conversion of Heat to Electricity" by Kaye, J. and Welsh, J. A. (Published by Wiley and Sons, Inc.), 1960.

VI-C-11 Commercial Literature, General Instrument Co.

ENERGY CONVERSION SYSTEMS REFERENCE HANDBOOK

Volume VI - Chemical Systems

Section D

FUEL STORAGE

W. R. Menetrey
Energy Research Division
ELECTRO-OPTICAL SYSTEMS, INC.

Manuscript released by the author
September 1960 for publication in this
Energy Conversion Systems Reference Handbook

WADD Technical Report 60-699

C O N T E N T S

I L L U S T R A T I O N S

TABLES

D. FUEL STORAGE

The fuel cell and combustion systems discussed in this volume require storage of monopropellant or bipropellant fuel in auxiliary tank structures. The fuel and tanks may be major weight items for long duration and/or high power level applications. Major problem areas for consideration include the following:

a. Minimum weight which will satisfy structural requirements resulting from high internal pressures, accelerations on launch, and minimization of evaporative losses.

b. Controlled fuel flow under zero-g conditions.

c. Additional power requirements and reliability of pumps, auxiliary heaters, controls, and other equipment.

Considered here will be the storage of hydrazine, hydrogen, and oxygen (fuels that will be of interest in the next decade) and the storage problem areas that can be applied to other fuels of interest.

1.0 LIQUID FUELS AT AMBIENT TEMPERATURE

Fuels such as hydrazine can be stored at ambient temperature in single skin structures with stiffening used only at tank openings, points of attachment, and similar locations. This type of construction maximizes strength/weight ratios. Exterior insulation or auxiliary heating is not normally required.

For minimum weight, the tank structure should be spherical, rather than cylindrical, in order to incorporate more surface area. For example, a cylinder with a L/D ratio of two has 54 percent more surface area than does a sphere of the same volume. Also the cylindrical skin must be thicker, particularly on the ends, to maintain minimum stress levels.

For operation at uniform pressure, the required wall thicknesses are as follows:

Cylinder (ASME Code)

$$t_t = \frac{f_s P_t D_t}{2 A_t - .2 P_t} \qquad \text{(D-1)}$$

Sphere (theoretical)

$$t_t = \frac{f_s P_t D_t}{4 A_t}$$

where

t_t = thickness of skin

f_2 = safety factor

P_t = internal pressure

D_t = tank diameter

A_t = yield strength of tank material.

Available tank materials include the following:

Heat treated titanium -- 140, 000 psi

Heat treated steel -- 240, 000 psi

Aluminum (Kaiser 5083) -- 18, 000 psi.

Recently, advanced techniques have decreased tank weight almost by a factor of two, using such materials as wound fiber glass filaments. However, these materials are more subject to failure at high temperatures.

The pressure at any height within the tank is the sum of the gas overpressure and the hydrostatic head due to the acceleration field of the tank. Hydrostatic pressures will be small for the quantities of fuel under consideration, and tanks should be designed with walls of uniform thickness. Using Equation D-1 and neglecting the tank ullage fraction, the ratio of tank weight to fuel weight can be derived as shown in Equation D-2:

Sphere

$$\frac{M_t}{M_f} = \frac{3}{2} \cdot \frac{\rho_t f_s P_t}{\rho_f s_t} \qquad (D-2)$$

Cylinder with 2:1 ellipsoidal caps

$$\frac{M_t}{M_f} = 4 \frac{(B + 0.69)}{(B + \frac{1}{3})} \cdot \frac{\rho_t f_s P_t}{\rho_f (2 s_t - 2 P_t)}$$

where

M_t = mass of tank

M_f = mass of fuel

ρ_t = density of tank material

ρ_f = density of fuel

B = length to diameter ratio of cylindrical tank.

Equation D-2 is depicted in Figure VI-D-1 by the diagonal lines. Several ordinate points are indicated which apply to the storage of hydrazine in titanium, steel, and aluminum tanks at 100 psi and to liquid and gaseous hydrogen/oxygen in titanium. The application of Equation D-2 is limited by the unreasonably thin skin wall resulting from low tank pressures. Using a limiting value of .025 inches for skin thickness, the tank/fuel weight ratio can be derived as a function of skin thickness, shown in Equation D-3 and by the horizontal lines of Figure VI-D-1.

$$M_t = \frac{\rho_t}{\rho_f} \cdot 6 t_t \left(\frac{6 M_f}{\pi \rho_f}\right)^{-1/3} \qquad (D-3)$$

Tank weight will be limited generally by the minimum skin thickness allowable at relatively low pressures.

On the basis of Figure VI-D-1, the total weight of the fuel storage system, derived as a function of propellant mass, is shown in Figure VI-D-2 for several cases (i.e., hydrazine stored in a titanium sphere at 100 psi and gaseous hydrogen and oxygen stored at 6,000 psi). Weight of the pump,

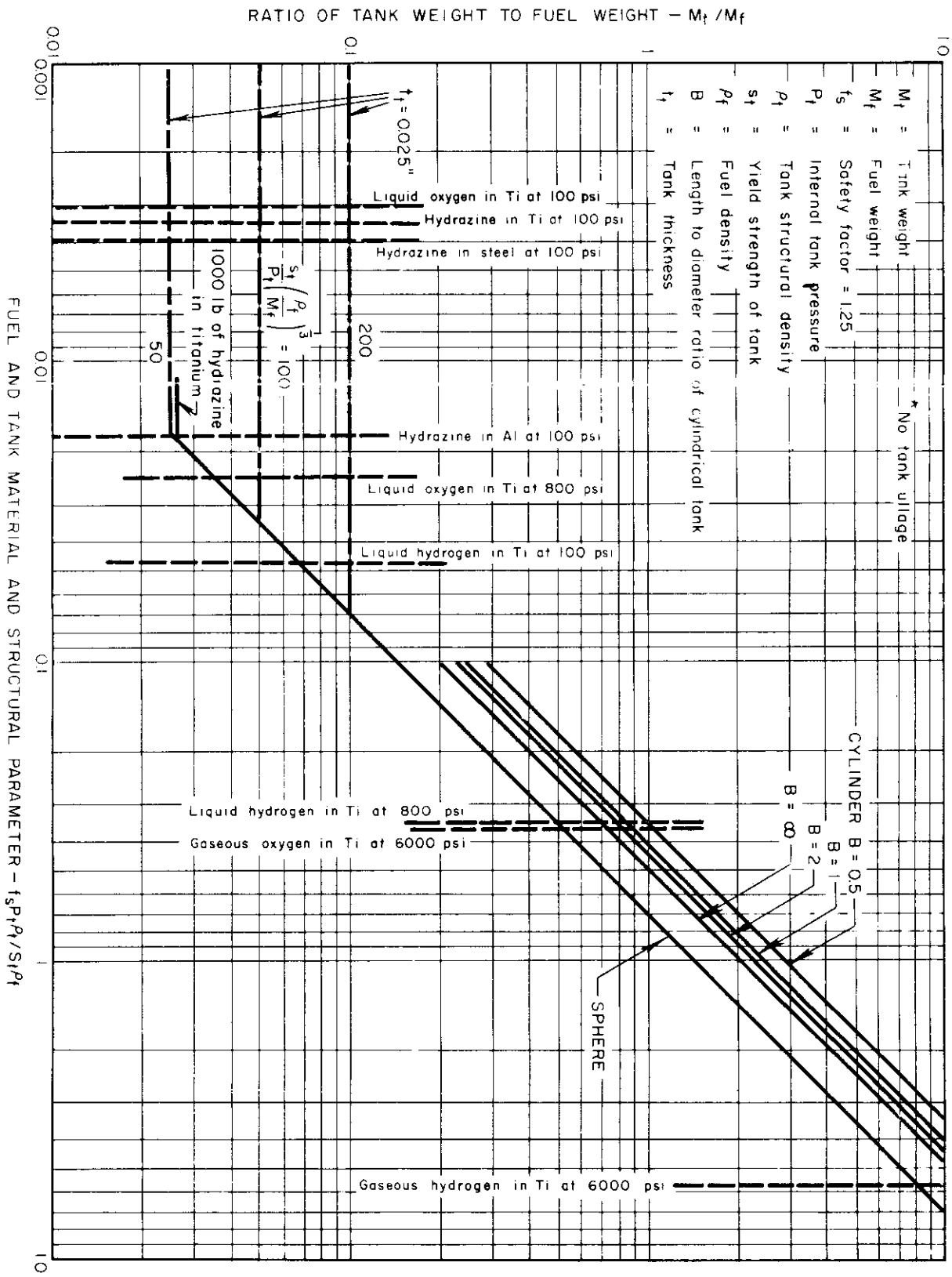

FIGURE VI-D-1 FUEL TANK TO WEIGHT RATIO - SINGLE SKIN STRUCTURE

piping, valves, and other auxiliaries is small and has not been considered in calculations. The weight required by the pressurization system in order to maintain fluid continuity is also relatively small, as compared with the tank and fuel weights.

2.0 GASEOUS STORAGE AT AMBIENT TEMPERATURE

Storage of gaseous hydrogen, oxygen, and other fuels at high pressure and ambient temperature offers the advantage of simplicity and long storage duration -- the only limiting factor in storage duration being the use rate. In addition, equipment associated with cryogenic storage, such as insulated tanks and transfer equipment, would not be required. Since heat transfer is not a problem with ambient temperature gaseous storage, insulation is unnecessary.

The weights of the fuel and tank are given by Equation D-4 and are depicted in Figure VI-D-2.

Sphere

$$M = \frac{M_f}{\left(1 - \frac{P_{ti}}{P_{tf}}\right)} \left(1 + \frac{3}{2} \frac{\rho_t}{\rho_f} \frac{f_s P_t}{s_t}\right) \qquad \text{(D-4)}$$

where

P_{ti} = initial tank pressure

P_{tf} = final tank pressure

M = total mass.

Heat-treated steel tanks would be only slightly heavier than titanium; however, aluminum is unsuitable because of its low tensile strength. As shown in Section 3.0, storage of gaseous hydrogen and oxygen at ambient temperature provides weight advantages only in applications requiring long duration and low power level. Wire-wound fibre-glass containers offer weight advantages, but lack the environmental versatility of metal.

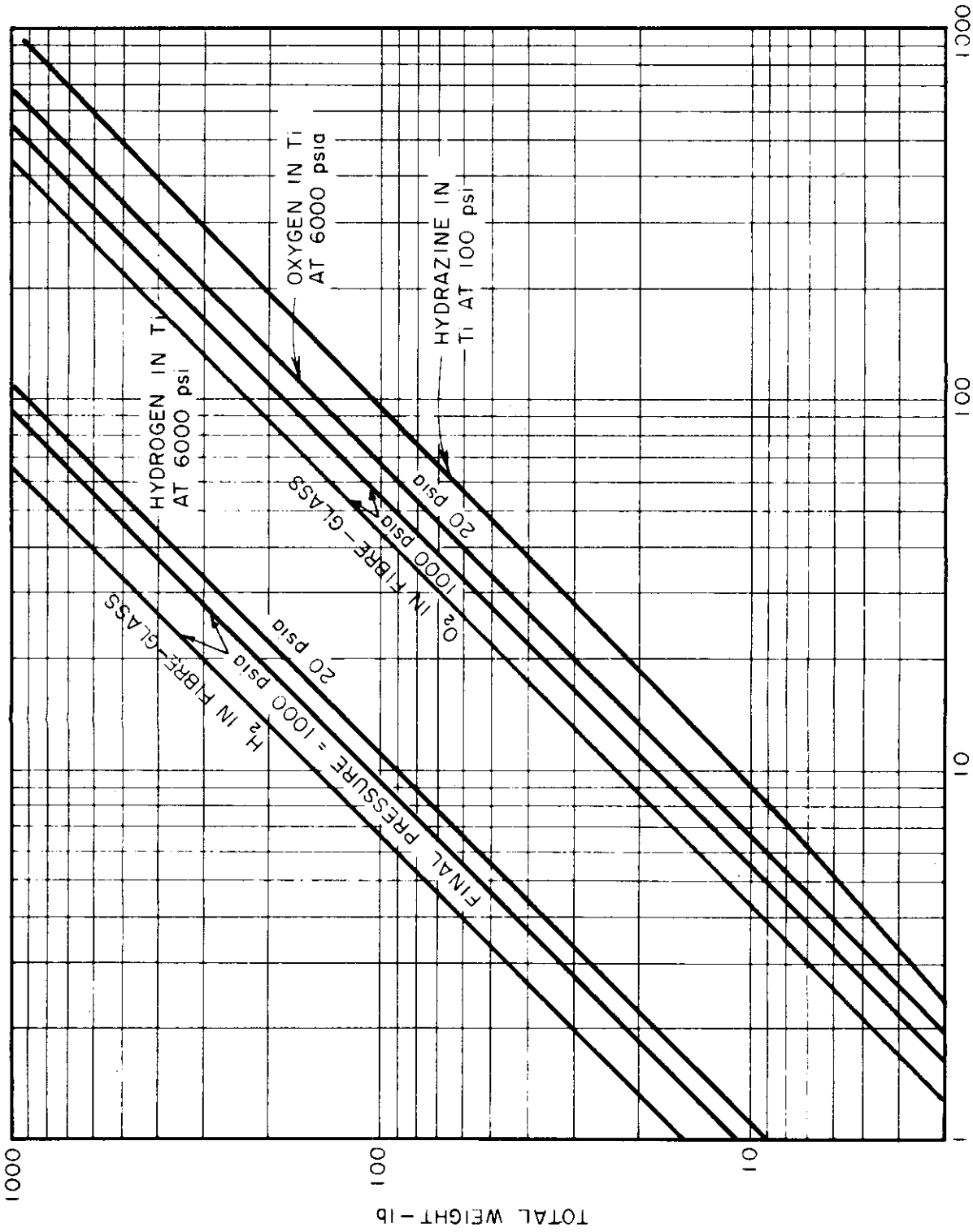

FIGURE VI-D-2 TANK WEIGHT REQUIRED TO STORE FUEL IN SPHERICAL CONTAINERS

3.0 CRYOGENIC STORAGE OF HYDROGEN AND OXYGEN

The purpose of this subsection is to discuss the storage of hydrogen (BP = -423°F) and oxygen (BP =-297.4°F) at cryogenic temperatures. More detailed information, including manufacturers of cryogenic equipment, can be obtained by consulting the list of references. In addition, a burgeoning interest in cryogenics during the last decade has resulted in a large amount of literature, such as that contained in the Proceedings of the Cryogenic Engineering Conference held annually.

The minimization of weight in a cryogenic H_2 - O_2 fuel storage system involves an optimum compromise among the type of insulation system, the materials used, the required outlet pressures, and other factors which entail a detailed analytical study. An excellent summary of these many factors is contained in Reference VI-D-1, along with summaries of anticipated storage weights as functions of power level and storage duration. However, since the publication of Reference VI-D-1, new insulation materials have appeared which will decrease insulation weight by factors of four or more, and new analyses of this current type are required.

In any system involving the storage of a cryogenic liquid, a transfer of heat into the liquid will cause evaporation of the liquid and/or a buildup of pressure within the container. In general, minimum weight is realized in any system having a use rate equaling the ventilation rate necessary to prevent an excessive pressure buildup.

The system, therefore, must be insulated to prevent a large heat transfer rate. However, for long-duration, low use-rate systems, a design in which some gas is vented but not used may result in less weight than would a design having sufficient insulation to eliminate venting. Such a system would sacrifice a small weight of gas and extra tank to save a larger weight of insulation, by using the refrigerating effect of the vented gas.

3.1 Equipment

Storage systems for space application are being developed. For example, a Beechcraft unit has been completed (for ground application) which will supply fuel to a high-pressure fuel cell with the following specifications:

Mission length	-	6 hours	
No loss standby	-	10 hours	
Storage pressure	-	800 psi	
Flow rate, H_2	-	1 lb/hr	heat must be supplied
Flow rate, O_2	-	8 lb/hr	to the unit.
Weight	-	180 lb empty	(an estimated 40 lb could be cut from weight with careful design)
Materials	-	All aluminum	

Although no test unit has yet included an outlet or auxiliary pressurization suitable for use under zero-g conditions, many ideas are available which appear to solve the problem of developing such a system. The following ideas have been presented for hydrogen tankage:

a. A capillary vent (for slow venting rates) with spherical tanks. The fundamental principle involves regulated flow of liquid within the dewar from a high-pressure region to a low-pressure region, with proper design for heat transfer to insure that liquid in the low-pressure region will evaporate before leaving the inner dewar container. In this manner, the available refrigeration in the vaporization process will be utilized. (See Ref. VI-D-2)

Calculated areas required for the capillary are approximately 2 sq in. for a 9 gram/hr flow rate for hydrogen with a pressure drop of 10 psi and 16 in^2 for a 72 gram/hr flow rate with oxygen at a pressure drop of 5 psi.

b. Cylindrical tanks with collapsible bellows (pressurized by a helium bottle) for positive expulsion.

c. Spherical tanks using a diaphragm that is pressurized by helium or an explosive compound. Increasing pressure would insure subcooling despite rising temperatures.

d. A helium-pressurized cylindrical hydrogen tank with a piston for positive expulsion, with subcooling insured by increasing pressure.

One basic limitation still remains in the development of a bellows or diaphragm material which will remain flexible at liquid hydrogen temperatures.

Some difficulties are encountered in storing cryogenic fluids under high pressure. At the critical temperature of liquid hydrogen, $-400^{\circ}F$, the critical pressure is 188.2 psi. Consequently, if the liquid is vaporized, the highest pressure realizable is 188.2 psi without superheating the gas formed. Since liquid and vapor at $-400^{\circ}F$ cannot coexist at pressures exceeding the critical, two possibilities arise: (1) gas at less than 188.2 psi can be taken and compressed to a higher working pressure or (2) liquid can be taken from the storage container with a pump and superheated to the required pressure. An advantage, however, is that no special zero-g apparatus is required for removal of fuel.

Alternatively, pressures above the critical point can be obtained by gradually warming the container and remaining gas in order to maintain a constant pressure as gas is withdrawn. The rate of heat transfer will depend on variations in specific heat with temperature, a gradually diminishing temperature

difference, and the gradually diminishing amount of gas remaining in the container.

As a result, the allowable heat input -- that required to maintain the pressure while withdrawing the contents at a constant rate -- varies with time or with percent of the material withdrawn from the container. Calculations in Reference VI-D-1 indicate that, for storage at 800 psi, only approximately 85 percent of the material could be used in a fuel cell without excessive heat input and that theoretically only 88 percent could ever be used. In any case, the vaporization of hydrogen with a minimum of waste is a delicate control problem.

In general, the storage and delivery of oxygen is appreciably simpler with the critical constants for oxygen being - 181.8°F and 730 psi. In high-pressure application, oxygen may be delivered by simple pressurization with an electric heater.

Two other methods of supplying gas at high pressures are as follows:

a. Store it as a liquid at low pressure, allow to evaporate and cool the shield, and then compress to the desired pressure.

b. Compress the liquid to the desired value and then warm it in a radiation shield or external heat exchanger to the desired value.

Pressurization by pumps is advantageous because lightweight container shields can be used and greater refrigeration is available in the liquid. However, this method requires more fuel and is less reliable than simply pressurizing the tank.

Estimated weights of the motor and compressor or gas pressurization range from 3 to 20 lb for power ratings of 1/10 to 10 kw. As an example, the power requirement for compression of the gases will amount to 15.4 percent of the power output if a compressor efficiency of 50 percent and a pressurization

from 20 to 800 psi are assumed. Thus, an additional 18.2 percent of fuel must be carried for the motors. This fuel weight is offset by the lighter internal tank required at lower pressures. Studies contained in Reference VI-D-2 indicate weight advantages of 5 to 10 percent for 100 and 300 watt systems (hydrogen and oxygen) that use vapor compression rather than pressurization of the internal tank. The use of new "super" insulations would negate this advantage, however. In addition, compressors operating for long periods of time without maintenance at cold temperatures are generally unreliable.

3.2 Construction Materials

The choice of structural materials is based primarily on strength properties, i.e., yield and tensile strength, ductility, impact strength, and notch insensitivity. Furthermore, low heat conductivity, low coefficient of thermal expansion, and low emissivity are advantageous properties for many structural components. Aluminum, copper, and austenitic stainless steel retain their ductility and are considerably stronger at 20°K than at room temperature. Teflon and Kel-F flourinated plastics retain just enough ductility for use at 20°K. Actual service background of metals and alloys at cryogenic temperatures -- plus experience concerning metallurgical stability and strengths at low temperatures -- led to the selection in Reference VI-D-2, of the materials listed in the following tabulation. Later data indicate that this selection is still valid.

Material	Yield Strength (psi)	Density ($lb/in.^3$)
Aluminum-Kaiser 5083	18,000	0.0961
Stainless Steel - Type 304, 321 (Austenitic)	30,000	0.287
Titanium - Ti-6A1-4V	160,000	0.161

Design must allow for thermal contraction in order to avoid leaks and ruptures. Stainless steel is advantageous for applications where low

thermal conductivity is required -- for example, the supports and piping within a dewar type of cryogenic container. Aluminum is useful where high thermal conductivity and light weight are important, such as in the outer shield of a dewar vessel which may use vapor cooling. Titanium combines high yield strengths with reasonable density and appears suitable for use in shells that must withstand high pressures. Data are not available for impact strength at liquid hydrogen temperatures (no tests below - 300°F), however, and satisfactory performance at this temperature may be borderline. Techniques have been developed for joining stainless steel to aluminum, the joining of titanium alloy, however, has not been solved satisfactorily.

3.3 Insulation

To obtain an optimum compromise between minimum evaporation rate and minimum container weight, the simplest and lightest method of insulation compatible with the duration requirements should be used. Many insulation types have been considered, as shown in the schematic diagrams of Figure VI-D-3. Because the durations obtainable depend upon whether oxygen or hydrogen is stored, it is necessary to make an independent calculation of storage weight for the hydrogen and oxygen systems.

Heat conduction through supports and piping must be considered in the design of a dewar or in the storage of liquid hydrogen or oxygen. The analysis in Reference VI-D-1 showed that detailed calculations resulted in performance not significantly different from that obtained by assuming a constant heat leak through piping and supports, i.e., a fixed percentage of the heat leak through the insulation on the order of 5 percent in a spherical tank without large openings.

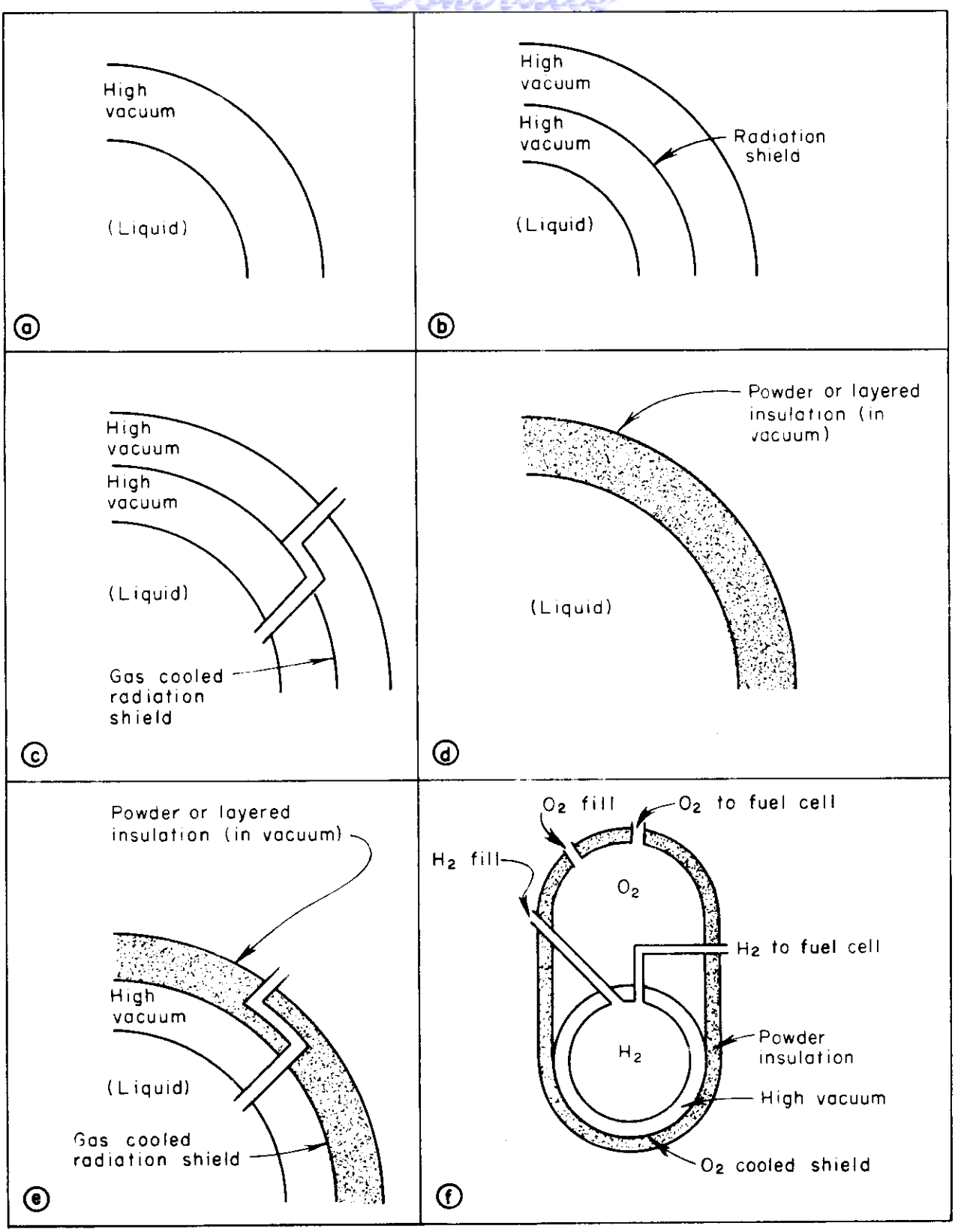

FIGURE VI-D-3 DEWAR INSULATION SYSTEMS

3.3.1 Vacuum Insulation

For systems in which no insulating powder is involved, the storage weight calculated in Reference VI-D-1 is still applicable. This weight is constant with respect to duration and power requirements for a single system. Methods of insulation include the following: high vacuum illustrated in Figure VI-D-3a; high vacuum with floating shield illustrated in Figure VI-D-3b; and high vacuum with gas-cooled shield illustrated in Figure VI-D-3c. The latter method employs the refrigeration available in the cold gas for cooling the radiation shield. When hydrogen is used, this method can be further improved by placing a para-orthoconversion catalyst in the outlet line in order to gain refrigeration obtainable by converting parahydrogen to equilibrium orthopara-hydrogen. The conversion of 100 percent parahydrogen to 25 percent parahydrogen results in refrigeration of 226 Btu/lb. A high vacuum insulation is assumed to have an evacuated space of less than 10^{-6} mm of mercury. Heat transfer is then entirely dependent upon radiation effects. If the insulation obtained from such a system is adequate, it has the advantage of relative simplicity and light weight. The heat transfer due to radiation for concentric spheres is given by

$$Q_r = \frac{\sigma A_1 (T_2^4 - T_1^4)}{\frac{1}{\epsilon 1} + \frac{A_1}{A_2}\left(\frac{1}{\epsilon_2} - 1\right)} \qquad \text{(D-5)}$$

where

σ = 0.1713×10^{-8} Btu/(hr) (ft^2) (^oR)^4

1 refers to inside sphere

2 refers to the outside sphere

A = surface area, ft^2

ϵ = emissivity

T = temperature ^oR

Q_r = heat transfer by radiation, Btu/hr.

Coatings with emissivities of approximately .03 (e.g., silvered) are readily obtainable. Theoretically, insertion of a radiation shield between the inner and outer shell of the dewar will reduce radiation heat transfer to one-half the value obtained without the shield. However, the additional weight of the shield (.025 in. aluminum) negates this advantage.

The ratios of total storage weight to fuel weight in hydrogen and oxygen systems without insulation powder are presented in Table VI-D-1 for internal pressures of 20, 90, and 800 psi.

TABLE VI-D-1
(Reference VI-D-1)

WEIGHT FACTORS FOR VARIOUS INSULATION SYSTEMS

Dewar System	Liquid Stored	Total Storage Weight to Fuel Weight Ratio		
		20 psia	90 psia	800 psia
High Vacuum	Oxygen	1.081	1.103	1.261
Shielded High Vacuum	Oxygen	1.112	1.14	1.3
High Vacuum With Gas-Cooled Shield	Oxygen	1.112	1.14	1.3
High Vacuum	Hydrogen	2.265	2.54	2.935
Shielded High Vacuum	Hydrogen	2.83	3.22	3.59
High Vacuum With Gas-Cooled Shield	Hydrogen	2.83	3.22	3.46

The ratios in the above table must be multiplied by a factor to account for the excess fuel evaporated over a given storage period. This factor is

$$\frac{M_s}{M_f} = \frac{1}{1 - \beta\tau} \qquad (D\text{-}6)$$

where

M_s = mass of liquid stored

M_f = mass of fuel consumed by converter

τ = time (days)

β = percent boiloff per day.

For example, with a reasonable value of 1 percent boiloff, storage for periods longer than 10 days would require 1.1 times the liquid used in the converter.

3.3.2 Powder and Layered Insulation

A decrease in radiation heat transfer can be effected in a vacuum system by the use of powder or layered insulation which has the effect of multiple radiation shields: Two systems using insulation material are shown in Figures VI-D-3d and VI-D-3e. The primary mode of heat transfer is conductive in the space filled with insulation. As shown in the equation below, heat transfer can be reduced by increasing the thickness of the insulation.

$$Q_r = \frac{4\pi K r_1 r_2 (T_2 - T_1)}{r_2 - r_1} \qquad \text{(D-7)}$$

where

K = thermal conductivity of the powder Btu/(hr)(ft^2)($^\circ$R/ft).

Recent developments by Linde Air Products Company and National Research Corporation have resulted in evacuated insulations with mean thermal conductivities about 1/10 of those found in the best evacuated powder types used commercially (Pearlite, Santocel). Their exact composition and structure are proprietary; however, they are of layer type construction using glass paper, foil, and other materials. A comparison of properties for some of

the available insulation materials is shown in Table VI-D-2. The thermal conductivity refers to the mean value measured between the specified temperature limits of column 3.

TABLE VI-D-2

PROPERTIES OF LOW TEMPERATURE INSULATION

-1- Insulation	-2- Density (lb/ft^3)	-3- Temperature (^oR)	-4- Thermal Conductivity $Btu/(hr)(ft^2)$ ($^oR/ft$)	-5- Manufacturer
Pearlite	6.0	540 - 37	.00041	Silbrico Corp., Chicago, Illinois
Silica Aerogel (Santocel, 85-5590, Al Powder 15-450 percent	6.0	540 - 37	.00035	Monsanto Chem. Co. Everett, Mass.
Max Efficiency Type S1 - 1	2.5	540 - 37	.000080	Linde Company Tonawanda, N. Y.
Max Efficiency Type S1-4	6.8	540 - 37	.000025	
Max Efficiency Type NRC-1	2.2	540 - 37	.000052	National Research Corp., Cambridge, Mass.

In order to calculate the heat transfer through the insulation, it is necessary to note the relationship between conductivity and temperature. A linear relationship was assumed in Reference VI-D-1 with $K = 0$ when $T = 0$, the midpoint value being given by the values in Table VI-D-2.

Two system configurations that have insulating material are shown in Figures VI-D-3d and VI-D-3e. The latter involves a high vacuum gas-cooled shield with para-orthoconversion combined with an insulated volume on the exterior of the vacuum region.

A schematic diagram of an oxygen-fueled system with insulating material is shown in Figure VI-D-3f. The temperature of the shield is maintained at the temperature of the boiling oxygen by evaporation. Refrigeration available in the cold hydrogen gas and para-orthoconversion is obtained at the boiling oxygen temperature. Preliminary heat transfer rate and weight calculations for such a system indicated that no saving in weight would be achieved (Ref. VI-D-1). In addition to complexity, the greater hazard of this system ruled it out.

The required thickness of insulation depends upon the liquid capacity of the tank, the properties of the insulation, and the allowable percentage boiloff, as shown in Equations D-8 and D-9.

$$\beta = \frac{7200\, K \Delta T}{\rho_f H_v r_i} \left(\frac{1}{t_{ins}} + \frac{1}{r_i} \right) \qquad \text{(D-8)}$$

where

β = percentage boiloff per day

K = thermal conductivity

ΔT = temperature drop

H_v = heat of vaporization (Btu/lb)

r_i = internal tank radium

t_{ins} = insulation thickness.

$$t_{ins} = \frac{r_i}{\frac{r_i^2}{A}\beta - 1} \qquad A = \frac{7200\ K\ \Delta T}{\rho_f H_v} \tag{D-9}$$

$$W_{ins} = \frac{4\ \pi\ A\beta\ r_i^5\ \rho_{ins}}{(r_i^2\ \beta - A)}$$

where

W_{ins} = insulation weight

ρ_{ins} = insulation density.

Several examples of the insulation thickness required for spherical tanks are shown in Figure VI-D-4. Also shown are the insulation requirements for typical cylindrical tanks (Linde Company) with a loss of 1 percent per day. Cylindrical tanks are more likely to be used for very large capacities (those greater than anticipated for auxiliary power use) primarily because of the necessity of fitting the tank within the missile structure. Consequently, the required insulation for large sizes will be almost double that predicted by calculations for spherical tanks. The effects of insulation thickness variations on the evaporation rate and tank weight are shown in Figure VI-D-5, which incorporates typical cylindrical storage tanks with L/d ratios of approximately 2 to 1.

In evaluating the heat loss for cylindrical tanks, as illustrated by the curve in Figure VI-D-4, heat leak through supports and piping was included. This contribution was taken into account by the fact that as capacity increases, supports and piping will contribute a logarithmically lower percentage of heat leak in typical vessels. These sources account for 70 percent of the total heat leak in a 10-gallon vessel and for 10 percent in a 100,000-gallon vessel. Ullage was considered 10 percent because of the comparatively rapid increase in volume with increasing saturation temperature (and pressure) that is characteristic of liquid hydrogen.

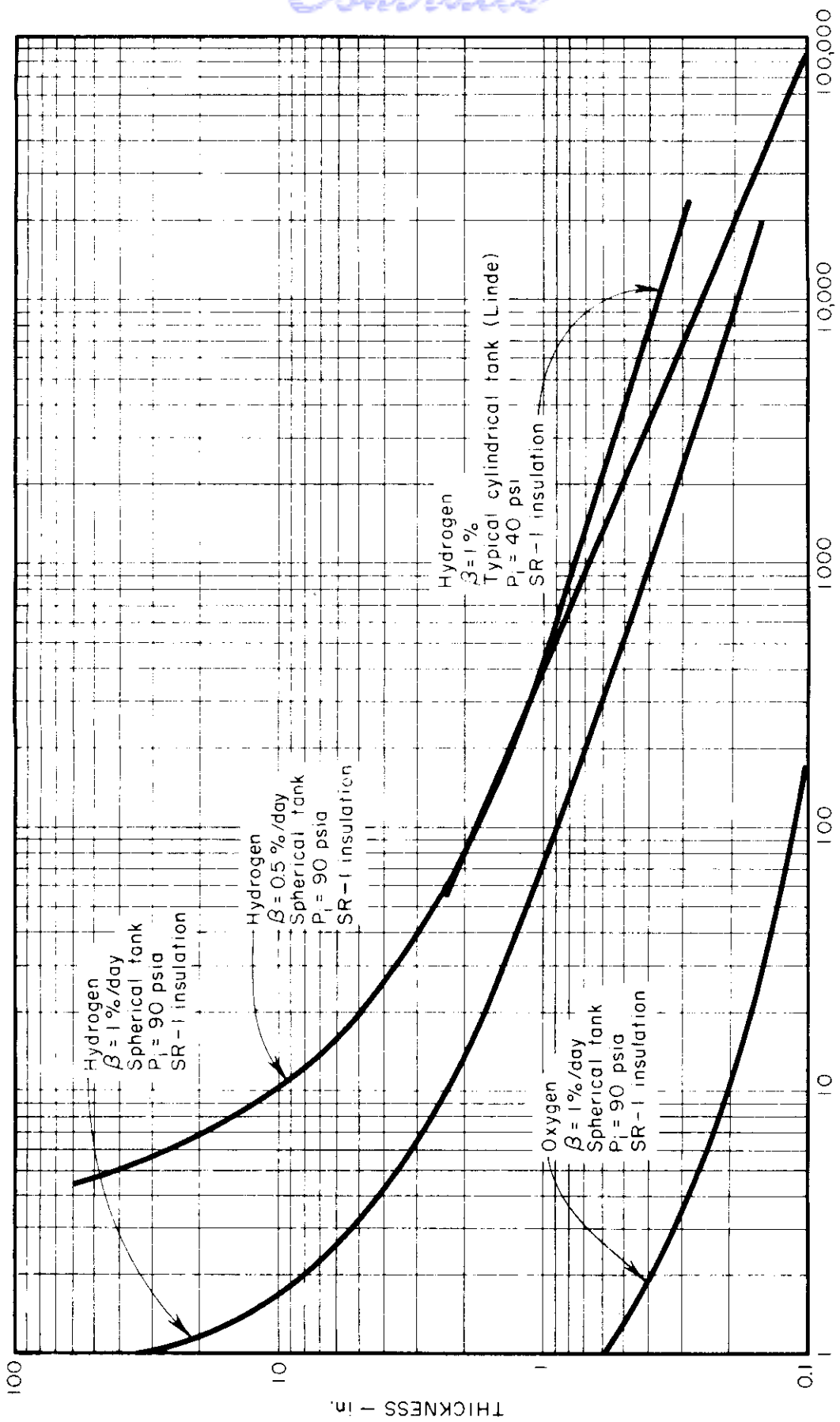

FIGURE VI-D-4 INSULATION THICKNESS FOR CRYOGENIC STORAGE

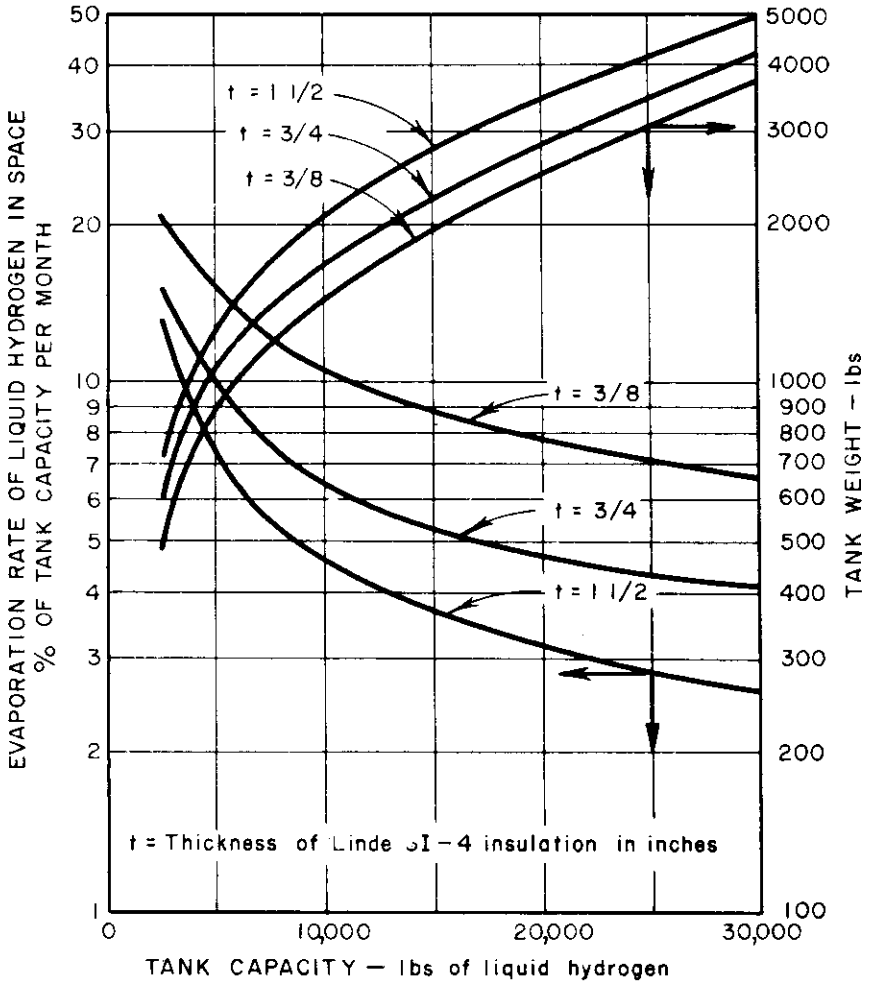

FIGURE VI-D-5 LIQUID HYDROGEN TANKAGE DESIGN (Linde)

As the curves show, it is relatively easy to limit heat leaks in large tanks. Since pressure rise or evaporation loss in percent per day is directly proportional to surface area and inversely proportional to capacity, large tanks provide better performance in terms of watt hr/lb than do small tanks. The heat required to vaporize the liquid is approximately the difference in internal energy between saturated liquid at internal tank pressure and vapor at slightly less pressure, held at the saturation temperature corresponding to internal tank pressure. Resulting vaporization heats are tabulated below for 20 and 90 psia.

Fluid	Liquid Density ($lb/in.^3$)	Tank Pressure (psia)	Vapor Pressure (psia)	Heat of Vaporization (Btu/lb)
Hydrogen	.00252	20	15	190.8
		90	80	161.8
Oxygen	.0411	20	15	90.83
		90	85	80.6

4.0 SYSTEM WEIGHT

Derivation of system weight involves complicated analysis deserving of computer techniques. Since the advent of the new "super" insulations (e.g., S1-4, Linde Company), it is of little interest to consider any other type of insulation system other than that illustrated in Figure VI-D-3d.

The performance of this type of system, weight-wise, is as good or better than any other system -- except in extremely short, high-power applications and extremely long, low-power applications. For the former case, simple radiation shielding can be used, and for the latter case, storage of gaseous fuel at high pressure seems best.

Figure VI-D-6 is abstracted from curves presented in Reference VI-D-4. These curves were derived from the following approximations:

1. Vacuum jacketed insulation
2. Insulation density = 5.0 lb/cu ft
3. Jacket temperature = $80^{\circ}F$
4. Insulation conductivity = $.02 \times 10^{-3}$ $\frac{Btu}{Hr\text{-}Ft^{\circ}F}$
5. Storage pressure = 14.7 psia
6. Jacket weight charged to vehicle structure
7. Remaining tank wt given by formula: $W_s = 20 + .5\ W_o$ (in lb)

   W_s (exclude insulation wt) includes shell weight, zero gravity fluid expulsion system, and zero-gravity vapor vent system.

   W_o = weight of hydrogen initially stored
8. Heat leak through fittings = Btu/hr
9. The thickness of insulation and the percentage boiloff were optimized in each case.

The weight of the entire hydrogen storage system is shown as a function of the storage duration. The curves in Reference VI-D-7 do not include the weight of the external shell, primarily because of its light weight and the possibility of using the missile structure for this purpose.

Also shown in Figure VI-D-6 are two curves derived from the calculations in Reference VI-D-1. As is shown, total storage weight will increase as the internal pressure is increased -- primarily because of the increase in internal tank weight. An optimization program is still required to ascertain the best storage weight obtainable for any given case. Until such a program is carried out, the curves of Figure VI-D-6 appear conservative and suitable for preliminary design. Variables would include internal pressure, storage duration, power level, and related factors.

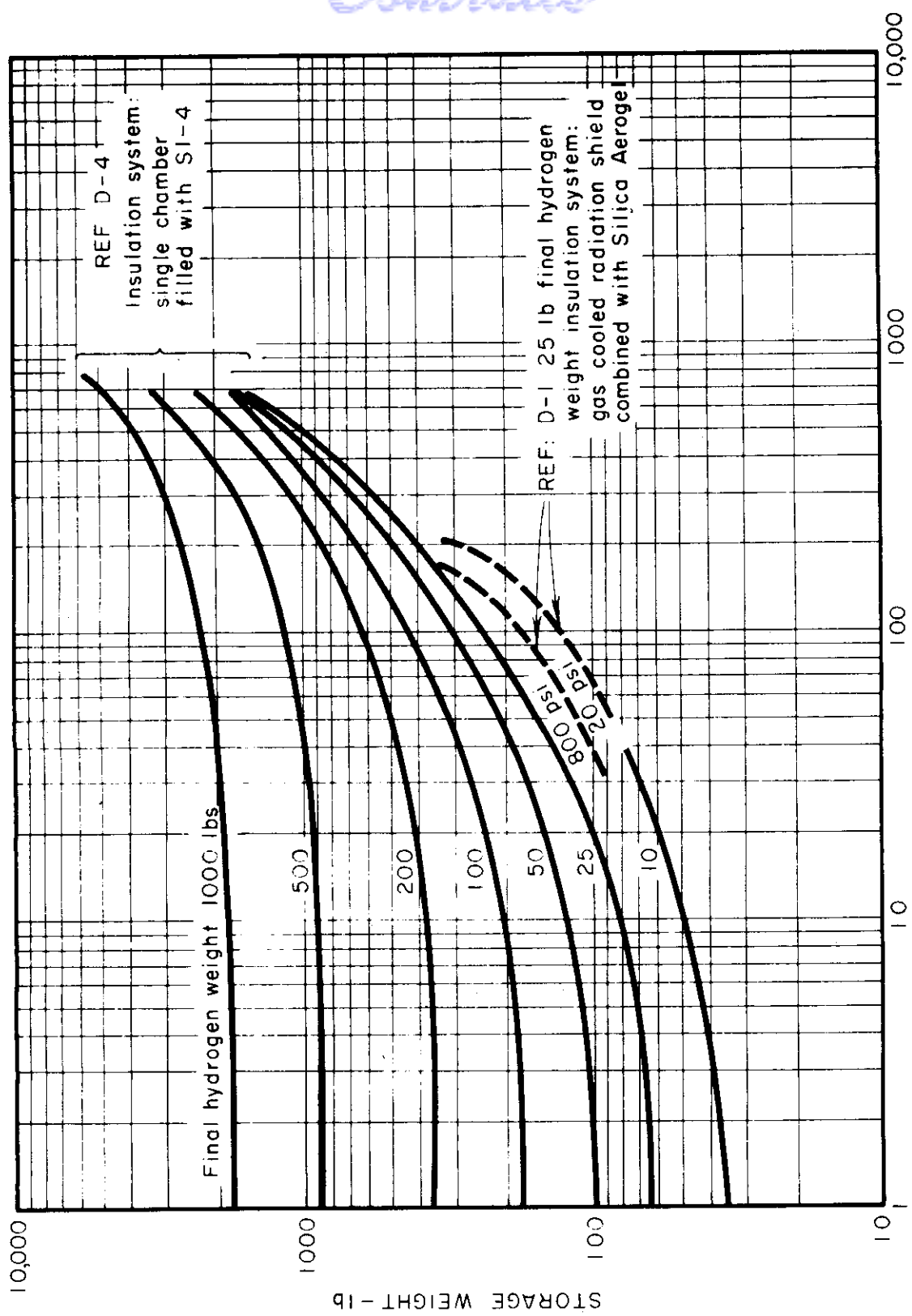

FIGURE VI-D-6 TOTAL STORAGE SYSTEM WEIGHT - HYDROGEN

Figure VI-D-7 is an approximation of the total weight required to store oxygen for a given duration. These calculations assumed S1-4 insulation with a spherical chamber in a configuration similar to that in Figure VI-D-3d. It was also assumed that the tank weight was 1/10 of the oxygen weight stored and that controls added another 1/10. As shown, a ratio of tank weight to storage weight is much less than the corresponding ratio for hydrogen, primarily because of hydrogen's higher density and higher heat of vaporization.

In systems calculations, Figures VI-D-6 and VI-D-7 can be used to approximate the total weight of the storage system. Hydrogen and oxygen requirements will vary according to the heat engine used. For example, the oxygen-to-hydrogen ratio for fuel cells will be stoichiometric; for the positive displacement engine, 1 lb. of hydrogen to .4 lb of oxygen; and for the turbine system, perhaps 1 lb of hydrogen to 1 lb of oxygen.

An idea of the components used and their interelation in the over-all system can be gained from Figure VI-D-8, which is designed to supply hydrogen and oxygen to a combustor at about 800 psia.

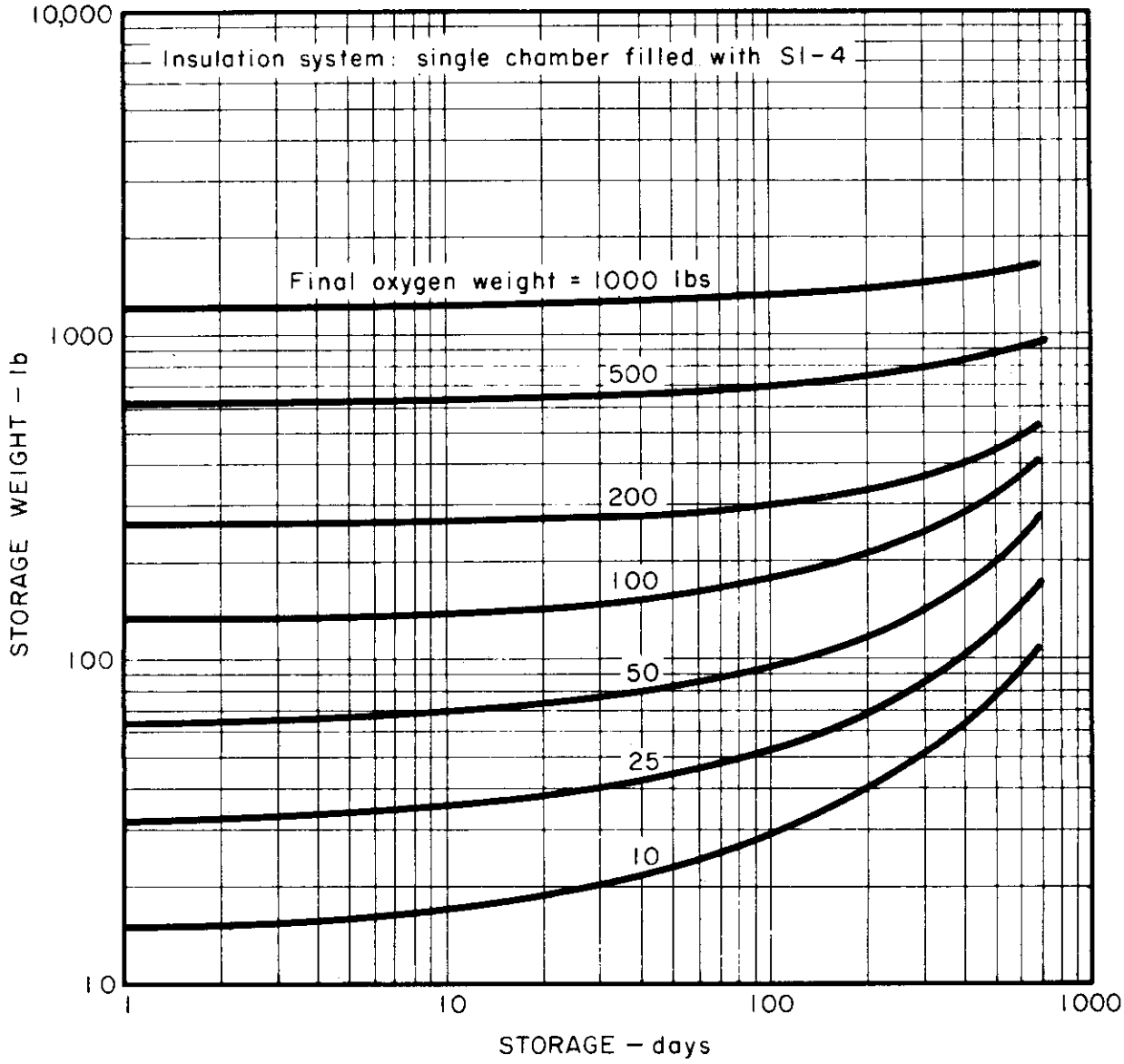

FIGURE VI-D-7 TOTAL STORAGE SYSTEM WEIGHT - OXYGEN

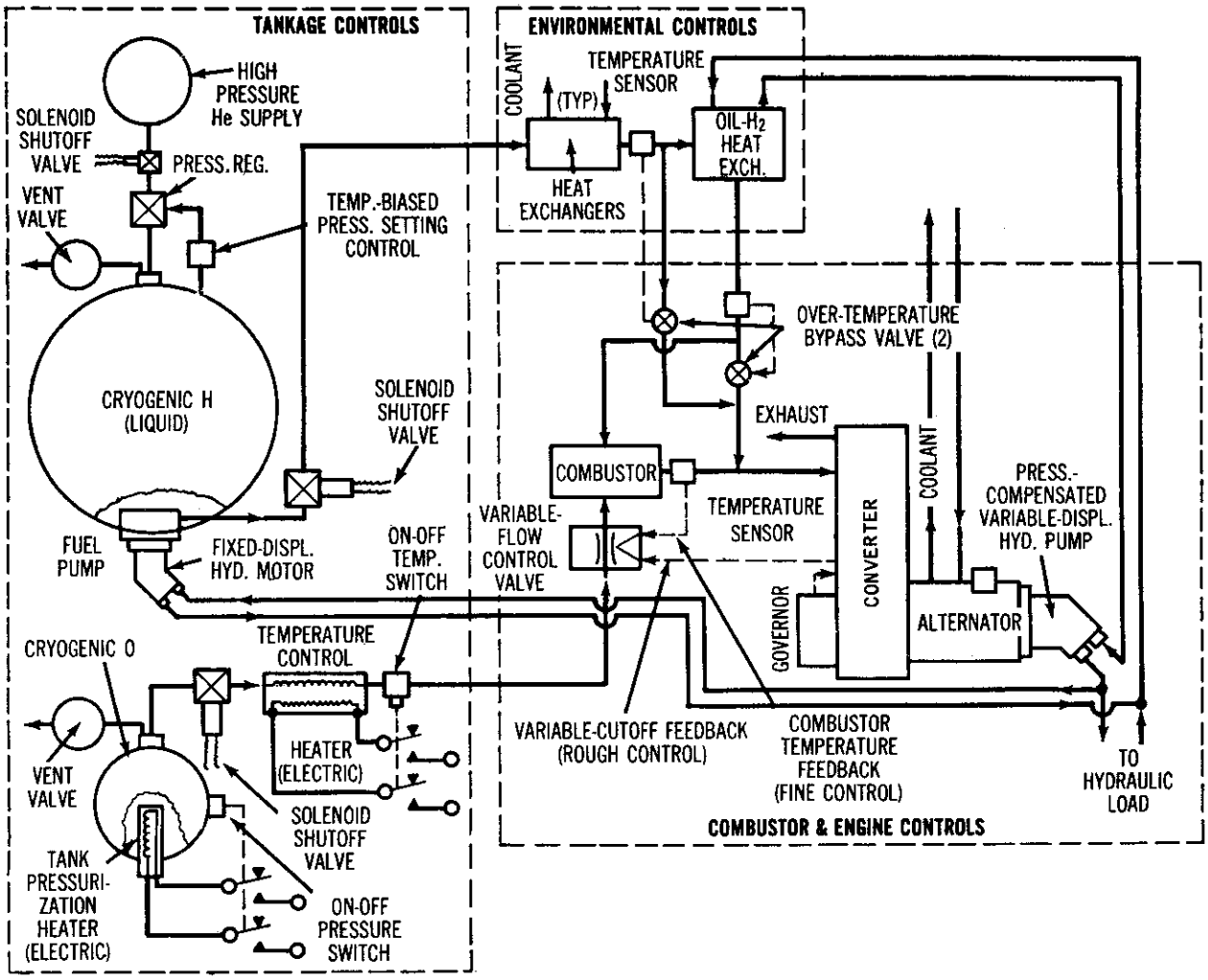

FIGURE VI-D-8 BASIC CONTROLS FOR TANKAGE AND COMBUSTOR

REFERENCE LIST

VI-D-1. DeHaan, James R., and Piccone, Marshall. (Beechcraft) "Hydrogen-Oxygen Fuel Electrolytic Battery Container Study," WADC Technical Report 58-542, October 1958.

VI-D-2. Alexander, L. R., et al. (Universal Winding Company, Inc., Patterson-Moos Division) "Continuous Feed Fuel Cell Systems," WADC Technical Report 57-605, September 1957.

VI-D-3. Bailey, B. M., et al. (Arthur D. Little, Inc.) "Handbook for Hydrogen Handling Equipment," WADC Technical Report 59-751, February 1960.

VI-D-4. Howard, H. J., and Laughlin, R. M. (Vickers, Inc.) "The Use of Chemical Power Systems in the Construction, Servicing and Operation of Manned Space Stations," Proceedings of the IAS Manned Space Stations Symposium, April 20-22, 1960.

VI-D-5. Kramer, K. R. "General Storage of Cryogenic Fluids," WADC Technical Note 58-282, October 1958.

VI-D-6. Smolak, G. R., and Knoll, G. R. "Cryogenic Propellant Storage for Round Trips to Mars and Venus," IAS Paper No. 60-23, January 25-27, 1960.

VI-D-7. Driscoll, D. G. "Cryogenic Tankage for Space Flight Applications," 1959 Cryogenic Engineering Conference, September 2-4, 1959.

VI-D-8. Menasco Manufacturing Company. "Pressure Vessels for the Space Age."

VI-D-9. Kinnaman, E. B., et al. (Boeing Airplane Company) "An Approach to the Practical Design of Reliable Lightweight High Strength Pressure Vessels," IAS Paper No. 59-109, June 16-19, 1959.

VI-D-10. Walter Kidde and Co., Inc. "Kidde Fiberglass Structures."

VI-D-11. Chelton, D. B., and Mann, D. B. "Cryogenic Data Book," U. S. Atomic Energy Commission, UCRL-3421, 1956, WADC Technical Report, 59.

VI-D-12. Perkins, W. E., and Franier, R. J. (Linde Company) "Practical Storage and Distribution of Liquid Hydrogen and Helium." Presented at 1959 Cryogenics Engineering Conference.

VI-D-13. Hansen, A. O. "Extremely Low Temperatures - Production and Commercial Uses," Chemical Engineering, February 23, 1959.

VI-D-14. Driscoll, D. B. (Linde Company) "Cryogenics Engineering Conference.